



University of Huddersfield Repository

Sabo, Sani

Chemical Modifications of Poly(dimethylsiloxane) For Permeation Analysis.

Original Citation

Sabo, Sani (2021) Chemical Modifications of Poly(dimethylsiloxane) For Permeation Analysis. Doctoral thesis, University of Huddersfield.

This version is available at <http://eprints.hud.ac.uk/id/eprint/35616/>

The University Repository is a digital collection of the research output of the University, available on Open Access. Copyright and Moral Rights for the items on this site are retained by the individual author and/or other copyright owners. Users may access full items free of charge; copies of full text items generally can be reproduced, displayed or performed and given to third parties in any format or medium for personal research or study, educational or not-for-profit purposes without prior permission or charge, provided:

- The authors, title and full bibliographic details is credited in any copy;
- A hyperlink and/or URL is included for the original metadata page; and
- The content is not changed in any way.

For more information, including our policy and submission procedure, please contact the Repository Team at: E.mailbox@hud.ac.uk.

<http://eprints.hud.ac.uk/>



Chemical Modifications of Poly(dimethylsiloxane) For
Permeation Analysis.

Sani Sabo (Researcher)
March 2021

Abstract

Absorption and distribution of any new drug candidate remain imperative components in the drug development process. For more than four decades, researchers have actively embarked on finding alternative ways to replace the use of human skin samples for *in-vitro* measurement of model drug absorption profiles. More recently, the use of polymeric materials has gained wide consideration as a viable alternative, largely due to physicochemical semblance that can be drawn from some of these polymeric membranes in comparison with the skin. However, an empirical resolve, strong enough to replicate surface activity of the skin, in terms of permeation data is yet to be achieved, which then necessitates the need to look for further approaches.

In this study, one of the polymer membranes widely considered as a potential skin mimic namely, poly(dimethylsiloxane) PDMS was studied and consequently, was chemically modified in an attempt to address some of the many constraints associated with the use of human skin samples.

In the first phase of the study, PDMS membrane was plasma treated using an atmospheric pressure non-thermal air plasma technique; structurally, this process replaces surface methyl groups present on the membrane surface with hydroxyl groups, thereby making the surface of the membrane susceptible for chemical treatments and grafting. This process was followed by silanisation processes using various active saline reagents such as dimethylphenylsilanol, tertbutyldimethylphenylsilanol, pentan-1,5-diol to mention but a few. A modified form of the membrane was characterised with a range of relevant analytical techniques such as scanning electron microscopy (SEM), water contact angle (WCA) analysis, Brunauer-Emmett-Teller (BET) technique and attenuated total reflectance-Fourier transform infrared spectroscopy (ATR-FTIR). Comparative permeation analysis was carried out between standard PDMS membrane and modified forms of the membrane, and drug permeation profiles were quantified using ultraviolet-visible spectroscopy (UV-vis) and high-performance liquid chromatography (HPLC) techniques.

As part of this research work, the concept of ‘smart polymers’ was also studied. Poly(dimethylsiloxane)-poly(ethylene oxide) block co-polymer (PEG-BCP) was identified and grafted onto plasma-treated PDMS membrane. The resultant membrane formed was able to smartly re-orient itself and selectively respond to changes based on sample drug hydrophilicity.

Overall, over-estimation of percutaneous absorption (which is a lingering constraint experienced with the use of polymeric membranes in permeation analysis) was remarkably reduced and reported difficulties experienced with analysing hydrophilic drugs, such as caffeine, were also addressed. Structural integrity, activity and selectivity of the membrane was also improved following modification processes reported herein.

Dedication

This work is dedicated to my favourite people; *my lovely wife Asiya Muhammad Kabir, and my two lovely children, Yahaya (Adnan) and Muhammad S. Sabo.*

Acknowledgement

In the name of Allah, the most beneficent the most merciful

I want to start by thanking my sponsors, the Petroleum Technology Development Fund (PTDF) - Abuja, Nigeria, without which this programme won't have been possible. I am grateful and mindful of the sponsorship, and I will strive to remain a good ambassador of the platform and try to contribute my little quota towards achieving the overall aim of the platform.

I also wish to extend my sincere gratitude to my supervisor- Prof. Laura Waters, her contribution in actualising completion of this programme can never be over-emphasised. As an international student, I am thankful to her support even towards issues which can otherwise be viewed not pertinent; her commitment to my doctoral success remained un-flinched right from the beginning of my programme up through the unprecedented COVID-19 pandemic period. Surely, it is difficult to justify her incredible support with words, but the plan is to demonstrate that I understand, and I am grateful.

Technical and supporting staff of my school (Applied Sciences) particularly Jim Rooney, Ibrahim George, Urfan Sabir and Richard Hughes have all contributed in one way or the other in the cause of this programme and I am grateful to all of them. I also wish to appreciate Prof. Krzysztof Kubiak from the school of Engineering who not only helped me with Water Contact Angle (WCA) analysis, but also trust me enough to completely move the instrument from his department down to my laboratory for easy access. I always look back to that moment and I am still in awe with his kindness.

Encouragement from my colleagues and friends both here in the UK and from back home Nigeria, also played a huge role in this journey. I particularly appreciate the time spent with Oliver Smith; a lab colleague turned friend, my close friends Hafiz Ibrahim and Aliyu Lawal Aliyu; aside tolerating all my complains, they have also played a very good role as friends. Tamunor Kingsley, Mustapha G., Sayfullahi Suleiman, Bello Sambo, Collins O, Umar Sani, Khalid H, Ishaq I, Malam Aliyu, Abubakar M., H. Ahmed to mention but a few are also appreciated. Shamsuddeen Ahmad and moreover, Hafiz Ibrahim who were instrumental towards my choice of institution have been of immense support also, and I appreciate them. All of these mates have made this journey a wonderful and memorable learning experience.

I am also very lucky to have an amazing family, there is a direct correlation between what I have become today, and the endless moral and financial support I have from my family. My uncle Alhaji Babangida Yahaya and his wife Haj. Hauwa, words are not enough to crown you. My siblings Isma'il Usman, Tasiu Sabo, Fatima, Rukayya, A/Rahman, Khadija, Ibrahim and Muhammad. I enjoyed all your support. To my wife Asiya Muhammad Kabir, alongside my family in-laws, and lastly but not by any stretch the least, my son, Yahaya (Adnan), I say thank you.

Publication and Conference presentations arising from this thesis

Publications

- Permeation of Pharmaceutical Compounds Through Silanized Poly(dimethylsiloxane) Journal of pharmaceutical sciences 109 (6), 2033-2037, 2020
- Poly(dimethylsiloxane): A Sustainable Human Skin Alternative for Transdermal Drug Delivery Prediction (A review) 110 (3), 1018-1024, 2021

Contributions

1. Introduction, materials, methods, data acquisition and results analysis
2. Introduction, materials, methods, data acquisition and results analysis

Published materials in the thesis

1. Chapter 1:

Section 1.1

Introduction to the concept of Transdermal drug delivery system, and background knowledge relating to the utility of human/animal skin for permeation analysis, prior to consideration of alternate systems, forms part of the work from this section that has been published. Moreover, background of polymer membranes and their relevance in TDDS have also been published, all of which were adopted from this thesis.

Page 2 and 3 of the journal - Poly(dimethylsiloxane): A Sustainable Human Skin Alternative for Transdermal Drug Delivery Prediction (A review) 110 (3), 1018-1024, 2021

Section 1.2.12

Table 1.2 from the above section appeared in page 4 of Poly(dimethylsiloxane): A Sustainable Human Skin Alternative for Transdermal Drug Delivery Prediction (A review) 110 (3), 1018-1024, 2021

2. Chapter 2:

Section 2.2

In this section, list of chemicals used forms part of an article that was published from this thesis. Therein, compounds used in this study were presented in a similar manner they appear in the section.

See Page 2 of Permeation of Pharmaceutical Compounds Through Silanized Poly(dimethylsiloxane)

Journal of pharmaceutical sciences 109 (6), 2033-2037, 2020

Section 2.3

In an attempt to discuss some of the findings presented in a published article that resulted from this work, critical concepts and spectroscopic mechanisms of techniques such as Attenuated total reflectance- Infrared

spectroscopy (ATR-FTIR) was highlighted, similar to the presentation made in this thesis (section 2.3.1.6)

Appeared in Pages 2 and 3 of Permeation of Pharmaceutical Compounds Through Silanized Poly(dimethylsiloxane)

Journal of pharmaceutical sciences 109 (6), 2033-2037, 2020

3. Chapter 3:

Section 3.2.1

Permeability studies that dealt with dose approach employed in this study, in-vitro method and reported inference was also published

Appeared in Page 4 of Poly(dimethylsiloxane): A Sustainable Human Skin Alternative for Transdermal Drug Delivery Prediction (A review) 110 (3), 1018-1024, 2021

Section 3.2.2

This section's optimisation process was adopted and reported. Effect of the steps involved and extent of the effect as it relates to permeation analysis was also highlighted in the published article. All of which was adopted from this thesis report.

Appeared in Page 3 of Poly(dimethylsiloxane): A Sustainable Human Skin Alternative for Transdermal Drug Delivery Prediction (A review) 110 (3), 1018-1024, 2021

4. Chapter 4:

Section 4.1

Background of this chapter as captured in this section and the literature it contains was cited in the published article arisen from this work. A similar layout and problem statement as contained in this chapter was also published.

Appeared in Page 1 of Permeation of Pharmaceutical Compounds Through Silanized Poly(dimethylsiloxane)

Journal of pharmaceutical sciences 109 (6), 2033-2037, 2020

Section 4.2/4.2.5

Silanisation method as reported herein was part of the areas that were published, and the results following from the process was also presented in part of the publication already published.

Appeared in Page 2, 3 and 4 of Permeation of Pharmaceutical Compounds Through Silanized Poly(dimethylsiloxane)

Journal of pharmaceutical sciences 109 (6), 2033-2037, 2020

Conference Presentations

- Postgraduate Research Conference, University of Huddersfield, April 2018
- 10th Association of Pharmaceutical Scientist (APS) International PharmSci Conference, University of Greenwich (Maritime Campus), September 2019.
- The JPAG pharmaceutical analysis research awards and careers symposium conference, Royal Society of Chemistry, London UK., November 2019
- Postgraduate Research Conference, University of Huddersfield, November 2020
- Africans in STEM symposium, University of Cambridge, April 2021 (In-view)

Table of Contents

Chapter 1	1
Introduction and literature review	1
1.1. Introduction.....	2
1.1.2. Model Polymeric Membranes for TDDS	4
1.2. Literature Review.....	7
1.2.1. Prospects in Transdermal Drug Delivery System	7
1.2.2. Topical and Transdermal Drug Delivery	10
1.2.3. Research Statement	10
1.2.4. Structure and Mechanism of Permeation Through the Skin	11
1.2.5. Permeation theory and measurements.....	19
1.2.6. Human tissue.....	25
1.2.7. Animal Tissue	26
1.2.8. Alternative models	29
1.2.9. Cell culture	31
1.2.10. QSPR.....	31
1.2.12. Poly(dimethylsiloxane)	34
1.3. Research Aim and Objectives	40
References.....	41
Chapter 2.....	49
Materials and methods	49
2.1. Introduction.....	50
2.2. Chemicals and Materials	51
2.3. Methods.....	60
2.3.1. Analytical and Experimental Procedures	60
2.4 Conclusion	81
References.....	82
Chapter 3.....	84
Poly(dimethylsiloxane): Membrane optimisations and Chemical vapour deposit process.....	84
3.1. Introduction.....	85
3.2. Results and Discussion	85
3.2.1. Standard PDMS membrane.....	85
3.2.2. Optimisation Processes	90
3.2.3. Glycerol Attachments on Plasma treated Poly(dimethylsiloxane) membrane	101
3.3. Conclusion	113
References.....	115
Chapter 4.....	118

Sequential Silanisation Processes in Modification of Plasma-treated Poly(dimethylsiloxane).....	118
4.1. Introduction.....	119
4.2. Sequential Silanisation using Dimethylphenylsilanol.....	120
4.2.1. Background.....	120
4.2.2. Silanisation method.....	121
4.2.3. Scanning Electron Microscopy of modified DMPS-PDMS membrane.....	123
4.2.4. Attenuated Total Reflectance-Fourier Transform Infra-red spectroscopy.....	127
4.2.5. Permeation analysis (Waters & Sabo, 2020).....	129
4.2.6. Brunauer-Emmett-Teller Technique	139
4.2.7. Optical Microscopy.....	141
4.3. Sequential Silanisation using Tertbutyldimethylsiloxane	143
4.4. Sequential Silanisation using Perfluorophenylsilanol.....	144
4.4.1. Comparative permeation profile between Perfluorophenylsilanol treated PDMS and PDMS membrane.....	145
4.5. Conclusion	147
References.....	149
Chapter 5.....	151
Development of a Smart Poly(dimethylsiloxane) alternative for permeation analysis.....	151
5.1 Introduction.....	152
5.2. Smart PDMS membrane	153
5.2.1. Background.....	153
5.2.2. D-PDMS - PDMS-PEG BCP method.....	154
5.2.3. Attenuated Total Reflectance-Fourier Transform Infra-red spectroscopy.....	157
5.2.4. Permeation analysis and measurement.....	159
5.3. Conclusion	167
References.....	168
Chapter 6:.....	170
Conclusion and Future work.....	170
6.1. Conclusion	171
6.2. Future work.....	173
References.....	175
Appendices.....	176
Appendix I	176
Appendix II.....	178

List of Figures

Figure 1. 1 Systemic illustration of transport route across layers of the skin	15
Figure 1. 2 Schematic representation of the ‘Bricks and mortar’ model	16
Figure 1. 3 Schematic diagram of potential drug permeation pathways.....	18
Figure 1. 4 Percentage of animals used in the United Kingdom for scientific experiments (3.4 million) in 2019.	27
Figure 1. 5 An illustration of some developed ‘Organ on a chip ‘systems.....	30
Figure 1. 7 General structure of poly(dimethylsiloxane), also known as PDMS.	35
Figure 2. 1 Schematic representation of a typical Plasma generator	63
Figure 2. 2 Typical Incident beam interactions with sample material in SEM analysis, adapted with modifications from (Dehm, Howe, & Zweck, 2012)p 4.	65
Figure 2. 3 A typical BET analyser (UoH Chemistry Lab, 2019)	72
Figure 2. 4 Schematic representation of a Dispersive IR.....	74
Figure 2. 5 Schematic illustration of ATR single bounce cell	75
Figure 2. 6 Graphical and schematic representation of ATR-FTIR technique, illustrating working methods of the technique. (FTIR laboratory UoH, 2020)	76
Figure 2. 7 Schematic representation of a flow-through system	77
Figure 2. 8 Schematic representation of a diffusion cell used for permeation analysis.....	78
Figure 3. 1 Caffeine calibration at 272 nm	88
Figure 3. 2 Salicylic acid calibration at 234 nm	88
Figure 3. 3 Steady state flux of benzoic acid through standard PDMS	89
Figure 3. 4 Steady state flux of caffeine through standard PDMS	90
Figure 3. 5 Steady state flux of diclofenac through standard PDMS.....	90
Figure 3. 6 Schematic representation of the plasma treatment mechanism employed in this study to modify the surface of PDMS membrane.	92
Figure 3. 7 SEM image of Standard PDMS prior to modification (× 500)	93
Figure 3. 8 SEM image of images of plasma treated PDMS (over cured) (× 500)	94
Figure 3. 9 SEM image of images of plasma treated PDMS (optimised) (× 500).....	95
Figure 3. 10 Steady state flux of diclofenac through standard and plasma treated PDMS membrane.	97
Figure 3. 11 SEM of normal (a), plasma treated (b) (over cured) and optimised (c), PDMS membranes (left), alongside their respective water contact angle measurements (right). 98	
Figure 3. 12 Schematic representation of chemical vapour deposit procedure - technique inspired by the atmospheric pressure chemical ionisation (APCI) process.....	104

Figure 4. 1 proposed reaction scheme (A) Un-modified membrane (B) Plasma-treated membrane (C) Modified membrane.	121
Figure 4. 2 SEM of DMPS-PDMS modified membranes with images (a), (b) and (c), representing the silanisation stage of the membrane modification process $\times 500$ magnification	124
Figure 4. 3 SEM of DMPS-PDMS modified membranes, following exposure to nitrogen with images (a), (b) and (c), representing different samples of membrane $\times 500$ magnification	125
Figure 4. 4 Comparative SEM images of PDMS, plasma treated (over cured), plasma treated (optimised), glycerol-coated, DMPS modified, and DMPS-modified (conditioned under nitrogen atmosphere) -PDMS membranes, respectively $\times 500$ magnification.....	126
Figure 4. 5 Comparative steady state flux of salicylic acid, ethyl paraben and diclofenac through PDMS, Plasma Treated, and DMPS modified membranes.....	131
Figure 4. 6 Comparative permeation profiles of model compounds, permeated through PDMS, Plasma Treated, and DMPS modified membranes	134
Figure 4. 7 Graphical representation of serially arranged log P values, in descending order, versus percentage increases in permeation profile (obtained between PDMS and modified PDMS).....	135
Figure 4. 8 Structural representation of lidocaine, benzocaine and tetracaine highlighting their similar functional groups	136
Figure 4. 9 Optical microscopy images for (A) PDMS, (B) plasma treated PDMS, and (C) D-PDMS at $\times 250$ magnification	141
Figure 4. 10 Optical microscopy image of D-PDMS at $\times 250$ magnification, illustrating the ATR-FTIR effective analysis area.....	142
Figure 4. 11 Permeability coefficient of alkyl 4-aminobenzoate permeated via silicon membrane. Adopted from Addicks <i>et al</i> , 1987.	144
Figure 4. 12 Comparative steady state flux of lidocaine and ibuprofen compounds through PDMS, DMPS and Perfluorophenylsilanol modified PDMS membranes, alongside PTFE	145
Figure 4. 13 Summary of silanisation processes employed in this study	147
Figure 5. 1 Schematic representation of proposed surface re-arrangement exhibited by PDMS-PEG BCP, when in contact with hydrophilic materials.	154
Figure 5. 2 Schematic illustration of distinct layers present in the formation of smart-PDMS membrane proposed in this study.	155
Figure 5. 3 Proposed reaction scheme in the development of a smart-PDMS membrane.....	156
Figure 5. 4 Independent ATR-FTIR spectra for PDMS-PEG BCP, smart-PDMS and PDMS membrane	158
Figure 5. 5 Chromatogram of caffeine at a concentration of 8 ppm, and a peak at approximately 3.02 minutes.	160
Figure 5. 6 Caffeine calibration at 271 nm using HPLC	161
Figure 5. 7 Chromatogram of caffeine solution at a concentration of 8 ppm, indicating a peak at approximately 3.0 minutes.....	162
Figure 5. 8 (a and b) Chromatogram of PDMS-PEG and PDMS respectively.	163

List of Tables

Table 1. 1 A summary of several studies proposing PDMS as a potential alternative to predict transdermal permeation. (Sabo & Waters, 2020)	37
Table 1. 2 Comparative description between PDMS membrane and skin equivalent models.	38
Table 1. 3 A summary of the main techniques employed for PDMS modifications.	39
Table 2. 1 Description of materials used in this study	52
Table 2. 2 Description of chemicals used in this study.....	53
Table 2. 3 Physicochemical properties of pharmaceutical compounds used in permeation studies	54
Table 2. 4 Summary of HPLC experimental conditions.....	79
Table 3. 1 Cumulative mass of model drugs used in this chapter alongside their biopharmaceutical classification, which are: caffeine (CAF), lidocaine (LID), benzoic acid (BZA), ethyl paraben (EPB), benzocaine (BEN), salicylic acid (SAL), ibuprofen (IBU), diclofenac (DCF), ketoprofen (KPF), antipyrine (ANT), tetracaine (TTC), procaine hydrochloride (PRC), and pentoxifylline (PTX) permeated through standard PDMS membrane following permeation analysis (mean \pm standard deviation, rounded to whole numbers, $n = 3$).	87
Table 4. 1 ATR-FTIR assignment of PDMS pre- and post-modification.....	127
Table 4. 2 A summary of log P, molecular weight, hydrogen bond donor (HBD), hydrogen bond acceptor (HBA) count, polar surface area (PSA), and log D of compounds i.e., antipyrine (ATP), benzocaine (BEN), caffeine (CAF), diclofenac (DF), ethyl paraben (EP), ibuprofen (IBU), ketoprofen (KTF), lidocaine (LID), pentoxifylline (PXF), procaine hydrochloride (PCN), salicylic acid (SA), and tetracaine (TTC).	130
Table 4. 3 Percentage increase (% incr.) of compounds i.e., antipyrine (ATP), benzocaine (BEN), caffeine (CAF), diclofenac (DF), ethyl paraben (EP), ibuprofen (IBU), ketoprofen (KTF), lidocaine (LID), pentoxifylline (PXF), procaine hydrochloride (PCN), salicylic acid (SA), and tetracaine (TTC), that permeated through normal and DMPS PDMS membranes	132
Table 4. 4 Cumulative mass ($\mu\text{g}/\text{cm}^2$), and permeation coefficient (K_p) $\times 10^{-4}$ cm/min) values of lidocaine (LID), ketoprofen (KTF), salicylic acid (SA), ethyl paraben (EP), ibuprofen (IBU), diclofenac (DF), procaine hydrochloride (PCN), antipyrine (ATP), pentoxifylline (PXF), tetracaine (TTC), caffeine (CAF) and benzocaine (BEN) permeated through N-PDMS and D-PDMS, alongside some K_p literature values.	138
Table 5. 1 ATR-FTIR assignment of PDMS pre- and post-modification.....	157
Table 5. 2 Physicochemical properties of ketoprofen (KTF), ethylparaben (EPB), ibuprofen (IBU), lidocaine (LID), tetracaine (TTC), and caffeine (CAF) model compounds used in present study, alongside their cumulative mass permeated ($\mu\text{g}/\text{cm}^2$) through PDMS and modified smart-PDMS.....	165
Table 5. 3 Percentage decrease (% decrse.) of compounds i.e., ketoprofen (KTF), ethyl paraben (EP), ibuprofen (IBU), lidocaine (LID), tetracaine (TTC) and percentage	

increase (% incr.) of caffeine (CAF), that permeated through smart PDMS membranes	166
---	-----

List of Abbreviation

ADMET	Absorption distribution metabolism excretion and distribution
AFM	Atomic force microscopy
APCI	Atmospheric pressure chemical ionisation
API	Active pharmaceutical ingredients
ATR-FTIR	Attenuated total reflectance – Fourier transform infrared spectroscopy
ATP	Antipyrine
BCS	Biopharmaceutical classification
BEN	Benzocaine
BET	Brunauer – Emmett - Teller
BSE	Back scattering electron
BZA	Benzocaine
CAF	Caffeine
CAT-Scan	Computerised axial tomography - Scan
CMP	Cumulative mass permeated
DCF	Diclofenac
DMPS	Dimethylphenylsilanol
ECHA	European chemical agency
EDX	Energy dispersive X-ray
EMA	European Medicines Agency
EPB	Ethyl 4-Hydroxybenzoate
ETD	Everhart – Thornley- Detector
EU	European Union
FTIR	Fourier transform infrared spectroscopy

FTS	Full Thickness Skin
HBA	Number of Hydrogen Bond Acceptor Groups
HBD	Number of Hydrogen Bond Donor Groups
HPLC	High Performance Liquid Chromatography
HSE	Health and Safety Executive
HtSE	Heat Separated Epidermis
IBU	Ibuprofen
IPM	Isopropyl Myristate
IR	Infrared
ISC	Isolated Stratum Corneum
KPF	Ketoprofen
LID	Lidocaine
Log K _{o/w}	Logarithmic of the Octanol/Water Partition Coefficient
LSE	Living Skin Equivalent
MA	Methyl acrylate
MRI	Magnetic Resonance Imaging
NSAID	Non-Steroidal Anti-Inflammatory Drugs
OECD	Organisation for Economic Cooperation and Development
PA	Polyamide
PAN	Polyacrylonitrile
PBS	Phosphate Buffer Saline
PC-BCP	Polycarbonate – Block co-polymer
PDMS	Poly(dimethylsiloxane)
PEG	Polyethylene glycol

PSA	Polar Surface Area
PTX	Pentoxifylline
QSAR	Quantitative Structure Activity Relationship
REACH	Registration Evaluation Authorisation and Restriction of Chemicals
RF	Radio Frequency
RHE	Reconstructed Human Epidermis
SCA	Static Contact Angle
SCCM	Standard Cubic Centimetre per Minute
SE	Secondary Electron
SEM	Scanning Electron Microscopy
STS	Split Thickness Skin
TBDMS	Tertiary Butyl Dimethylsilanol
TDDS	Transdermal Drug Delivery System
TEM	Transmission Electron Spectroscopy
TTC	Tetracaine
UV	Ultraviolet
UV-vis	Ultraviolet - visible
UK	United Kingdom
WCA	Water Contact Angle
XPS	X-ray Photoelectron Spectroscopy

List of symbols

C^o	Initial concentration of permeant on membrane surface (Donor compartment)
C^h	Concentration of permeant within the membrane
C^D	Donor compartment concentration (aqueous solution)
C^R	Receiver compartment concentration (aqueous solution)
D	Diffusion coefficient
Da	Daltons
d_c	Concentration of permeant
d_x	Position (spatial dimension of the membrane surface)
I	Intensity of coloured light
I_o	Intensity of transmitted light
J_{ss}	Steady state flux
J	Diffusion/Permeant flux
K_p	Permeability coefficient
K	Partition coefficient
γ_{SV}	Solid-vapour interface
γ_{SL}	Solid-liquid interface
γ_{LV}	Liquid-vapour interface
P_o	Saturation pressure
T	Transmittance
V_m	Monolayer capacity
ϑ	Theta
Ω	Ohms

Chapter 1

Introduction and literature review

1.1. Introduction

There is considerable interest in utilising the skin as a route for drug delivery, thus requiring assessment of percutaneous absorption. The early stages of the transdermal drug development process rely heavily on skin permeation data, largely obtained from permeation analysis using human skin. However, in the initial development of a new drug candidate, such studies using human skin are practically not feasible, due to the shortage in availability of skin and how costly it can be. Also, given the number of experiments required before any medicine is fine tuned for clinical studies, further explains how difficult it is to rely on human skin for such purposes. However, the concept of using a transdermal drug delivery system (TDDS) has continued to be widely explored and considered, and this is due to the numerous advantages this route of drug administration offers. It is almost impossible to not consider this route of drug delivery in this era of human development, thus, in an attempt to address human skin availability which tends to impede development of this system and pose one of the major challenges in biopharmaceutical transdermal research, a promising approach involves the use of sustainable and synthetic polymeric membranes. The development of these membranes would not only address availability concerns often associated with human skin samples, but would also provide a shorter and more economical drug development process (Godin & Touitou, 2007). Hence, the creation of an alternative membrane that can correlate human data for prediction of percutaneous absorption in TDDS is critically needed.

Prior to consideration of synthetic membranes in the percutaneous absorption research processes, their broad application in biochemical related fields such as gas separation (Restrepo-Flórez & Maldovan, 2019), (Vopička, Randová, & Friess, 2014) and ultrafiltration have resulted in an increase in their production and characterisation, hence, concerns related to availability and compatibility have been addressed long before now (S.-F. Ng, J. Rouse, D.

Sanderson, & G. J. P. Eccleston, 2010b). Specifically, in the area of TDDS, these polymers and some of their additives have not only eased availability and cost-related concerns but have also provided an extensive database with numerous designs and flexibility for diverse applications. An impressive technical know-how that encompasses physicochemical and mechanical properties of various polymers commercially available has also been achieved and documented, making it even easier to apply in TDDS. More recently, polymers are considered the backbone of TDDS (Kandavilli, Nair, & Panchagnula, 2002).

Despite the extensive commercialisation of the polymer industry, there are limitations in terms of commercially available membranes that are suited for TDDS, especially considering the numerous and distinct properties required of such membranes. This is because commercial demands to develop a certain polymer for a specific purpose may still not address all the specific qualities needed for an effective TDDS membrane. The ability to create modifications is a promising advantage polymeric membrane offers, which largely addresses issues relating to specifics needed for certain purposes. It is well established that most of the conventional polymers produced in bulk do not necessarily meet the demand required for both their bulk and surface properties, especially when considered as biomaterials (Ikada, 1994). Therefore, materials proven to have excellent bio-functionality could be identified, modified and tailored appropriately to give a better clinically applicable material. These materials (although modified mostly only at the surface) could give new functionalities such as increased hydrophilicity, biocompatibility, adhesion, conductivity, anti-fogging and anti-fouling, amongst other properties (Uyama, Kato, & Ikada, 1998). Based on this knowledge, researchers are embarking on polymer modification processes, thereby bridging the gap between the numerous advantages of polymers and some of the distinct features they may lack for more specific purposes. It is also safe to say certain developments associated with such research have led to the production of many new materials, some of which are at an industrial scale.

1.1.2. Model Polymeric Membranes for TDDSs

Generally, polymeric membranes considered effective for drug permeation studies can be grouped as porous and non-porous membranes, and the mechanism through which drug compounds pass through them differs depending on which membrane type is used. In the case of a non-porous membrane, the drug molecule passes through the membrane via diffusion across a concentration gradient with the major influential factor being the drug molecules ability to adsorb on the membrane surface. Considering these factors, scientists have been able to cascade the three stages of permeation on these membranes, (S Ebnesajjad & Khaladkar, 2005; Sina Ebnesajjad & Morgan, 2019) :

1. Liquid take-up on the membrane surface, mainly determined by solubility parameters and the surface chemistry of the membrane
2. Migration of the liquid via the membrane matrix (determined by diffusivity), and
3. Desorption from the membrane once diffused.

Porous membranes on the other hand, are more utilised in separation processes based on drug molecule size, provided any interaction between the membrane and molecule is avoided, a sort of sieving mechanism is employed in this approach. Such membranes are often used in ultrafiltration studies.

When trying to mimic percutaneous absorption of the skin, non-porous membranes have been reported as better alternatives over the porous membranes. This is largely attributed to comparisons with reported permeation profiles using human skin. Hence, non-porous membranes are considered more closely related to the skin due to their relatively low permeation (Misra, 2014).

To better utilise synthetic polymeric membranes for investigating transdermal permeation, numerous modifications and theories have tried to explain certain principles and several

approaches have been considered. Methods involving co-polymerisation are amongst the most widely reported approaches. This approach is interesting as the principle behind it is to mimic the morphological structure of the skin. An example is polydimethylsiloxane-polycarbonate copolymers. Reported selectivity of polydimethylsiloxane was harnessed in this system, alongside the ultra-sieving nature of the polycarbonate co-polymer. Fourteen model drugs were used in this particular report, spanning a wide range of therapeutic classes. Permeability coefficients of these drugs across an actual skin membrane were determined and analysed, physicochemical parameters such as permeant molecular weight, octanol-water partition coefficient, solubility in aqueous solution and melting point were also considered. Results obtained using the actual human skin sample were then compared with results obtained from the synthetic membranes. There was a significant relationship between the two membranes ($R^2 = 0.886$) but this approach experienced phase segregation between the two co-polymers, which is a major problem with copolymers (Feldstein, Raigorodskii, Iordanskii, & Hadgraft, 1998), and as such was not considered an effective alternative at the time.

Another interesting approach previously attempted was by creating an artificial lipid membrane using isopropyl myristate (IPM), which was principally chosen to represent barrier function of the stratum corneum (top layer of the skin) (Hadgraft & Ridout, 1987). This approach was also inspired by skin morphology, which guided their choice of selection. Although a positive correlation was demonstrated in transport resistance between IPM and excised human skin, this approach still suffered from low resistance when compared with actual skin, it was therefore suggested in the paper that further modifications should be made to improve predictability and stability of the system.

Synthetic membranes such as cellulose nitrate (Borgia, Schlupp, Mehnert, & Schäfer-Korting, 2008), polyethersulfone and polycarbonate (S.-F. Ng, Rouse, Sanderson, & Eccleston, 2012),

amongst others, have also been used in skin mimicry studies with poor correlation compared with excised human skin.

However, Borgia *et al* (Borgia et al., 2008) and Shiow-Fern *et al* (S.-F. Ng, Rouse, et al., 2010b) have separately reported in their findings that silicon membrane has proven superior compared with other synthetic polymers such as polyether sulfone, polycarbonate or cellulose nitrate. Silicon membranes distinctly exhibit mechanistic diffusion of materials similar to the stratum corneum, as a consequence of their non-porous nature and compound selectivity. More specifically, silicon membranes have the ability to maintain penetrant permeation profiles via a concentration gradient. Moreover, differences in the permeation amongst different permeants remains a subjective measure which is a function of concentration and diffusivity of the permeant (Wijmans & Baker, 1995).

1.2. Literature Review

This section summarises the strengths, weaknesses, opportunities and challenges of this study. Challenges that may have prevented development of a cost-effective alternative prior to this study are also highlighted.

1.2.1. Prospects in Transdermal Drug Delivery Systems

Routes for drug delivery are broadly divided into three categories, namely, the oral route, intradermal route and the transdermal route. The oral drug delivery route has been reported as the most popular route of drug delivery; an online journal released a report in June 2019 estimating the sale of pain relief drugs at a value of £628.6 million, with the Nurofen brand having the highest sale value of £93 million (Statista, 2019), and this is excluding cold, cough, sore throat, vitamins and minerals medication. Notwithstanding this popularity, approximately 74 % of drugs taken orally have been reported not to be as effective as desired (Marwah, Garg, Goyal, & Rath, 2016). The intradermal drug delivery route on the other hand, has been reported to suffer from low patient compliance, due to its invasive method of delivery, especially by patients that require routine medications. The third option is the transdermal drug delivery route, which utilises the skin (with a large surface area) for drug delivery. Studies has shown increased patient compliance when using this route for drug delivery purposes (Thomas & Finnin, 2004). Other advantages in using the skin for drug delivery purposes includes minimised systematic delivery to other sites, as well as a reduced likelihood of uncertain absorption from degradation by stomach acid and enzymes. It also eliminates the need to use needles (or their re-use), which is still a problem particularly in developing countries (Bartosova & Bajgar, 2012), (Waghule et al., 2019). Other advantages include reduced hospitalisation and the release of drug via this route can be sustained and controlled (Pegoraro, MacNeil, & Battaglia, 2012). These advantages have made the utilisation of skin for drug

delivery a basis of several billion-dollar industries, such as cosmetics, pharmaceutical and personal care industries (Menon, 2002). This has also made TDDSs a rapid area of research and development.

In addition, new medicines are constantly designed for topical administration. A substantial number of existing drugs are also re-formulated from their original oral forms to creams, gels or ointments to utilise this promising transdermal route. Typical examples of these re-formulated drugs include ibuprofen gel and diclofenac gel. Another major reason why some of these drugs are re-formulated is as a result of studies carried out to compare efficacies and adverse effects between oral and topical forms of a drug. Findings have suggested that in terms of efficacy, there were no significant differences drawn either from the primary efficacy endpoint, the median rated time for the injury to be considered completely better by the patients or other efficacy measures, including clinical relief from pain or swelling (Whitefield, O'Kane, Anderson, & therapeutics, 2002).

Moreover, despite a proven effectiveness in the oral forms of non-steroidal anti-inflammatory drugs (NSAIDs), (mostly prescribed for musculoskeletal and soft tissue injuries) over the years, a major concern is their propensity to induce duodenal or gastric ulceration (Sanna, Peana, & Moretti, 2009). Studies have shown a significant number of patients (68 %) taking the oral form of an NSAID experience peptic ulceration, perforation, mucosal erosion or bleeding (Andrianakos et al., 1992). On the other hand, there have been rare reports suggesting adverse effects associated with topical forms of these drugs (Fernando, Thomas, Temple, & Lee, 1994), (Moore, Tramer, Carroll, Wiffen, & McQuay, 1998) and (Patil, Datir, Saudagar, & Therapeutics, 2019). These findings further encouraged researchers to develop more compounds with a wide range of therapeutic classes in a topical form, thereby providing a broader spectrum of topical drugs for combating more challenging health concerns. More

recent examples of drugs converted to transdermal formulations are compounds for the treatment of diseases such as Parkinson's and Alzheimer's which are currently in their final stages of development (Benson, Grice, Mohammed, Namjoshi, & Roberts, 2019). Also, within America alone, more than 35 transdermal products have already been approved to treat conditions ranging from hypertension, female menopause, severe pain from local muscle injuries, contraception, eczema, psoriasis and nicotine dependence, amongst others (Hillery, Lloyd, & Swarbrick, 2002). Misra *et al* also highlighted the increasing level of support from the pharmaceutical industry towards supporting this alternate route of drug delivery (Misra, 2014) .

Another key factor when considering TDDS is the concept of controlled drug release which it exemplifies, by not only minimising drug side effects but also optimised therapeutic efficacies by maximising bioavailability. Common examples are insulin patches for diabetic patients, nicotine patches for addiction withdrawal purposes, along with many other forms of these marketed compounds. The non-invasive nature, convenience and prolonged administration of therapeutic agents from these wearable TDDS remains a cornerstone in this field.

However, just like other forms of drug delivery processes, topical administration of drugs also has several issues of concern, necessitating evaluation in efficiency of these novel formulations before administration to the skin. These concerns include the fact that there is a continuous application of therapeutic compound on the skin, raising issues such as the potential to cause skin cancer (Klimová, Hojerová, & Beránková, 2015). Or, in the case of formulations such as sunscreen, can cause blockages of skin surface pores, which may decrease efficiency (Klimová et al., 2015). It also remains a challenge to researchers when trying to overcome the primary (i.e. barrier) function of skin, in the formulation development process.

As a consequence of this, there has been a lot of research within this area, not only to propose alternative formulations but to also enhance, optimise and mitigate certain issues related to such systems (Malvey, Rao, & Arumugam, 2019), (Anissimov & Roberts, 2011).

1.2.2. Topical and Transdermal Drug Delivery

It is important to highlight that utilising the skin for drug delivery purposes has been used for many years. Galen's classical formulation of cold cream, which is still in use today with some modifications, is evidence of this aged practice (Hadgraft & Lane, 2005). Although, TDDS pre-date recorded literature, recent advancements in biophysical techniques have paved the way for more appreciation in terms of the therapeutic usefulness of this route. More recently, researchers have been able to navigate and shape understanding in this field, owing to the commercialisation of several transdermal delivery systems. However, a mechanistic understanding of this route remains a concern. Scientists suggest a more detailed understanding still needs to be achieved in terms of the skin structure, which will then help when trying to develop an alternative to skin that can mimic how it functions.

1.2.3. Research Statement

Primarily, this research focuses on developing and modifying a synthetic polymeric membrane that can be used for transdermal drug development and research purposes in place of skin (both human and animal) for the prediction of skin permeation. It is, therefore, necessary to consider the structure and mechanistic properties of skin, particularly human skin, and understand how materials are transported through skin, so as to have an informed position and background as to what type of alternative is actually needed to address the many challenges associated with the use of skin.

As part of the initial research, concerted efforts were made to identify a promising skin mimic membrane, which was then modified in an attempt to create a better fit for permeation analysis, thus achieving the production of a suitable alternative to skin.

1.2.4. Structure and Mechanism of Permeation Through the Skin

The skin is the largest organ of the human body (Ghafourian, Samaras, Brooks, & Riviere, 2010), it consists of complex tissues, each performing a distinct function based on its cell type. It defines the boundary between the human body and its surrounding, thus, allowing selective movement of material in and out of the body, and at what rate (K. W. Ng & Lau, 2015). This is the primary function of skin (Menon, 2002) along with maintenance of constant internal conditions. The skin can be broadly divided into three different layers; the epidermis, dermis and the hypodermis or subcutaneous tissue (Shahzad, Louw, Gerber, & Du Plessis, 2015). The epidermis represents the outermost layer of the skin which can further be subdivided histologically into five distinct sub-layers, namely: stratum corneum (horny layer), stratum granulosum (granular layer), stratum spinosum (prickle cell layer), and stratum basale (also called the stratum germinativum). The stratum basale and stratum spinosum are sometimes collectively referred to as the Malpighian layer (K. W. Ng & Lau, 2015).

The stratified epidermis is mainly made up of keratinocyte cells and these cells synthesise the protein called keratin. This protein is in a constant state of growth and transition from which the division of these distinct sub-layers emerge. The growth and transition are such that it starts from the deeper sublayer to the superficial stratum corneum and each sub-layer typically represents a certain stage of keratin maturation (Malvey et al., 2019). Stratum basale which forms the innermost layer, is attached to the basement by a protein bridge called desmosomes, this protein also connects sub-layers of keratinocytes which are in a constant state of division. In the stratum basale, the keratinocytes are able to grow and differentiate continuously, pushing the older cells up towards the outer layer (Tobin, 2006). Stratum basale also host melanocytes,

which produce melanin, the pigment responsible for pigmentation and provides a shielding effect from ultraviolet radiation, hence chronic exposure to light increases the melanocyte ratio when compared to keratinocytes (Malvey et al., 2019).

As the basal cells continue to grow and mature, they form the stratum spinosum consisting of cells with many sides, the keratinocytes at this division, when viewed at a microscopic level form spin-like projections owing to the name 'spinosum' (L. A. Cole & Kramer, 2015). They play an important aspect in immune reactions of the skin. As opposed to the prickled keratinocytes in the stratum spinosum, the stratum granulosum which is the next sub-layer of the epidermis consists of flattened keratinocytes with granules from which a hydrophobic lipid is released. This lipid helps protect the body from loss of excessive fluid, while also contributing to guarding the entry of foreign substances into the body. At this stage, the cells also lose their nuclei and cytoplasm forming granules that contributes to their water retention capacity. These lower three sub-layers within the epidermis collectively are referred to as the viable epidermis, because 95 % of the keratinocytes are viable (Tobin, 2006).

At this stage of the keratinocyte development, the cells become enucleated, flattened and lack cellular organelles, forming the superficial layer known as the stratum corneum which serves as the principal sub-layer that mainly provides the barrier property of skin (Choe, Lademann, & Darvin, 2016). This barrier property provided by the stratum corneum makes it the most interesting layer to study when considering the overall barrier property of the skin.

The stratum corneum and stratum lucidum (the latter only present in thick skin of the body, such as soles of the feet and palms of the hand) form the outermost layers of skin. Skin owes its selective absorption and barrier functions mainly to the stratum corneum (the primary barrier). This function is possible as a consequence of the unique composition of the stratum corneum and can be envisaged from a theoretical point of view as a 'bricks and mortar' structure, comprising of the keratinocytes (corneocytes) 'bricks' and the intracellular 'lipids',

which are both key determinants of skin permeability and, in turn, relates to drug permeation through the skin. It is this structure-activity relationship that permits prediction of drug permeation (K. W. Ng & Lau, 2015).

It is important to note that detailed structure of the skin is still circumstantial and remains an interesting area of research for scientists (Lundborg et al., 2018), therefore, to fully understand TDDS, it is paramount to focus more on the main theories that try to explain the skin structure more specifically, as it relates to its barrier functions.

Advances in TDDS are largely attributed to understanding the mechanism behind skin permeation. Studies in this field suggests a chemical defence property is exhibited by the skin. Efforts, therefore, were channelled towards understanding, identifying and studying the stratum corneum as this is known to be responsible for this barrier or defence property.

Routes of drug delivery via the skin surface have been debated over the years, and it has not yet been unequivocally resolved (Hadgraft & Lane, 2005). However, this discussion will focus on the plethora of evidence that supports some of the more popular claims. It is widely accepted that permeation of drugs occurs via the intact area of the stratum corneum and that the skin appendages or trans-appendageal pathways, only provide negligible amounts of permeable substance compared to the overall permeation profile of any xenobiotic permeating the skin at a steady state. It is argued under this context that the appendageal pathways grossly occupy an average of 0.1 % of the total skin surface (Lane, 2013), and a fraction of these pathways are sometimes blocked by dried sebum or have to compete with outflow of sebum from hair follicles (Moss, Gullick, & Wilkinson, 2016). Even though xenobiotics (especially water soluble or ionic compounds) might permeate this route faster compared to the intact area of the stratum corneum, it is believed that the relative contribution is still negligible. Furthermore, there have been various studies conducted in the 1960's and 1970's that involved the use of

spectroscopic techniques and radiolabelled compounds to determine the actual route of drug transport via the skin. Attenuated total reflectance (ATR) infrared spectroscopy for instance, was used to quantify drug components on the skin surface following topical application over a specified period of time. Skin conductivity and impedance measurement on skin was also used to research and described the structure of the skin, and consequently transport of material via the skin. Transmission electron spectroscopy (TEM) was also used to describe the ultra-layered structure of skin. All these findings pointed at the intact part of the stratum corneum as the main route for drug delivery. The mechanism and potential of using an intact part of the stratum corneum for drug delivery was further exemplified by transdermal drug delivery of nitroglycerin to the myocardium for the treatment of *Angina pectoris* in 1989. It was reported in the paper, that for any drug topically administered, it has to be distributed first into the papillary layer following skin permeation, through to the capillary network, before distribution to target tissues with the help of blood capillaries embedded within inner layers of the skin, as illustrated in Figure 1.1 (Chien, Siddiqui, Shi, Lelawongs, & Liu, 1989).

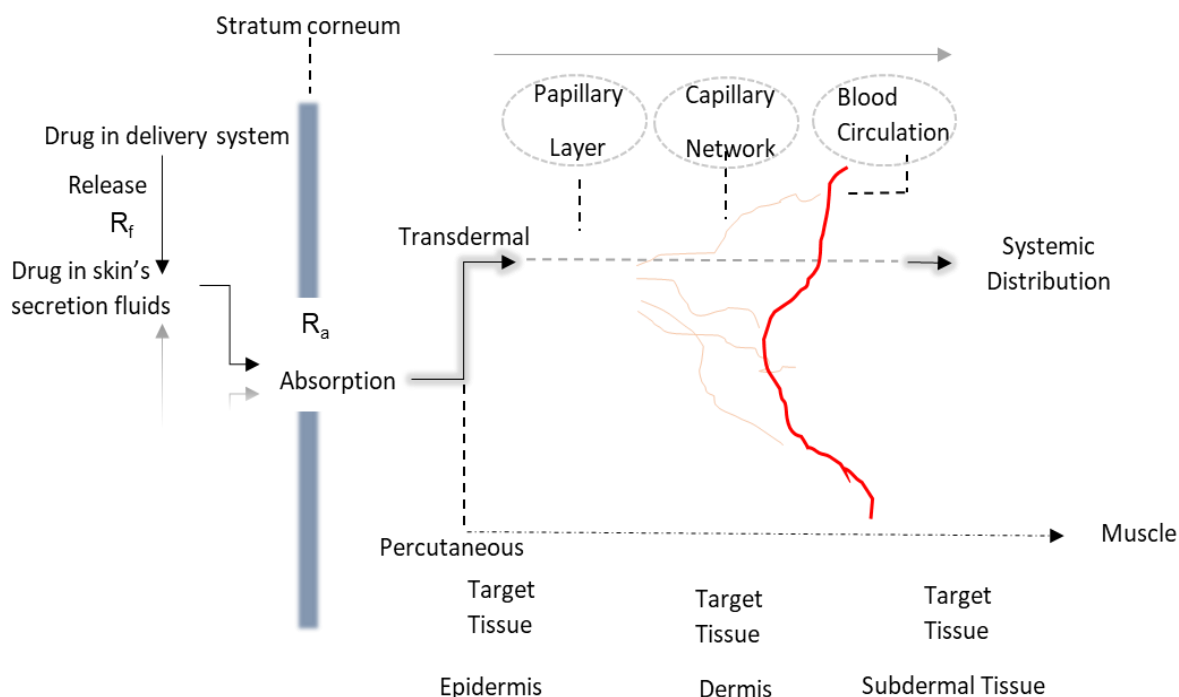


Figure 1. 1 Systemic illustration of transport route across layers of the skin

This finding and many other findings alike, contributed to understanding how transport of materials via the skin occurs, thus paving the way for rapid development of TDDS in the 1980's. However, within the intact part of the stratum corneum, there is a plethora of evidence that suggests a well-defined hetero-type composition exists between corneocytes and an intercellular lipid region. This region was described as a structurally complex and presumably lipid rich region which provides a continuous pathway through the skin. If this is the case, then scientists suggest that stacking of the corneocytes becomes an area of interest when trying to predict the mechanism of permeation, since their composite materials are distinct and may react differently to xenobiotics. A structure was then proposed in 1975 by Michael *et al* which tries to propose a layered structure of the skin (Michaels, Chandrasekaran, & Shaw, 1975) with a semblance of bricks and mortar wall. This arrangement that exemplifies a heterogeneous skin surface is illustrated in Figure 1.2.

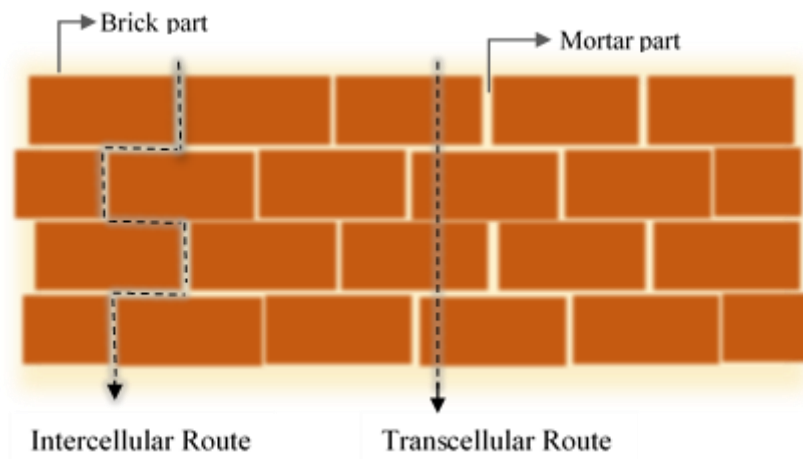


Figure 1. 2 Schematic representation of the ‘Bricks and mortar’ model

The ‘bricks and mortar’ model of the stratum corneum allows a conceptualisation of how the skin works. The corneocytes (bricks), which are largely agreed as terminally differentiated keratinocytes are comprised mainly of keratin microfibers, and are protected externally by a cornified cell envelop, held together by desmosomes protein (Hoath, 2014a) (Feingold & Elias, 2014). The intercellular lamellar (mortar) lipid membrane comprises of three different lipid components, found in approximately a 3:1:1 relative ratio, based on the stratum corneum - lipid composition (% by weight) which comprises of ceramide (50 %), free fatty acid (10-15 %) and cholesterol (25 %) (Feingold & Elias, 2014). It is important to note that these lipids, are produced from lamellar bodies within the stratum granulosum, some of which (upon entry into the stratum corneum, after extrusion) are converted enzymatically to ceramides (Del Rosso & Levin, 2011).

Ceramide plays a vital role in the water retention capacity of the stratum corneum, this is evidenced by the fact that any change in the percentage composition of the stratum corneum can result in skin diseases such as psoriasis and eczema. (Imokawa, Akasaki, Hattori, & Yoshizuka, 1986). Some of these diseases play an essential role in understanding barrier disruption, relationships and interactions between various lipid classes hence helps in a better

understanding of membrane permeability. Unsaturated free fatty acid has been suggested also to contribute in disrupting the barrier structure of the stratum corneum (Meckfessel & Brandt, 2014), and is known to exist as sebaceous contamination (Harding, 2004). Linoleic and oleic acid are believed to be the only two members of the fatty acid group that are not bound and are unsaturated. Linoleic acid particularly, plays a vital role in controlling the loss of trans epidermal water (Prottey, 1976). Cholesterol provides the needed fluidicity to the stratum corneum at room temperature (Zbytovská et al., 2008), which prevents the skin from being brittle. Additionally, cholesterol sulphate (which constitutes about 2-5 % of the stratum corneum lipids), helps in the formation of the lipid lamellae and serves as a laminating agent which in turn gives the stacked parallel nature of the stratum corneum, thus, stabilising it (Sato, Nakanishi, Denda, Nomura, & Koyama, 1997). It is on this basis, that the majority of mechanisms for drug permeation via the skin are built. Recently, Hoath *et al* (Hoath, 2014b) also reported the intercellular lipid region as the only continuous route through the stratum corneum. In other words, the intercellular route is predominantly packed with lipophilic compounds, and substances can only pass through them via physicochemical interaction in a description shown in Figure 1.3.

Dermis is the second layer of human skin, found underneath the epidermis. It comprises of two distinct layers namely; papillary layer (superficial layer) (Figure 1.1) and the reticular or capillary layer (Lai-Cheong & McGrath, 2017). The papillary layer is thinner and has contact with the epidermis through its loose connective tissue (Yousef, Alhadjj, & Sharma, 2019). It has an extensive network of blood vessels which helps in providing needed nutrients that are utilised in producing keratinocyte cells in the epidermis. It also helps in removing excess waste (cellular waste) from the skin which otherwise will be harmful if left to accumulate. The result of these activities generates heat which helps provide maintenance of internal temperature. The reticular layer on the other hand, is mainly home to collagen and elastin and are primarily

responsible for providing strength and elasticity respectively. Hence, perturbation in molecular organisation of this protein network results in a compromise of the skins mechanical properties leading to a reduced resilience and elasticity (M. A. Cole, Quan, Voorhees, & Fisher, 2018). These nerves are also responsible for transport of xenobiotics into the body system via blood streams.

The hypodermis (often referred to as subcutaneous tissue) is adipose tissue. It is the deepest layer of the skin after the dermis. It contains fat deposits, and due to the well-integrated nature with the dermis, it contains hair follicles, skin appendages, blood vessels and sensory neurons (Yousef et al., 2019).

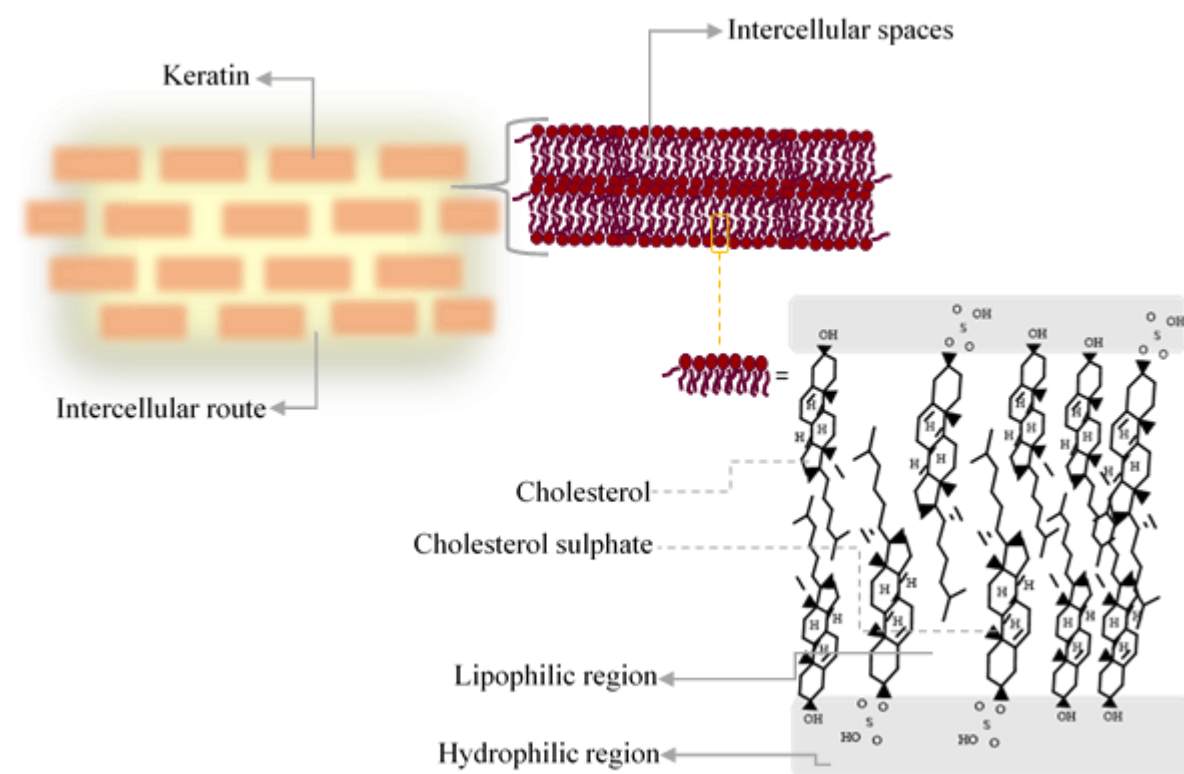


Figure 1. 3 Schematic diagram of potential drug permeation pathways

1.2.5. Permeation theory and measurements

Quantitative measurements of materials across the skin can never be over-emphasised and are of paramount importance to scientists concerned with TDDS. Principles that govern this transport of materials via the skin such as permeation rate after attaining a steady-state, breakthrough time and cumulative drug release over a therapeutic window are equally important for mechanistic understanding of the process. These parameters are achieved and monitored by permeation analysis processes, which ultimately determines the suitability of a drug for TDD. The principle behind permeation of drugs when applied to the skin, can best be described by Fick's first law of diffusion. The law states that 'flux in a certain direction is directly proportional to the concentration gradient' (Equation 1.1), this is however, under the assumption of a steady state (Comyn, 1985).

$$J = D \frac{dC}{dx} \quad \text{Equation 1.1}$$

Where J is diffusion flux (or sometimes referred to as the permeant flux), reported in units of $\text{mol m}^{-2} \text{s}^{-1}$, or in the case of lower concentration, it can be units of $\mu\text{g cm}^{-2} \text{s}^{-1}$. D is the diffusion coefficient in units of $\text{m}^2 \text{s}^{-1}$ or $\text{cm}^2 \text{s}^{-1}$, C is the concentration of the permeant in mol cm^{-3} or in $\mu\text{g cm}^{-3}$ as the case might be, and x is the position, or spatial dimension of the membrane surface thus represented in units of m or cm.

The *in vitro* analytical permeation process is such that it comprises of a donor phase and receptor phase, where a pre-heated membrane is carefully mounted between these two phases. Often in analysis a saturated solution is mounted on the membrane surface within the donor compartment. All openings within the donor top and the receptor bottom are occluded to ensure

a stable temperature and prevent the loss of solvent through evaporation (S.-F. Ng, J. Rouse, D. Sanderson, & G. Eccleston, 2010a).

During the permeation process it is important to maintain sink conditions, whereby the receptor compartment would have zero-drug concentration. This condition is challenging to achieve when using static cells (S.-F. Ng, Rouse, Sanderson, Meidan, & Eccleston, 2010), and this led to the development of a system known as the flow-through system, which takes into consideration variables such as temperature, stirring, and flow rate. Temperature is an important property in permeation studies, it immensely affects passive diffusion of drugs, and the ideal temperature within the membrane matrix is expected to be maintained at $32\text{ }^{\circ}\text{C} \pm 1\text{ }^{\circ}\text{C}$. It has been reported that an increase in temperature affects permeation profiles. For example, approximately $8\text{ }^{\circ}\text{C}$ increase in temperature alters the permeation of caffeine, methyl paraben and butyl paraben by more than two-fold (F. Akomeah, Nazir, Martin, & Brown, 2004).

Generally, two distinct approaches are employed in drug permeation analysis namely, a finite and infinite dose approach. The basic difference between the two approaches is such that the former requires a certain drug concentration that can be changed and varied according to suitability of the intended experiments, while the latter employs a constant concentration usually from the saturated form of the drug in question. Another important factor to consider is a constant agitation of the fluid in the receptor compartment using a magnetic stirrer at an optimum speed, especially when experiments last for many hours. Stirring should be such that the speed is not too fast to create a vortex, which may disturb the flow rate, leading to the formation of bubbles that can affect the permeation profile.

If a permeable compound is added to the donor chamber then a steady-state diffusion from the donor phase, across the membrane to the receptor phase, is attained, i.e. movement of

molecules from a region of higher concentration to a region of lower concentration through a semi-permeable membrane will occur. Hence, the concentration gradient across the membrane would be constant or linear. Thus, Equation 1.1 can be re-written as:

$$J_{ss} = D \frac{[C^o - C^h]}{h} \quad \text{Equation 1.2}$$

Where J_{ss} is the steady state flux, C^o is the initial concentration of permeant on the surface of the membrane, (the donor compartment concentration) and C^h is the concentration of permeant within the membrane at a certain position, h , i.e. the receiver compartment. These permeant concentrations are difficult to ascertain in practical terms, hence a partition coefficient that describes the partitioning between the permeant and the aqueous solution is introduced for convenience, therefore, concentrations of the aqueous solution in the donor and receiver compartments are obtained practically (Avdeef, 2012). Equation 1.2 can therefore be written as:

$$J_{ss} = DK \frac{[C^D - C^R]}{h} \quad \text{Equation 1.3}$$

Where K is the introduced membrane partition co-efficient, C^D the donor compartment aqueous solution concentration and C^R the receiver compartment aqueous solution concentration.

Equation 1.3 can be simplified further considering the fact that the diffusion coefficient (D) is still practically difficult to ascertain, hence, the kinetic parameter D , the thermodynamic and the membrane thickness parameters K and h respectively, can be combined to give the permeability coefficient parameter K_p . The equation can then be written as:

$$J_{ss} = K_p (C^D - C^R) \quad \text{Equation 1.4}$$

Furthermore, the concentration of the receptor compartment is effectively zero, in comparison with the donor compartment. This is practically obtainable if the permeant concentration in the receptor compartment does not exceed 10 % of the donor compartment (Moss et al., 2016). Hence, Equation 1.4 becomes simplified to:

$$J_{ss} = K_p C^D \quad \text{Equation 1.5}$$

Having met the conditions previously highlighted, the permeability coefficient K_p becomes experimentally obtainable and provides useful information regarding permeation in topical and transdermal drug formulations. The convenience in comparing these experimentally determined datasets and existing skin data can be seen further in Flynn's work, where a significant amount of data has been published using this approach (Flynn, 1990). More recently, a larger dataset has been collected using this approach which includes (but not limited to) the previous dataset of 283 compounds (Baba, Takahara, & Mamitsuka, 2015).

It is quite important at this juncture to mention some of the specifications for *in vitro* permeation studies according to the European Medicines Agency Guideline (EMA). It stipulates that, *in vitro* permeation analysis is meant to evaluate the permeation of drugs across the skin and is not necessarily expected to establish a correlation to that of *in vivo* permeation.

Permeation studies allow the use of artificial or synthetic membranes, as well as human skin or skin from animals such as rodents, snakes, pigs and other animals. It is expected that when using synthetic membrane, information such as membrane thickness, integrity of the membrane and at least six repeatable data sets should be provided. The solvent used should be an aqueous buffer for water soluble drugs. However, hydroalcoholic media or the use of solubility enhancers are allowed for poorly water-soluble drugs.

1.2.3.1 Properties of Penetrants

Having understood to a large extent theory about how the skin works, and the principle that tries to explain how permeation of drugs across the skin occurs, another interesting area for researchers is physicochemical properties of the permeant when formulating topical drugs. From Fick's law, it became apparent that diffusion coefficient (D) and permeation co-efficient (K) need to be appropriately considered, as each factor can influence the overall effect of permeation, thus can assist in the design of an appropriate drug candidate. It is also vital to establish the main factors that affect skin permeability which are size and shape of the permeant, superficial charges, lipophilicity, penetration enhancers, and physical state of the skin (Verma, Verma, Blume, & Fahr, 2003), to be able to mitigate them and understand how best to predict permeation.

The physical parameter K , that represents partition co-efficient in this instance the stratum corneum, describes the relative concentration of the permeate present in the stratum corneum and in the vehicle, at equilibrium. As such, the rate determining state depends largely on the solubility of the penetrant in each phase. Since the stratum corneum is mainly a lipophilic barrier, molecules with high log P (octanol-water partition co-efficient) values should be able to absorb better, thus permeate faster. Yet, compounds with a balanced partition co-efficient of approximately one (1), tend to permeate the skin better, compared to compounds with a higher value of log P . Examples of such compounds with moderate log P values are nicotine, estrogen, scopolamine and nitroglycerin. Even with this empirical data, recent compounds specifically designed for TDDS still tend to have lipophilic values that are comparatively low (Y. Chen, Quan, Liu, Wang, & Fang, 2014).

Most topically formulated compounds rely on the theory that the lipid domains between corneocytes provides the only continuous route when transcending through the skin hence,

lipophilic compounds have greater tendencies to permeate skin. Practical science still somewhat suggests that it is not enough to have an affinity to the lipophilic route, but also tendencies of partitioning out of this route should also be considered. In essence, the lipophilic pathway should serve as a route rather than a rate limiting step. In relation to this, Moss *et al* in 2016 was able to publish a large dataset of compounds that explains how compounds with high lipophilic values ($\log P > 3$) exhibit poor clearance from the viable tissues, and suggests that compounds with $\log P$ values of $1 < \log P < 3$, are the most suitable candidates for topical delivery, when considering $\log P$ values (Moss et al., 2016). This is to say drugs with $\log P$ values > 3 , would rather stay longer on the lipophilic pathways instead of permeating easily via this route.

However, following the general aqueous state topical compounds are formulated in, it becomes necessary for compounds to show some hydrophilic favourability (Malvey et al., 2019) and when comparing molecular size, solubility and melting points with regards to TDDS, it is considered that an inverse relationship exists between transdermal flux and molecular weight. Therefore, since there is fair comparison between molecular weight and size, compounds having a smaller molecular size make better candidates. In this case, lipophilic compounds are often not favoured given their relatively large molecular size. Moreover, the diffusion coefficient is heavily influenced by molecular size and temperature (F. Akomeah et al., 2004; Shahzad et al., 2015) with the diffusion coefficient directly related to an increase in temperature and inversely proportional to hydrodynamic radius. This forms the basis of a general ceiling of 500 Da for compounds considered as transdermal drug candidates. In addition, organic molecules tend to have low relative aqueous solubility at standard temperatures and pressures, hence lipophilic solutions also prevail in terms of TDDS, when strictly considering these factors.

The balance of opinions supported by practical data further points to the necessity of having an alternate surrogate skin sample which can mimic the activity of the skin. Furthermore, it could provide another perspective for researchers to further understand how the skin works, consequently helping to harness the full potential skin has to offer as a route for drug delivery.

1.2.6. Human tissue

The use of human skin equivalent models (*ex-vivo*) obtained from cadavers or cosmetic surgery, when used for percutaneous absorption studies, are often considered as the gold standard (Elnaggar, El-Massik, & Abdallah, 2011) and a potentially viable alternative to skin. However, the skin as a living entity itself is not fully represented when used in this form. Furthermore, inconsistencies in uniformity and reproducibility in skin-based membrane experiments have been suggested as issues related with such systems (Batheja, Song, Wertz, & Michniak-Kohn, 2009). In addition, limited availability of these samples often hinders their widespread usage. Even when samples are available, de-freezing and disinfection treatment can be problematic too (Abd et al., 2016). Scientists as far back as the 1980's proposed that not only biological tissues with viable cells can effectively predict permeation (Bronaugh, Stewart, Congdon, & Giles Jr, 1982). Development of biophysical techniques have also helped in amplifying this idea. It is now established and universally accepted that other forms of membranes can effectively predict and mimic permeation of the skin without necessarily having viable cells.

However, in trying to address availability concerns posed by human skin, scientists have tried to create skin analogues often referred to as the 'living skin equivalent (LSE)' model. This model comprises of full thickness skin (FTS), split thickness skin (STS), isolated stratum corneum (ISC) and heat separated epidermis (HtSE), which have all proven to be very effective

in histological studies. In measurement and prediction of permeation analysis, these membranes fall short, and considering their relative cost makes them a challenging alternative.

It is important to note that permeants diffuse the skin via three different routes; the skin appendages (hair follicles and sweat glands), the intercellular lipid lamellar within the stratum corneum and via keratin bundles, and these routes collectively gives the net amount of drugs permeating the skin. Any model that tends to ignore any of these routes, outrightly negates its potential of making a viable alternative. In the LSE model, full thickness skin (FTS), has partially separated stratum corneum which gives relatively low permeability results, whereas the split thickness skin (STS) lacks appendages such as hair follicles and sweat glands (Godin & Touitou, 2007). Other options such as isolated stratum corneum (ISC) and heat separated epidermis (HtSE) are too fragile to handle and require an underlying support (F. K. Akomeah, Martin, & Brown, 2007). Thus, it has been concluded that models such as the LSE model have limited use in *in vitro* permeation studies (Schmook, Meingassner, & Billich, 2001) and (Roy, Fujiki, & Fleitman, 1993).

1.2.7. Animal Tissue

Another alternative considered is the use of animals, based on their far wider availability compared with human tissue. These animals are used in the development of drugs, determination of toxicity for compounds destined to be used by humans, and this practice can be traced as far back as 500 BC.

Most frequently used in TDDS studies are the excised skin from mice, albino rats, pigs, guinea pigs and rabbits (Balakrishnan et al., 2009), (Özgüney et al., 2006), (Qvist, Hoeck, Kreilgaard, Madsen, & Frokjaer, 2000), (Dalton, Graham, & Jenner, 2015) and (Nicoli, Penna, Padula, Colombo, & Santi, 2006). This is largely a general phenomenon, as a similar profile is also seen in the UK (Figure 1.4), according to an article report titled ‘Animal research in the UK’.

It is reported that tissues from snakes and fish are also used, but these types of skin samples suffer from a relative shortage in availability (Lee, Conradi, & Shanmugasundaram, 2010).

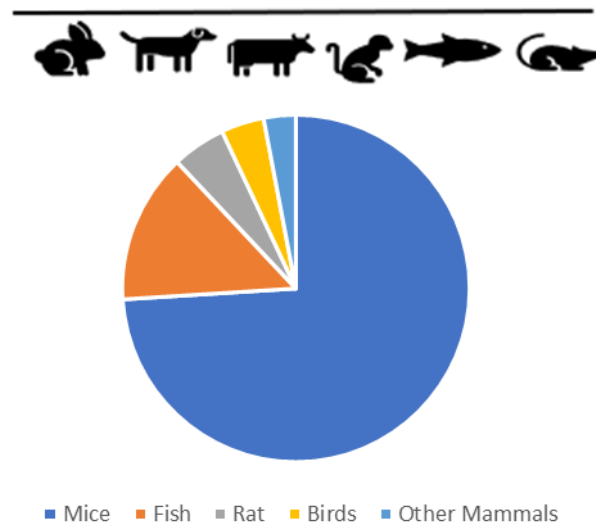


Figure 1. 4 Percentage of animals used in the United Kingdom for scientific experiments (3.4 million) in 2019.

A vital point of arguments often presented in supporting the use of animals for scientific experiments is the area of biomedical research. It is argued that viable cells in the animals helps researchers study numerous diseases. The common practice involves inducing these animals with artificial diseases and conducting experiments on them. This then allows researchers to test a new drug intended to cure the induced disease (Barnard & Kaufman, 1997; Botting & Morrison, 1997). However, often times there is one observation per animal, which increases the number of animals used for a given set of experiments. During the experiments, the animals are often restrained which makes it difficult for animals to escape the pain. Vivisection is sometimes employed to induce or infect the animals with desired diseases. Every known human disease has been tested on animals and even ‘predictive’ ones are being tried on animals, with the aim of quantifying, curing, or discovering a treatment. This is how the animal testing model works in the context of drug delivery (Carstens & Moberg, 2000; Hutson, 1994).

Invasive procedures such as traumatic injuries, burns, social deprivation, force-feeding, creating an artificial heart-attack, implanting electrodes in the body to induce brain traumas, motion sickness, irregular heart rhythms, migraines, and other environmental manipulations to cause distress and other more severe injuries including spinal cord injury and paralysis are all part of this practice (Bhanu Prasad, 2016a; Mukerjee, 1997).

Variation in the biology of animals used for scientific experiments can affect the outcome of results, even within animals of the same species. Animals of different development stages, ages and sex, can result in immense differences in the outcome of a result. More specifically, in the prediction of percutaneous drug delivery, the use of animal tissue results in over-estimation of permeability data (Lu, Lee, & Rao, 1992), and difficulty in the preparation set-up. Mice skin for instance is thinner than human skin, and most of the animals used have more hair follicles than humans, thereby increasing the issues for percutaneous predictions (Geusens et al., 2011). It is reported that for skin permeation experiments there is an increase of 3-5 folds in permeation values when using rabbit skin as the membrane (Chowhan & Pritchard, 1978), about 11 folds with rat skin (Van Ravenzwaay & Leibold, 2004), and close to 100 folds with nude mouse (Lu et al., 1992), making it increasingly difficult to compare the data with that of humans.

In addition, over the last decade, there has been an increase in the laws and regulations regarding the use of animal testing. Notable amongst the laws are the Registration, Evaluation, Authorisation and Restriction of Chemicals (REACH), which was signed on the 1st of June 2007, which promotes the use of alternative methods in data analysis and prediction such as using quantitative structure-activity relationship models (QSARs). The law also requires manufacturers of certain materials to submit all dossiers with relevant data including skin corrosion, dermal toxicity and other factors related to health and safety. The European

Chemical Agency (ECHA) and the Health and Safety Executive (HSE) have all restricted and addressed various ethical and safety issues about the use of animal models. There is also a global debate in using animals for cosmetic testing (Y. Wang, Zhao, & Song, 2020). For example, there is a complete ban for animal-cosmeceutical practices in places such as the EU (cosmetic directive 76/768/EEC), i.e. all of these factors pose a serious constraint in the use of animal testing (Sreedhar, Manjula, Pise, Pise, & Ligade, 2020).

The use of animals for scientific purposes often boils down to an ethical question and the question of whether it works. It is largely agreed that without animal testing most of the successful drugs and advancements we have seen medically wouldn't have been possible. However, progressive scientists argue that there is the need for a rise in efforts from a data quality and ethical perspective to find alternative models, and minimise the many problems associated with this aged practice.

1.2.8. Alternative models

Alternatives to human and animal testing are largely based on biochemical assays, *in-vitro* analysis, and computational models which are based on algorithms. These alternatives are technically more robust, sophisticated, easily maintained and controlled, more so than the classical methods of human and animal tests. In addition, recent research is increasingly focusing on developing models that can mimic the living system, which are less expensive and experimentally efficient and sustainable. Moreover, regulators and generics are fast moving towards accepting some of these *in-vitro* techniques. Recently, the Organisation for Economic co-operation and Development (OECD) has accepted cell culture models for their usage in *ex-vivo* purposes in place of laboratory animals (Garcia et al., 2018).

Other remarkable milestones achieved with these alternate methods includes the development of human brain cells (microbrain) which can be used to study brain tumours, as well as the development of artificial skin (Epiderm) and bone marrow (Bhanu Prasad, 2016b).

Institutes including inter-disciplinary researchers are currently working on a distinct field referred to as ‘lab on chip’. This type of research is primarily aimed at recapitulating the physiological functions of living organs, such as lungs, hearts, skin and intestine. These organs on a chip (Figure 1.5) could one day mimic functions of traditional organs. Because these devices are made up of translucent flexible polymers that contain hollow microfluidic channels lined by living human cells, they provide an avenue to observe the inner workings of human organs.

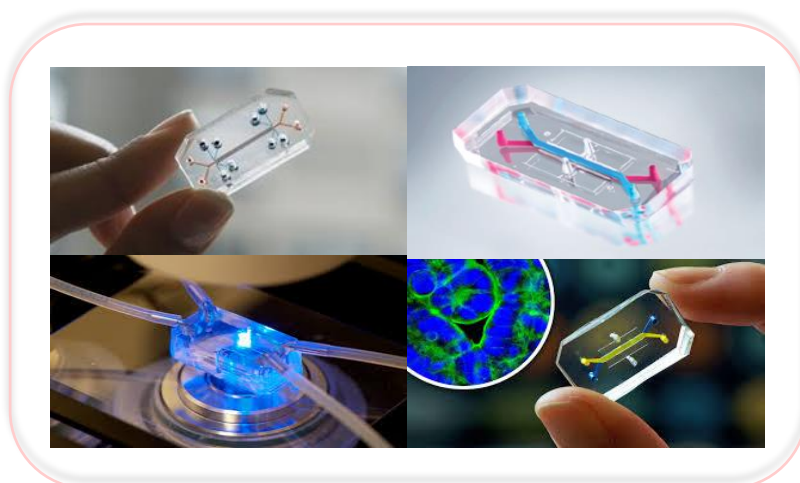


Figure 1. 5 An illustration of some developed ‘Organ on a chip ‘systems.

In general, given the development of biophysical techniques, it is no longer acceptable to use animals for purposes of studying what happens within the body. Advanced X-rays, MRI and CAT scans all allow researchers to look inside the human body in real time (Bhanu Prasad, 2016a).

This progressive route is akin to the overall principle of the study employed in this work.

1.2.9. Cell culture

Success stories have been recorded regarding acceptance of cell culture models in place of laboratory animals as it relates to this study. Notable amongst these models are reconstructed human epidermis (RHE) and some living skin equivalents (LSEs). These models try to mimic the human skin structure, for example, RHE consists of a three-dimensional framework, which is grown from keratinocytes and possesses stratum corneum equivalent on its surface.

These models have proven promising especially in histological studies and related research areas (Hausmann et al., 2019). Despite promising features of these models, barrier functions and by extension prediction of percutaneous absorption crucial to this study, have been found to have limitations. For instance, these skin equivalent models over-estimated permeation when compared with isolated human tissue (Batheja et al., 2009). Similar findings were reported by (Küchler, Strüver, Friess, & toxicology, 2013), who attributed these limitations to immaturity of the stratum corneum. Poor reproducibility, its delicate nature, un-ease of handling, and high cost has contributed to limiting its widespread use and acceptance, especially for use in percutaneous predictions.

1.2.10. QSPR

Another major alternative to the use of skin samples and *in vivo* analysis in research is computer modelling. This area of research has also opened new areas, with the advent of neural network modelling and non-invasive imaging. In some cases, more indirectly, the internet has allowed the reduction of duplicate animal testing via the pooling of data.

Understanding the relationships between physicochemical properties of permeant and their extent of permeation when used as active pharmaceutical ingredients (APIs) is an area of interest for researchers that deals with study related to permeation analysis. This has led to

extensive work in related areas. Derived mathematical relationships have become an important aspect in this field. Pioneering work by Potts and Guy (R.O. Potts & P.R. Guy, 1992), has been described as one of the most widely accepted models. Using data from Flynn's work (Flynn, 1990), the authors were able to relate the $\log K_{o/w}$ partition co-efficient, permeability co-efficient K_p , and molecular weight of different drugs. Although the data used was from Flynn's dataset, the model has stood the test of time, as more recent QSPR models also use the same empirical data and principle of steady-state transport across excised human epidermis, and as such their main output theme remains the prediction of a human skin permeability co-efficient K_p (Pecoraro et al., 2019).

Potts and Guy built their model with the assumption that, despite the stratum corneum being the rate limiting barrier of the skin, it is considered to have highly organised lipids, hence, diffusion can occur by sink conditions, which correlates to the steady state condition described by Fick's law. Employing a logarithmic form of Fick's equation, and assuming an exponential relationship between molecular weight and diffusivity (free-volume theory) (Potts & Guy, 1992) provided the following model:

$$\text{Log } K_p = -6.3 + 0.71 \log K_{OW} - 0.0061 \text{ MW} \quad \text{Equation 1.6}$$

The work was based on using the 'bricks and mortar' concept, as the appendageal pathway was neglected. This model explains the relationship between highly hydrophilic compounds and their low molecular weights, which translates to their low diffusivity via the lipid lamellae. The simplicity of this model coupled with its correlation value ($R^2 = 0.86$), in relation to the approximately 90 compounds it was developed upon, makes it the most frequent model cited of its kind (Mitragotri et al., 2011).

It is clear that the Potts and Guy model neglected the appendageal route, whereas work by Mitragotri proposed four different routes via the stratum corneum. These routes are diffusion through the lipid lamellae, along the lipid lamellae, through defects in the stratum corneum and diffusion via the appendages. The latter of which being the most relevant route, (which was considered not relevant in the Potts and Guy model) and also divided properties of the permeant into low and high molecular weight, hydrophobic and hydrophilic drugs (Mitragotri et al., 2011) and (Mitragotri, 2003).

Consequently, Mitragotri was able to devise the following model:

$$\text{Log } K_p = -2.39 + 0.74 \log K_{ow} - 0.0091 \text{ MW} \quad \text{Equation 1.7}$$

This stark difference between the Potts and Guy model alongside Mitragotri's model, presents an interesting challenge in the QSPR approach. Moss *et al* observed in their findings while testing the Potts and Guy model that steroids are frequent outliers. They further suggest that data used in the study was extracted from a single data source, more challenging is how it displays poor compatibility with recent data. The authors proceeded in creating their model (n =116 compounds), incorporating steroidal compounds and other therapeutic classes (Moss et al., 2016).

In theory, it appears that predictive models could address all the problems that relate to ethical issues, labour-intensiveness, cost and perhaps time-consuming problems associated with current systems. However, the lack of a universal model that can take into consideration all of the potential routes of drug permeation via the skin, stands out to be a limiting factor for all predictive models presented to date. Moreover, variability in changes any model is built upon could render the model inefficient. More puzzling is the complexities for newly developed drugs, hence some of these models have evidently failed to provide an effective tool that will capture new drugs, and thus creating the need to rely on *in vivo* analysis.

1.2.12. Poly(dimethylsiloxane)

Desirable properties of poly(dimethylsiloxane) (PDMS), as a silicon polymeric membrane, such as simplicity in usage, increased obtainability, susceptibility to surface modification and reduced cost (S.-F. Ng et al., 2012) has led to the choice of PDMS for this study. Additionally, PDMS addresses most of the major challenges encountered with the use of human or animal skin in permeation analysis, including uniformity, stability, ease of handling, sufficiency for large scale studies, ethical and legal issues. In addition, certain properties PDMS membrane offers makes it even more attractive for utilisation, particularly as a substitute for biological tissues in permeation analysis. While the advantages are clear, it is imperative to highlight some of the challenges (and numerous modifications recently developed to overcome such challenges) encountered in tailor-fitting the membrane to the desired outcome.

As far back as the early 1940's, polyorganosiloxanes, a family of compounds to which PDMS belongs, have been produced on an industrial scale (via Muller–Rochow direct synthesis) (Pouget et al., 2010). The overall estimation of silicon based materials available as far back as 2002 was estimated to be over 2 million tonnes, and one of the major reasons for the high production and demand of silicon based polymers is a consequence of their un-paralleled thermal stability and flexibility properties, compared with other polymer membranes (Owen & Dvornic, 2012; Pouget et al., 2010). Most of these properties are largely attributed to the Si-O-Si backbone of these polymers. PDMS has a Si-O-Si bond angle of 140° (Hurd, 1946) exhibiting a certain orientation in space and has a glass transition temperature of -123°C (Tan & Rodrigue, 2019) due to its molecular backbone orientation, which allows a level of torsional motion. It also has low intermolecular forces, and therefore a large molar volume of $75.5\text{ cm}^3\text{mol}^{-1}$. The low cohesion energy, poor solubility and surface energy can all be attributed to this low intermolecular force. However, the value of the Si-O-Si bond is high (110 kCal mol^{-1}), compared with Si-C (76 kCal mol^{-1}), C-C ($82.6\text{ kCal mol}^{-1}$) and C-O ($85.5\text{ kCal mol}^{-1}$)

bonds, which explains the excellent thermal stability of the polymer (Hurd, 1946). Methyl groups present on the membrane surface are largely responsible for the hydrophobic nature of the membrane.

The basic structure of PDMS can be seen in Figure 1.7.

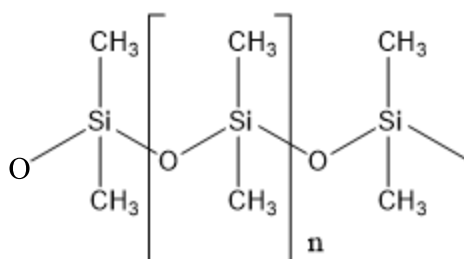


Figure 1. 6 General structure of poly(dimethylsiloxane), also known as PDMS.

Other remarkable properties of the membrane include: gas permeability making it transparent to visible and UV light (the methyl groups do not absorb radiation above 300 nm) (Pouget et al., 2010), relative environmental friendliness (it does not bio-accumulate), low-cost and non-toxicity (Roychowdhury, Cushman, Synowicki, & Linford, 2018; Tan & Rodrigue, 2019; Tibbe et al., 2018). These properties, amongst others too numerous to mention, gives PDMS advantages over other polymeric membranes, making it the most commonly used polymer among the polyorganosiloxanes (Pang, Koh, Li, & He, 2020). These desirable features also facilitate using it for biological mimic functions, such as a human skin mimic.

For more than sixty years, there has been considerable research to enhance, or incorporate, the use of polymeric membranes for drug delivery purposes (Arora & Mukherjee, 2002; Quinn, Bonham, Hughes, & Donnelly, 2015; Yiyun et al., 2007). However, in the last decade there has been an increase in PDMS-biological research. For example, its optical transparency and gas permeability has made it a good candidate for eye lenses and glasses (Shih & Yu-Lung, 2020)

as well as discreet oxygen sensors (Jiang, Thomas, Forry, DeVoe, & Raghavan, 2012). More recently, powdered PDMS has been utilised for the delivery of genes into cultured animals (López, Rubio, Sadek, & Vega, 2020) and as mimics in fluids analogous to blood particulates (Pinho, Muñoz-Sánchez, Anes, Vega, & Lima, 2019). Following the same route, the selectivity, stability and very low permeation profile of the membrane prompted scientists to consider it as a potential candidate to mimic the barrier function of human stratum corneum. Interestingly, its ability to adhere to modifications also makes it an outstanding candidate for such studies.

It is also reported that tailored properties can be achieved by the judicious choice of the chemical substitute, including skin-like properties. A plethora of data have shown how PDMS possesses some intrinsic flexibilities, where modifications on the membrane can lead to an overall effect on how it works (Lei et al., 2017; Lin, Zhao, & Yan, 2016; Shahsavan, Quinn, d'Eon, & Zhao, 2015; Shin, Kim, & Hong, 2018; Sondhi, Hwangbo, Yoon, Nishida, & Fan, 2018; Trantidou, Elani, Parsons, & Ces, 2017).

Over the last decade, a plethora of research has been published that involves modifications carried out on the membrane which subsequently alters the permeation profile compared with the un-modified form of the membrane. For example, a recent study has shown how the use of plasma treated PDMS membrane resulted in significant changes in the permeation profiles of some sample drugs when compared with permeation profiles from an un-modified form of the membrane (Waters, Finch, Bhuiyan, Hemming, & Mitchell, 2017). Such studies further highlight the possibility of tailoring the membrane into a desired outcome and how surface treatment can affect the membrane permeation profile.

Table 1 is a summary of vital studies carried out that have considered PDMS as a potential alternative to skin. Relevant findings related to percutaneous absorption, their limitations and some of the advantages they possess over other alternatives are also highlighted.

Table 1. 1 A summary of several studies proposing PDMS as a potential alternative to predict transdermal permeation. (Sabo & Waters, 2020)

Polymer model	Compared model	Model compds Used	Findings related to percutaneous absorption	Physicochemical Parameters used in the experiments				Limitations	Advantages	Reference
				Temp.	Medium pH	Flow rate	Exp. Duration			
PDMS – PC BCP	Human skin epidermis (Inner thigh)	14	Share similar mechanism of drug transport (solubility-diffusion process)	35°C ± 0.5 °C	-	100 rpm ± 1	48 hours	Over prediction of percutaneous absorption	Easily achieved	(Feldstein et al., 1998)
PDMS – PA Carbowax	Porcine skin	32	Shows a good correlation with model compounds (R ² = 0.93)	37 °C	7.3 – 7.5	400 rpm	12 hours	Performs best under precise and fine conditions, lot-to-lot variabilities could lead to variable results	Provides a good relationship with porcine skin	(Xia, Baynes, Monteiro-Riviere, & Riviere, 2007)
PDMS - PEG	Human skin	12	Can be used to predict permeability of the human skin for both hydrophilic and lipophilic drugs	37° C	-	-	-	Less reliable when predicting hydrophilic compounds	Provides a suitable alternative to human skin	(Miki et al., 2015)
PDMS	Pig skin	1	Absorption was slightly higher compared to that of pig skin	37 ± 0.5 °C	7.4	-	24 hours	Limited sample size	Cost effective	(Simon, Amaro, Healy, Cabral, & de Sousa, 2016)
PDMS	Human skin and Hairless rat skin	15	Results obtained show correlations with compounds having low log P values yet more pronounced with drugs having high log P values	32 °C	7.4 (except for 1 compound)			Overestimation of percutaneous absorption	Could serve as a screening test for permeation analysis	(Uchida et al., 2016)
PDMS - MA	Human skin	11	Drug permeation was similar to human skin	37° C	7.4		-	The membrane was delicate, and more studies need to be carried out between polymer materials and the drug	Provides a linear relationship between membrane permeation and that of human skin, which could provide an avenue for a mathematical model	(Yamaguchi et al., 1997)
PDMS	Porcine skin	2	Percutaneous absorption of the synthetic membrane, fits a normal distribution curve	37 ± 0.5 °C	7.4		24 hours	A correlation wasn't achieved between synthetic membrane and porcine skin	The permeation profile was good, and results were reproducible	(Khan, Frum, Sarheed, Eccleston, & Meidan, 2005)

Based on the findings presented in Table 1, along with some other examples that can be found in literature, it is fair to say that PDMS membrane has been receiving immense consideration over the past few years as a potential alternative to skin for permeation analysis. However, some scientists still show reservations in accepting artificial membranes, proposing that it will not successfully model the lipid perturbation effects undergone by biological tissues (Küchler, Strüver, & Friess, 2013). A comparison of PDMS with skin equivalent models is summarised in Table 2 which tries to compare the membrane advantages over these biological models and how these advantages point to the need to actually consider the membrane as an alternative.

Table 1. 2 Comparative description between PDMS membrane and skin equivalent models.

Skin model	Advantages	Limitations
Reconstructed Human Skin equivalent (RHE)	Good correlation compared with human skin data	-Fragile -Expensive -Variable -Instability
Animal skin	Traditionally used	-Ethical constraints -Legal constraints -Questionable barrier property -Age, anatomical site and animal type impede prediction of percutaneous absorption
Human skin	Gold standard	-Ethical permission required -Availability and storage constraints -Variance resulting from anatomical site used, gender, age and race
PDMS silicon membrane	-Cost effective -Reproducible -Modifiable	-Non-biological -Over prediction of percutaneous absorption

1.2.10.2 Broad classification in modifications of PDMS.

A brief overview of the broad classification on the general methods employed in modification of PDMS is presented in Table 1.

Table 1. 3 A summary of the main techniques employed for PDMS modifications.

Main Techniques	Principle	Post treatment effect as it relates to TDDS	Advantages	Disadvantages
Dynamic Modification	This method of modification is mostly a physisorbed process that relies on interactions of materials chiefly by the principle of weak attractions such as Van der Waal forces. A solution-based approach is mostly used, that comprises the membrane and a desired solvent solution. Amphiphilic groups from the selected solvent, interacts with PDMS membrane and attach their lipophilic group on the hydrophobic surface of the membrane, thereby altering its surface chemistry. These surfactants referred to as ‘dynamic modifiers’ are utilised in different ways ranging from the exposure of the already prepared membrane in a solution containing the surfactants (A.-J. Wang, Xu, & Chen, 2006), to direct introduction of the surfactants in the pre-cured monomer mixture during the polymer synthesis. (Holczer & Fürjes, 2017).	Significant changes in surface chemistry of the membrane have been observed following this type of modification, using water contact angle analysis. It is reported that a significant reduction in water contact angle (from 110 °C to 23 °C) was observed (Madadi & Casals-Terré, 2013), in the modified form of the membrane, following this process. It is also reported that this surface change can affect the overall permeation profiles of these membranes when used in permeation analysis. (Bhuiyan & Waters, 2017).	It is in-expensive and effective process. In some instances, the principles of this modification process gives similar outcomes to the plasma modification process which is a more expensive technique (Madadi & Casals-Terré, 2013)	It is superficial and mostly short term. Depletion of the modifiers can easily occur when such membranes are utilised for permeation analysis. The modifiers simply diffuse into the aqueous solution, thus exposing the membrane back to its original form
Surface Oxidation	This process is more of a chemisorbed process. It involves more stronger bonds, which can bring about a more robust change and effect almost at a molecular level. The process largely oxidises the surface methyl groups of this membrane, thereby altering its chemistry. It is more robust in terms of wettability and reactivity of the membrane, and also more stable compared to dynamic modification. Example of such process involves the use of Piranha solution (H_2O_2 / H_2SO_4) (Maji, Lahiri, & Das, 2012), UV/ O_3 treatment, and plasma treatment.	This process largely results in the cleavage of the alkoxysilane group ($Si-CH_3$), and formation of a silanol group ($Si-OH$) (I.-J. Chen & Lindner, 2007). This change has also been reported to alter the permeation profile of PDMS membranes (Waters et al., 2017)	Relatively more stable, compared to membranes modified using the dynamic method.	Different chemical entities are utilised in this method, which could be corrosive and has a high risk. Some of the techniques employed are expensive and requires a certain level of training to use.
Covalent Attachment	This process is basically an extension of the ‘surface oxidation’ process. It involves attaching various chemical functionalities on the already oxidised membrane surface. Organosilanes have received a lot of attention for such purpose. Largely attributed to their moderate reaction protocols and in-expensive nature (Chuah, Kuddannaya, Lee, Zhang, & Kang, 2015)	The process provides a wide array of modification possibilities thus substantive literature have reported membranes that have undergone this type of modification	It is comparatively in-expensive and requires moderate reaction conditions.	Considering potential application in <i>in vitro</i> analysis, limited attempts have been made to modify PDMS membrane using this process.

1.3. Research Aim and Objectives

The aim of this research is to chemically modify poly(dimethylsiloxane) polymer membrane in order to effectively mimic surface activity of the skin in permeation analysis, consequently, addressing the challenges often associated with the use of skin in transdermal drug delivery processes. This aim is set to be achieved according to the following set of objectives:

- ❖ To identify and acknowledge various methods and works previously employed on the membrane, in an attempt to address and bridge the research aim, thereby constructively identifying existing gaps.
- ❖ To identify, study and apply different functionalities that are compatible with PDMS membrane and are capable of driving effects strong enough to result in permeation profile changes
- ❖ To employ a range of analytical techniques to characterise the newly developed membranes, hence provide an avenue for replication of the process
- ❖ To compare obtained data from modified membranes with human skin data from literature to investigate their potential as skin mimics.

References

- Abd, E., Yousef, S. A., Pastore, M. N., Telaprolu, K., Mohammed, Y. H., Namjoshi, S., . . . Roberts, M. S. (2016). Skin models for the testing of transdermal drugs. *Clinical pharmacology: advances and applications*, 8, 163.
- Akomeah, F., Nazir, T., Martin, G. P., & Brown, M. B. (2004). Effect of heat on the percutaneous absorption and skin retention of three model penetrants. *European Journal of Pharmaceutical Sciences*, 21(2-3), 337-345.
- Akomeah, F. K., Martin, G. P., & Brown, M. B. (2007). Variability in human skin permeability in vitro: comparing penetrants with different physicochemical properties. *Journal of pharmaceutical sciences*, 96(4), 824-834.
- Andrianakos, A., Avouac, B., Bijlsma, J., Bolten, W., Delmas, P., Grasedyck, K., . . . inflammation. (1992). Prevention of non-steroidal anti-inflammatory drug (NSAID) induced gastropathy. *European journal of rheumatology and inflammation* 12(3), 23-29.
- Anissimov, Y. G., & Roberts, M. S. (2011). Modelling dermal drug distribution after topical application in human. *Pharmaceutical research*, 28(9), 2119.
- Arora, P., & Mukherjee, B. (2002). Design, development, physicochemical, and in vitro and in vivo evaluation of transdermal patches containing diclofenac diethylammonium salt. *Journal of pharmaceutical sciences*, 91(9), 2076-2089.
- Avdeef, A. (2012). *Absorption and drug development: solubility, permeability, and charge state*: John Wiley & Sons.
- Baba, H., Takahara, J.-i., & Mamitsuka, H. (2015). In silico predictions of human skin permeability using nonlinear quantitative structure–property relationship models. *Pharmaceutical research*, 32(7), 2360-2371.
- Balakrishnan, P., Shanmugam, S., Lee, W. S., Lee, W. M., Kim, J. O., Oh, D. H., . . . Choi, H.-G. (2009). Formulation and in vitro assessment of minoxidil niosomes for enhanced skin delivery. *International journal of pharmaceutics*, 377(1-2), 1-8.
- Barnard, N. D., & Kaufman, S. R. (1997). Animal research is wasteful and misleading. *Scientific American*, 276(2), 80-82.
- Bartosova, L., & Bajgar, J. (2012). Transdermal drug delivery in vitro using diffusion cells. *Current medicinal chemistry*, 19(27), 4671-4677.
- Batheja, P., Song, Y., Wertz, P., & Michniak-Kohn, B. (2009). Effects of growth conditions on the barrier properties of a human skin equivalent. *Pharmaceutical research*, 26(7), 1689-1700.
- Benson, H. A., Grice, J. E., Mohammed, Y., Namjoshi, S., & Roberts, M. S. J. C. d. d. (2019). Topical and Transdermal Drug Delivery: From Simple Potions to Smart Technologies. *Current drug delivery*, 16(5), 444-460.
- Bhanu Prasad, C. (2016a). A review on drug testing in animals. *Transl Biomedicine*, 7, 4.
- Bhanu Prasad, C. (2016b). A review on drug testing in animals. *Translational Biomedicine*, 7(4), 2172-0479.100099.
- Bhuiyan, A., & Waters, L. J. (2017). Permeation of pharmaceutical compounds through silicone membrane in the presence of surfactants. *Colloids and Surfaces A: Physicochemical and Engineering Aspects*, 516, 121-128.
- Borgia, S. L., Schlupp, P., Mehnert, W., & Schäfer-Korting, M. (2008). In vitro skin absorption and drug release—a comparison of six commercial prednicarbate preparations for topical use. *European Journal of Pharmaceutics and Biopharmaceutics*, 68(2), 380-389.

- Botting, J. H., & Morrison, A. R. (1997). Animal research is vital to medicine. *Scientific American*, 276(2), 83-85.
- Bronaugh, R. L., Stewart, R. F., Congdon, E. R., & Giles Jr, A. L. (1982). Methods for in vitro percutaneous absorption studies I. Comparison with in vivo results. *Toxicology and applied pharmacology*, 62(3), 474-480.
- Carstens, E., & Moberg, G. P. (2000). Recognizing pain and distress in laboratory animals. *Ilar Journal*, 41(2), 62-71.
- Chen, I.-J., & Lindner, E. (2007). The stability of radio-frequency plasma-treated polydimethylsiloxane surfaces. *Langmuir*, 23(6), 3118-3122.
- Chen, Y., Quan, P., Liu, X., Wang, M., & Fang, L. (2014). Novel chemical permeation enhancers for transdermal drug delivery. *Asian Journal of Pharmaceutical Sciences*, 9(2), 51-64.
- Chien, Y. W., Siddiqui, O., Shi, W.-M., Lelawongs, P., & Liu, J.-C. (1989). Direct current iontophoretic transdermal delivery of peptide and protein drugs. *Journal of pharmaceutical sciences*, 78(5), 376-383.
- Choe, C., Lademann, J., & Darvin, M. E. (2016). A depth-dependent profile of the lipid conformation and lateral packing order of the stratum corneum in vivo measured using Raman microscopy. *Analyst*, 141(6), 1981-1987.
- Chowhan, Z., & Pritchard, R. (1978). Effect of surfactants on percutaneous absorption of naproxen I: comparisons of rabbit, rat, and human excised skin. *Journal of pharmaceutical sciences*, 67(9), 1272-1274.
- Chuah, Y. J., Kuddannaya, S., Lee, M. H. A., Zhang, Y., & Kang, Y. (2015). The effects of poly (dimethylsiloxane) surface silanization on the mesenchymal stem cell fate. *Biomaterials science*, 3(2), 383-390.
- Cole, L. A., & Kramer, P. R. (2015). *Human Physiology, Biochemistry and Basic Medicine*: Academic Press.
- Cole, M. A., Quan, T., Voorhees, J. J., & Fisher, G. J. (2018). Extracellular matrix regulation of fibroblast function: redefining our perspective on skin aging. *Journal of cell communication and signaling*, 12(1), 35-43.
- Comyn, J. (1985). Introduction to polymer permeability and the mathematics of diffusion. In *Polymer permeability* (pp. 1-10): Springer.
- Dalton, C., Graham, S., & Jenner, J. (2015). Effect of exposure area on nerve agent absorption through skin in vitro. *Toxicology in Vitro*, 30(1), 454-461.
- Del Rosso, J. Q., & Levin, J. (2011). The clinical relevance of maintaining the functional integrity of the stratum corneum in both healthy and disease-affected skin. *The Journal of clinical and aesthetic dermatology*, 4(9), 22.
- Ebnesajjad, S., & Khaladkar, P. (2005). Selecting Fluoropolymers for Corrosion Control. *Fluoropolymers Applications in the Chemical Processing Industries*. William Andrew Applied Science Publishers, 117-160.
- Ebnesajjad, S., & Morgan, R. (2019). *Fluoropolymer additives*: William Andrew.
- Elnaggar, Y. S., El-Massik, M. A., & Abdallah, O. Y. (2011). Fabrication, appraisal, and transdermal permeation of sildenafil citrate-loaded nanostructured lipid carriers versus solid lipid nanoparticles. *International journal of nanomedicine*, 6, 3195.
- Feingold, K. R., & Elias, P. M. (2014). Role of lipids in the formation and maintenance of the cutaneous permeability barrier. *Biochimica et Biophysica Acta (BBA)-Molecular and Cell Biology of Lipids*, 1841(3), 280-294.

- Feldstein, M. M., Raigorodskii, I. M., Iordanskii, A. L., & Hadgraft, J. (1998). Modeling of percutaneous drug transport in vitro using skin-imitating Carbosil membrane. *Journal of Controlled Release*, 52(1-2), 25-40.
- Fernando, A., Thomas, S., Temple, R., & Lee, H. J. B. B. M. J. (1994). Renal failure after topical use of NSAIDs. *British Medical Journal* 308(6927), 533.
- Flynn, G. (1990). Physiochemical determinants of skin absorption. *Principles of route-to-route extrapolation for risk assessment*, 93-127.
- Garcia, M. T., de Vasconcellos, F. L. L., Raffier, C. P., Roberts, M. S., Grice, J. E., Benson, H. A. E., & Leite-Silva, V. R. (2018). Alternative methods to animal studies for the evaluation of topical/transdermal drug delivery systems. *Current Topics in Medicinal Chemistry*, 18(4), 287-299.
- Geusens, B., Strobbe, T., Bracke, S., Dynoodt, P., Sanders, N., Van Gele, M., & Lambert, J. (2011). Lipid-mediated gene delivery to the skin. *European Journal of Pharmaceutical Sciences*, 43(4), 199-211.
- Ghafourian, T., Samaras, E. G., Brooks, J. D., & Riviere, J. E. (2010). Modelling the effect of mixture components on permeation through skin. *International journal of pharmaceutics*, 398(1-2), 28-32.
- Godin, B., & Touitou, E. (2007). Transdermal skin delivery: predictions for humans from in vivo, ex vivo and animal models. *Advanced drug delivery reviews*, 59(11), 1152-1161.
- Hadgraft, J., & Lane, M. E. J. I. J. o. P. (2005). Skin permeation: the years of enlightenment. *International journal of pharmaceutics*, 305(1-2), 2-12.
- Hadgraft, J., & Ridout, G. (1987). Development of model membranes for percutaneous absorption measurements. I. Isopropyl myristate. *International journal of pharmaceutics*, 39(1-2), 149-156.
- Harding, C. R. (2004). The stratum corneum: structure and function in health and disease. *Dermatologic therapy*, 17(s1), 6-15.
- Hausmann, C., Zoschke, C., Wolff, C., Darvin, M. E., Sochorová, M., Kováčik, A., . . . Kleuser, B. J. S. r. (2019). Fibroblast origin shapes tissue homeostasis, epidermal differentiation, and drug uptake. *Scientific reports*, 9(1), 2913.
- Hillery, A. M., Lloyd, A. W., & Swarbrick, J. (2002). *Drug delivery and targeting: for pharmacists and pharmaceutical scientists*: CRC Press, 243-256.
- Hoath, S. (2014a). Development of the stratum corneum. *British Journal of Dermatology*, 171(s3), 2-5.
- Hoath, S. (2014b). Development of the stratum corneum. *British Journal of Dermatology*, 171, 2-5.
- Holczer, E., & Fürjes, P. (2017). Effects of embedded surfactants on the surface properties of PDMS; applicability for autonomous microfluidic systems. *Microfluidics and Nanofluidics*, 21(5), 81.
- Hurd, C. B. (1946). Studies on siloxanes. I. The specific volume and viscosity in relation to temperature and constitution. *Journal of the American Chemical Society*, 68(3), 364-370.
- Hutson, G. (1994). Animal Welfare Science-a discipline for the future or an ephemeral preoccupation. *Animal Welfare in the Twenty-First Century: Ethical, Educational and Scientific Challenges*, 47-52.
- Ikada, Y. (1994). Surface modification of polymers for medical applications. *Biomaterials*, 15(10), 725-736.

- Imokawa, G., Akasaki, S., Hattori, M., & Yoshizuka, N. (1986). Selective recovery of deranged water-holding properties by stratum corneum lipids. *Journal of Investigative Dermatology*, 87(6), 758-761.
- Jiang, K., Thomas, P. C., Forry, S. P., DeVoe, D. L., & Raghavan, S. R. (2012). Microfluidic synthesis of monodisperse PDMS microbeads as discrete oxygen sensors. *Soft Matter*, 8(4), 923-926.
- Kandavilli, S., Nair, V., & Panchagnula, R. (2002). Polymers in transdermal drug delivery systems. *Pharmaceutical technology*, 26(5), 62-81.
- Khan, G. M., Frum, Y., Sarheed, O., Eccleston, G. M., & Meidan, V. M. (2005). Assessment of drug permeability distributions in two different model skins. *International journal of pharmaceutics*, 303(1-2), 81-87.
- Klimová, Z., Hojerová, J., & Beránková, M. (2015). Skin absorption and human exposure estimation of three widely discussed UV filters in sunscreens—In vitro study mimicking real-life consumer habits. *Food and Chemical Toxicology*, 83, 237-250.
- Küchler, S., Strüver, K., & Friess, W. (2013). Reconstructed skin models as emerging tools for drug absorption studies. *Expert opinion on drug metabolism & toxicology*, 9(10), 1255-1263.
- Küchler, S., Strüver, K., Friess, W. J. E. o. o. d. m., & toxicology. (2013). Reconstructed skin models as emerging tools for drug absorption studies. 9(10), 1255-1263.
- Lai-Cheong, J. E., & McGrath, J. A. (2017). Structure and function of skin, hair and nails. *Medicine*, 45(6), 347-351.
- Lane, M. E. (2013). Skin penetration enhancers. *International journal of pharmaceutics*, 447(1-2), 12-21.
- Lee, P. H., Conradi, R., & Shanmugasundaram, V. (2010). Development of an in silico model for human skin permeation based on a Franz cell skin permeability assay. *Bioorganic & medicinal chemistry letters*, 20(1), 69-73.
- Lei, W.-W., Li, H., Shi, L.-Y., Diao, Y.-F., Zhang, Y.-L., Ran, R., & Ni, W. (2017). Achieving enhanced hydrophobicity of graphene membranes by covalent modification with polydimethylsiloxane. *Applied Surface Science*, 404, 230-237.
- Lin, D., Zhao, Q., & Yan, M. (2016). Surface modification of polydimethylsiloxane microfluidic chips by polyamidoamine dendrimers for amino acid separation. *Journal of Applied Polymer Science*, 133(25).
- López, M., Rubio, M., Sadek, S., & Vega, E. (2020). A simple emulsification technique for the production of micro-sized flexible powder of polydimethylsiloxane (PDMS). *Powder Technology*, 366, 610-616.
- Lu, M.-y. F., Lee, D., & Rao, G. S. (1992). Percutaneous absorption enhancement of leuprolide. *Pharmaceutical research*, 9(12), 1575-1579.
- Lundborg, M., Narangifard, A., Wennberg, C. L., Lindahl, E., Daneshmandi, B., & Norlén, L. (2018). Human skin barrier structure and function analyzed by cryo-EM and molecular dynamics simulation. *Journal of structural biology*, 203(2), 149-161.
- Madadi, H., & Casals-Terré, J. (2013). Long-term behavior of nonionic surfactant-added PDMS for self-driven microchips. *Microsystem technologies*, 19(1), 143-150.
- Maji, D., Lahiri, S., & Das, S. (2012). Study of hydrophilicity and stability of chemically modified PDMS surface using piranha and KOH solution. *Surface and Interface analysis*, 44(1), 62-69.

- Malvey, S., Rao, J. V., & Arumugam, K. M. (2019). Transdermal drug delivery system: A mini review. *Pharma Innov. J*, 8, 181-197
- Marwah, H., Garg, T., Goyal, A. K., & Rath, G. (2016). Permeation enhancer strategies in transdermal drug delivery. *Drug delivery*, 23(2), 564-578.
- Meckfessel, M. H., & Brandt, S. (2014). The structure, function, and importance of ceramides in skin and their use as therapeutic agents in skin-care products. *Journal of the American Academy of Dermatology*, 71(1), 177-184.
- Menon, G. K. (2002). New insights into skin structure: scratching the surface. *Advanced drug delivery reviews*, 54, S3-S17.
- Michaels, A., Chandrasekaran, S., & Shaw, J. (1975). Drug permeation through human skin: theory and in vitro experimental measurement. *AIChE Journal*, 21(5), 985-996.
- Miki, R., Ichitsuka, Y., Yamada, T., Kimura, S., Egawa, Y., Seki, T., Morimoto, Y. (2015). Development of a membrane impregnated with a poly (dimethylsiloxane)/poly (ethylene glycol) copolymer for a high-throughput screening of the permeability of drugs, cosmetics, and other chemicals across the human skin. *European Journal of Pharmaceutical Sciences*, 66, 41-49.
- Misra, A. (2014). *Applications of polymers in drug delivery*: Elsevier.
- Mitragotri, S. (2003). Modeling skin permeability to hydrophilic and hydrophobic solutes based on four permeation pathways. *Journal of controlled release*, 86(1), 69-92.
- Mitragotri, S., Anissimov, Y. G., Bunge, A. L., Frasc, H. F., Guy, R. H., Hadgraft, J., . . . Roberts, M. S. (2011). Mathematical models of skin permeability: an overview. *International journal of pharmaceuticals*, 418(1), 115-129.
- Moore, R. A., Tramer, M., Carroll, D., Wiffen, P. J., & McQuay, H. J. B. (1998). Quantitative systematic review of topically applied non-steroidal anti-inflammatory drugs. *British Medical Journal*, 316(7128), 333-338.
- Moss, G. P., Gullick, D. R., & Wilkinson, S. C. (2016). *Predictive Methods in Percutaneous Absorption*: Springer.
- Mukerjee, M. (1997). Trends in animal research. *Scientific American*, 276(2), 86-93.
- Ng, K. W., & Lau, W. M. (2015). Skin deep: the basics of human skin structure and drug penetration. In *Percutaneous Penetration Enhancers Chemical Methods in Penetration Enhancement* (pp. 3-11): Springer.
- Ng, S.-F., Rouse, J., Sanderson, D., & Eccleston, G. (2010a). A comparative study of transmembrane diffusion and permeation of ibuprofen across synthetic membranes using Franz diffusion cells. *Pharmaceutics*, 2(2), 209-223.
- Ng, S.-F., Rouse, J., Sanderson, D., & Eccleston, G. J. P. (2010b). A comparative study of transmembrane diffusion and permeation of ibuprofen across synthetic membranes using Franz diffusion cells. 2(2), 209-223.
- Ng, S.-F., Rouse, J. J., Sanderson, F. D., & Eccleston, G. M. (2012). The relevance of polymeric synthetic membranes in topical formulation assessment and drug diffusion study. *Archives of pharmacological research*, 35(4), 579-593.
- Ng, S.-F., Rouse, J. J., Sanderson, F. D., Meidan, V., & Eccleston, G. M. (2010). Validation of a static Franz diffusion cell system for in vitro permeation studies. *Aaps PharmSciTech*, 11(3), 1432-1441.
- Nicoli, S., Penna, E., Padula, C., Colombo, P., & Santi, P. (2006). New transdermal bioadhesive film containing oxybutynin: In vitro permeation across rabbit ear skin. *International journal of pharmaceuticals*, 325(1-2), 2-7.

- Owen, M. J., & Dvornic, P. R. (2012). Surface Applications of Silicones. In *Silicone Surface Science* (pp. 355-374): Springer.
- Özgüney, I. S., Karasulu, H. Y., Kantarci, G., Sözer, S., Güneri, T., & Ertan, G. (2006). Transdermal delivery of diclofenac sodium through rat skin from various formulations. *Aaps Pharmscitech*, 7(4), E39-E45.
- Pang, Y., Koh, J. J., Li, Z., & He, C. (2020). Reactive Functionally Terminated Polyorganosiloxanes. *Silicon Containing Hybrid Copolymers*, 23-61.
- Patil, P., Datir, S., Saudagar, R. J. J. o. D. D., & Therapeutics. (2019). A Review on Topical Gels as Drug Delivery System. *Journal of Drug Delivery and Therapeutics*, 9(3-s), 989-994.
- Pecoraro, B., Tutone, M., Hoffman, E., Hutter, V., Almerico, A. M., Traynor, M. J. J. o. c. i., & modeling. (2019). Predicting Skin Permeability by Means of Computational Approaches: Reliability and Caveats in Pharmaceutical Studies. *Journal of chemical information and modelling*, 59(5), 1759-1771
- Pegoraro, C., MacNeil, S., & Battaglia, G. (2012). Transdermal drug delivery: from micro to nano. *Nanoscale*, 4(6), 1881-1894.
- Pinho, D., Muñoz-Sánchez, B., Anes, C. F., Vega, E., & Lima, R. (2019). Flexible PDMS microparticles to mimic RBCs in blood particulate analogue fluids. *Mechanics Research Communications*, 100, 103399.
- Potts, R. O., & Guy, R. H. (1992). Predicting skin permeability. *Pharmaceutical research*, 9(5), 663-669.
- Pouget, E., Tonnar, J., Lucas, P., Lacroix-Desmazes, P., Ganachaud, F., & Boutevin, B. (2010). Well-architected poly (dimethylsiloxane)-containing copolymers obtained by radical chemistry. *Chemical reviews*, 110(3), 1233-1277.
- Prottey, C. (1976). Essential fatty acids and the skin. *British Journal of Dermatology*, 94(5), 579-587.
- Quinn, H. L., Bonham, L., Hughes, C. M., & Donnelly, R. F. (2015). Design of a dissolving microneedle platform for transdermal delivery of a fixed-dose combination of cardiovascular drugs. *Journal of pharmaceutical sciences*, 104(10), 3490-3500.
- Qvist, M. H., Hoeck, U., Kreilgaard, B., Madsen, F., & Frokjaer, S. (2000). Evaluation of Göttingen minipig skin for transdermal in vitro permeation studies. *European Journal of Pharmaceutical Sciences*, 11(1), 59-68.
- Restrepo-Flórez, J. M., & Maldovan, M. J. A. J. (2019). Anisotropic Membrane Materials for Gas Separations. *AIChE Journal* e16599.
- Roy, S., Fujiki, J., & Fleitman, J. (1993). Permeabilities of alkyl p-aminobenzoates through living skin equivalent and cadaver skin. *Journal of pharmaceutical sciences*, 82(12), 1266-1268.
- Roychowdhury, T., Cushman, C. V., Synowicki, R., & Linford, M. R. (2018). Polydimethylsiloxane: Optical properties from 191 to 1688 nm (0.735–6.491 eV) of the liquid material by spectroscopic ellipsometry. *Surface Science Spectra*, 25(2), 026001.
- Sabo, S., & Waters, L. J. (2020). Poly (dimethylsiloxane): A sustainable human skin alternative for transdermal drug delivery prediction. *Journal of pharmaceutical sciences*. 110 (3), 1018-1024.
- Sanna, V., Peana, A. T., & Moretti, M. D. (2009). Effect of vehicle on diclofenac sodium permeation from new topical formulations: in vitro and in vivo studies. *Current drug delivery*, 6(1), 93-100.

- Sato, J., Nakanishi, J., Denda, M., Nomura, J., & Koyama, J. (1997). Cholesterol sulfate inhibits proteases which are involved in desquamation of stratum corneum. *Journal of Investigative Dermatology*, 4(108), 603.
- Schmook, F. P., Meingassner, J. G., & Billich, A. (2001). Comparison of human skin or epidermis models with human and animal skin in in-vitro percutaneous absorption. *International journal of pharmaceutics*, 215(1-2), 51-56.
- Shahsavan, H., Quinn, J., d'Eon, J., & Zhao, B. (2015). Surface modification of polydimethylsiloxane elastomer for stable hydrophilicity, optical transparency and film lubrication. *Colloids and Surfaces A: Physicochemical and Engineering Aspects*, 482, 267-275.
- Shahzad, Y., Louw, R., Gerber, M., & Du Plessis, J. (2015). Breaching the skin barrier through temperature modulations. *Journal of controlled release*, 202, 1-13.
- Shih, W.-C., & Yu-Lung, S. (2020). Fabrication of polydimethylsiloxane optical material. *U.S Patent Application No. 16/747,871*
- Shin, S., Kim, N., & Hong, J. W. (2018). Comparison of surface modification techniques on polydimethylsiloxane to prevent protein adsorption. *BioChip Journal*, 12(2), 123-127.
- Simon, A., Amaro, M. I., Healy, A. M., Cabral, L. M., & de Sousa, V. P. (2016). Comparative evaluation of rivastigmine permeation from a transdermal system in the Franz cell using synthetic membranes and pig ear skin with in vivo-in vitro correlation. *International journal of pharmaceutics*, 512(1), 234-241.
- Sondhi, K., Hwangbo, S., Yoon, Y.-K., Nishida, T., & Fan, Z. H. (2018). Airbrushing and surface modification for fabricating flexible electronics on polydimethylsiloxane. *Journal of Micromechanics and Microengineering*, 28(12), 125014.
- Sreedhar, D., Manjula, N., Pise, A., Pise, S., & Ligade, V. (2020). Ban of Cosmetic Testing on Animals: A Brief Overview. *International Journal of Current Research and Review*, 12(14), 113-116.
- Statista. (2019). Pain relief treatments sales value in Great Britain 2009-2019. Retrived from <https://www.statista.com/statistics/521802/otc-pain-relief-treatments-sales-value-great-britain/>
- Tan, X., & Rodrigue, D. (2019). A review on porous polymeric membrane preparation. Part ii: Production techniques with polyethylene, polydimethylsiloxane, polypropylene, polyimide, and polytetrafluoroethylene. *Polymers*, 11(8), 1310.
- Thomas, B. J., & Finnin, B. C. J. D. d. t. (2004). The transdermal revolution. 9(16), 697-703.
- Tibbe, M., Loessberg-Zahl, J., Do Carmo, M. P., Van Der Helm, M., Bomer, J., Van Den Berg, A., . . . Eijkel, J. (2018). Large-scale fabrication of free-standing and sub-µm PDMS through-hole membranes. *Nanoscale*, 10(16), 7711-7718.
- Tobin, D. J. (2006). Biochemistry of human skin—our brain on the outside. *Chemical Society Reviews*, 35(1), 52-67.
- Trantidou, T., Elani, Y., Parsons, E., & Ces, O. (2017). Hydrophilic surface modification of PDMS for droplet microfluidics using a simple, quick, and robust method via PVA deposition. *Microsystems & nanoengineering*, 3(1), 1-9.
- Uchida, T., Yakumaru, M., Nishioka, K., Higashi, Y., Sano, T., Todo, H., & Sugibayashi, K. (2016). Evaluation of a silicone membrane as an alternative to human skin for determining skin permeation parameters of chemical compounds. *Chemical and Pharmaceutical Bulletin*, 64(9), 1338-1346.

- Uyama, Y., Kato, K., & Ikada, Y. (1998). Surface modification of polymers by grafting. In *Grafting/Characterization Techniques/Kinetic Modeling* (pp. 1-39): Springer.
- Van Ravenzwaay, B., & Leibold, E. (2004). A comparison between in vitro rat and human and in vivo rat skin absorption studies. *Human & experimental toxicology*, 23(9), 421-430.
- Verma, D. D., Verma, S., Blume, G., & Fahr, A. (2003). Particle size of liposomes influences dermal delivery of substances into skin. *International journal of pharmaceutics*, 258(1-2), 141-151.
- Vopička, O., Randová, A., & Friess, K. (2014). Sorption of vapours and liquids in PDMS: novel data and analysis with the GAB model of multilayer adsorption. *European Polymer Journal*, 60, 49-57.
- Waghule, T., Singhvi, G., Dubey, S. K., Pandey, M. M., Gupta, G., Singh, M., . . . Pharmacotherapy. (2019). Microneedles: a smart approach and increasing potential for transdermal drug delivery system. *109*, 1249-1258.
- Wang, A.-J., Xu, J.-J., & Chen, H.-Y. (2006). Nonionic surfactant dynamic coating of poly (dimethylsiloxane) channel surface for microchip electrophoresis of amino acids. *Analytica chimica acta*, 569(1-2), 188-194.
- Wang, Y., Zhao, Y., & Song, F. (2020). The Ethical Issues of Animal Testing in Cosmetics Industry. *Humanities and Social Sciences*, 8(4), 112.
- Waters, L. J., Finch, C. V., Bhuiyan, A. M. H., Hemming, K., & Mitchell, J. C. (2017). Effect of plasma surface treatment of poly (dimethylsiloxane) on the permeation of pharmaceutical compounds. *Journal of pharmaceutical analysis*, 7(5), 338-342.
- Whitefield, M., O'Kane, C., Anderson, S. J. J. o. c. p., & therapeutics. (2002). Comparative efficacy of a proprietary topical Ibuprofen gel and oral Ibuprofen in acute soft tissue injuries: a randomized, double-blind study. *National library of medicine Pubmed*, 27(6), 409-417.
- Wijmans, J. G., & Baker, R. W. J. J. o. m. s. (1995). The solution-diffusion model: a review. *Journal of membrane science*, 107(1-2), 1-21.
- Xia, X.-R., Baynes, R. E., Monteiro-Riviere, N. A., & Riviere, J. E. (2007). An experimentally based approach for predicting skin permeability of chemicals and drugs using a membrane-coated fiber array. *Toxicology and applied pharmacology*, 221(3), 320-328.
- Yamaguchi, Y., Usami, T., Natsume, H., aoyagi, T., nagase, Y., sugibayashi, K., & morimoto, Y. (1997). Evaluation of skin permeability of drugs by newly prepared polymer membranes. *Chemical and Pharmaceutical Bulletin*, 45(3), 537-541.
- Yiyun, C., Na, M., Tongwen, X., Rongqiang, F., Xueyuan, W., Xiaomin, W., & Longping, W. (2007). Transdermal delivery of nonsteroidal anti-inflammatory drugs mediated by polyamidoamine (PAMAM) dendrimers. *Journal of pharmaceutical sciences*, 96(3), 595-602.
- Yousef, H., Alhajj, M., & Sharma, S. (2019). Anatomy, skin (integument), epidermis.
- Zbytovská, J., Kiselev, M., Funari, S., Garamus, V., Wartewig, S., Palát, K., & Neubert, R. (2008). Influence of cholesterol on the structure of stratum corneum lipid model membrane. *Colloids and Surfaces A: Physicochemical and Engineering Aspects*, 328(1-3), 90-99.

Chapter 2

Materials and methods

2.1. Introduction

The aim of this project was to experimentally modify and characterise poly(dimethylsiloxane) PDMS membrane. To achieve this a theoretical background in relevant topics was acquired, as highlighted in Chapter 1. This background knowledge was itemised to include chemical composition and description of the membrane surface, methods involved in altering the surface and possible re-orientation of these surface elements that may occur as a result of different modifications.

This chapter highlights materials, chemicals and methodologies needed to achieve the research aim. Differences and similarities in the methodology used in comparison with existing literature are also described. Pre-experimental work carried out, mainly in standardising model drugs and understanding their chemistry, to permit comparative analysis with established standards are also highlighted. Design and optimisation processes, in terms of permeation analysis, is aimed to mimic *in-vivo* scenarios, are also described.

In Table 2.1 and 2.2, a full list of materials and chemicals employed in this research are highlighted. The purpose of these materials and their overall importance in terms of the experimental procedures is also described. Table 2.3 provides a detailed description of the model drugs and other related compounds used, their physicochemical properties such as molecular weight, log P and charge are also presented.

2.2. Chemicals and Materials

A detailed list of chemicals and materials used in this research are presented in Table 2.1 and 2.2.

A list of pharmaceutical compounds used is presented separately in Table 2.3

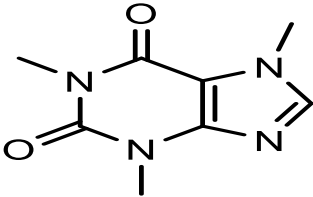
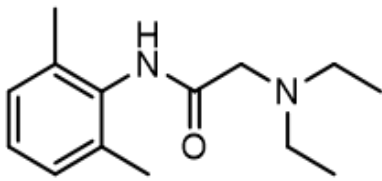
Table 2. 1 Description of materials used in this study

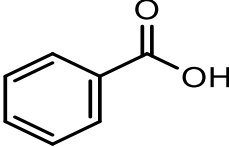
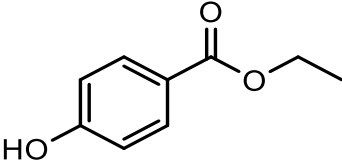
Materials	Symbol	Man./ Supplier	Grade/Model/Specifications	Note
Silatos™ silicon sheeting	N/A	Silex, Hampshire, UK.	Dimension 150 x 200 x 0.3 mm	This was used as received for normal membrane processes and was subjectively modified, which where applicable are reported as modified membranes.
Tempered clear glass with laminated surface	N/A	NA	Thickness: 6mm	It was used as a support to cut the membrane into required pieces and had good adhesion to the membrane surface.
Re-usable scalpel blades	N/A	Swann-Morton	N/A	Was used to cut the membrane into required pieces.
pH/Temperature meter	N/A	Jenway instruments	3510 pH Meter	It was used to measure pH of solutions and for temperature measurement, which was mainly as a control in permeation analysis
Oven	N/A	Thermo scientific	Fisherbrand	This was used in drying samples and activating the membrane in some instances
Magnetic stirrer	N/A	Stuart Hot Stirrer	N/A	N/A
Plasma generating system	HPT-100	Henniker plasma, UK	HPT-100	Used for preliminary membrane surface oxidation, optimised to operate at 100 W and 8 SCCM

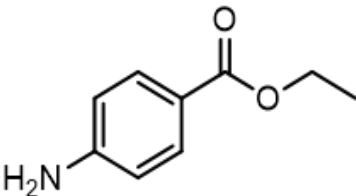
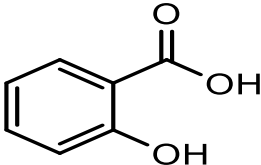
Table 2. 2 Description of chemicals used in this study

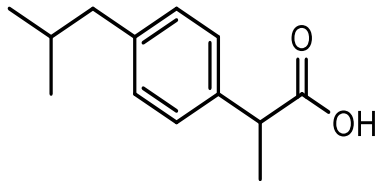
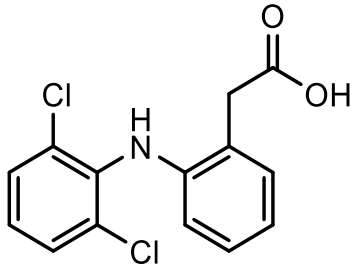
Chemicals	Formulae/Symbol	Supplier	Grade	Note
Potassium phosphate dibasic	K_2HPO_4	Sigma-Aldrich	Laboratory grade	These were used as purchased and were used to prepare a phosphate buffer saline (PBS)
Potassium phosphate monobasic	KH_2PO_4			
Hydrogen chloride	HCl		AR grade 99%	
Sodium chloride	NaCl	Tokyo Chemical Industry	-	These were used primarily to adjust the pH of solutions as appropriate.
Sulphuric Acid	H_2SO_4	Fisher Scientific	AR grade >95%	
Sodium hydroxide	NaOH	Fluorochem Limited	-	
Glycerol	$C_3H_8O_3$	Sigma-Aldrich	99%	These were used as precursors in modification processes.
Dimethylphenylsilanol	$C_8H_{12}OSi$		-	
Pentan-1,5-diol	$C_5H_{12}O_2$			
Tertbutyldimethylphenylsilanol	$C_6H_{15}SiOH$		99%	
(Perfluorophenyl)silanol				
Poly(dimethylsiloxane)-poly(ethylene oxide) block co-polymer	PDMS-PEG BCP	Gelest, inc	-	
Ethanol	C_2H_5OH	Fisher Scientific	-	-
Water	H_2O	Millipore corporation	Millipore grade	Used for preparations of solutions, unless stated otherwise

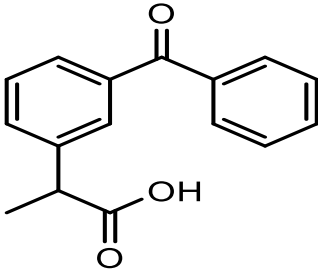
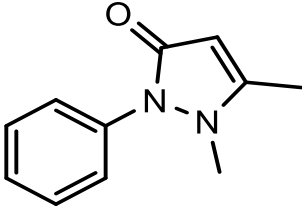
Table 2. 3 Physicochemical properties of pharmaceutical compounds used in permeation studies

Caffeine		
^b Abbreviation	CAF	^a 
Suppliers	Sigma- Aldrich	
Grade used	≥ 99.5 %	
Molecular Weight	194.19 g mol ⁻¹	
^c Log P	-0.07	
Charge	Cationic	
^d pKa	10.4	
λ _{max}	271 nm	
^d BCS	Class I	
Lidocaine		
^b Abbreviation	LID	^a 
Suppliers	Sigma- Aldrich	
Grade	≥ 99 %	
Molecular Weight	234.34 g mol ⁻¹	
^c Log P	2.44	
Charge	Cationic	
^d pKa	7.8	
λ _{max}	230 nm	
^d BCS	Class II	

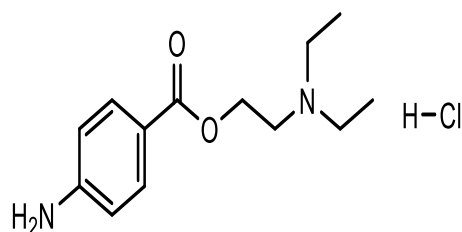
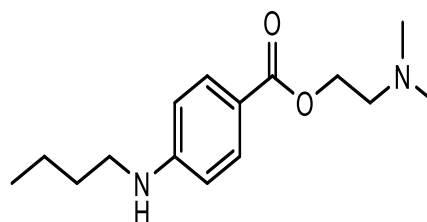
Benzoic acid		
^b Abbreviation	BZA	^a 
Suppliers	Sigma Aldrich	
Grade	≥ 99 %	
Molecular Weight	122.12 g mol ⁻¹	
^c Log P	1.89	
Charge	Anionic	
^d pKa	4.2	
λ _{max}	228 nm	
^d BCS	Class II	
Ethyl 4-hydroxybenzoate		
^b Abbreviation	EPB	^a 
Suppliers	Sigma-Aldrich	
Grade	≥ 99 %	
Molecular Weight	166.17 g mol ⁻¹	
^c Log P	2.47	
Charge	Anionic	
^d pKa	8.34 pc	
λ _{max}	254 nm	
BCS	Class II	

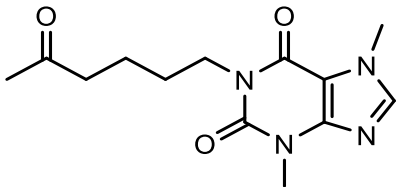
Benzocaine		
^b Abbreviation	BEN	^a 
Suppliers	Sigma- Aldrich	
Grade	≥ 99 %	
Molecular Weight	165.19 g mol ⁻¹	
^c Log P	1.86	
Charge	Cationic	
^d pKa	2.51	
λ _{max}	287 nm	
^d BCS	Class II	
Salicylic acid		
^b Abbreviation	SAL	^a 
Suppliers	Sigma- Aldrich	
Grade	≥ 99.5 %	
Molecular Weight	138.12 g mol ⁻¹	
^c Log P	2.26	
Charge	Anionic	
^d pKa	2.71	
λ _{max}	234 nm	
^d BCS	Class I	

Ibuprofen		
^b Abbreviation	IBU	^a 
Suppliers	Tokyo Chemical Ind	
Grade	≥ 99 %	
Molecular Weight	206.28 g mol ⁻¹	
^c Log P	3.97	
Charge	Anionic	
^d pKa	4.85	
λ _{max}	221 nm	
^d BCS	Class II	
Diclofenac		
^b Abbreviation	DCF	^a 
Suppliers	Tokyo Chemical Ind	
Grade	≥ 99 %	
Molecular Weight	296.15 g mol ⁻¹	
^c Log P	4.51	
Charge	Anionic/Cationic	
^d pKa	4.13	
λ _{max}	275 nm	
^d BCS	Class II	

Ketoprofen		
^b Abbreviation	KPF	^a 
Suppliers	Fluorochem Ltd	
Grade	≥ 99 %	
Molecular Weight	254.28 g mol ⁻¹	
^c Log P	3.12	
Charge	Anionic	
^d pKa	3.88	
λ _{max}	261 nm	
^d BCS	Class II	
Antipyrine		
^b Abbreviation	ANT	^a 
Suppliers	Sigma-Aldrich	
Grade	≥ 98 %	
Molecular Weight	188.22 g mol ⁻¹	
^c Log P	0.38	
Charge	Cationic	
^d pKa	1.45	
λ _{max}	242 nm	
^d BCS	Class I	

Tetracaine		a
^b Abbreviation	TTC	
Suppliers	Tokyo Chemical Ind	
Grade	≥ 98 %	
Molecular Weight	264.36 g mol ⁻¹	
^c Log P	2.79	
Charge	Cation	
^d pKa	8.42	
λ _{max}	310 nm	
^d BCS	Class II	
Procaine		a
^b Abbreviation	PRC	
Suppliers	Sigma-Aldrich	
Grade	≥ 97 %	
Molecular Weight	236.31 g mol ⁻¹	
^c Log P	2.14	
Charge	Cation	
^d pKa	8.95	
λ _{max}	290 nm	
BCS	Class I	



Pentoxifylline		
^b Abbreviation	PTX	^a 
Suppliers	Tokyo Chemical Ind	
Grade	≥ 99.5 %	
Molecular Weight	278.3 g mol ⁻¹	
^c Log P	0.32	
Charge	Cation	
^d pKa	19.64	
λ _{max}	274 nm	
^d BCS	Class III	

*a- Sited from PubChem and drawn with ChemDraw Application

*b- Locally adopted for purposes of this study

*c- Adopted from Drugbank

*d- Adopted from PubChem

2.3. Methods

2.3.1. Analytical and Experimental Procedures

In this section, laboratory procedures and spectroscopic techniques used are broadly highlighted. Their principles and how they relate to this work are also described.

Poly(dimethylsiloxane) PDMS silicon membrane with a thickness of 0.3 mm was used throughout this study and is referred to as standard membrane. Its selective permeability is studied in this research, which forms the main basis for its consideration to replace skin in permeation analysis. In trying to address issues such as the leaching effect and reduced permeability associated with the membrane, a variety of modification processes were carried out. Aromatic polymers or polymers with multiple bonds tend to have favourable structures for

chemical modifications, sometimes their reactivity is influenced by the nature of their branch chains or groups (Botvay, Máthé, & Pöpl, 1999). In contrast, PDMS has straight chains, with a very stable silicon-oxygen bond, which makes it comparatively more difficult to chemically modify. Nonetheless, the work presented in this thesis is a series of attempts made to effectively modify the membrane, and this chapter reports the analytical techniques employed to help achieve this aim.

2.3.1.1 Atmospheric Pressure Nonthermal Air Plasma Treatment of Poly(dimethylsiloxane)

For many years, successes have been recorded in using solventless processes such as plasma, corona, flame, x-ray treatments, electrons or ion beams to modify polymer surfaces (Chan, Ko, & Hiraoka, 1996). These solventless treated membranes have been applied successfully to serve as adhesives, in microfluidic devices, biomaterials or as coatings in some specialised materials. In general, certain surface properties such as crosslinking density, conductivity, lubricity, hydrophilicity, increased reactivity and roughness have been altered or improved as a result of such surface treatments. This study is interested in these solventless methods to help activate the inert surface of PDMS membrane, thereby making it susceptible for chemical reactions, without altering its bulk properties or compromising integrity.

Polyethylene, for example, which is used in huge quantities in industry to make films for packaging, due to its excellent mechanical properties, has a major problem with bondability, and this is due to its inertness and hydrophobic nature. To overcome this problem, oxygen plasma treatment is employed to increase its hydrophilicity, consequently addressing the bondability problem.

However, a more delicate and well-crafted method needs to be adopted in application of these processes especially when the membranes are intended to be used as biomaterials, such as the membrane considered in this study. Therefore, parameters such as intensity of the plasma used,

type of reaction gas employed, depth of the treatment, mechanical strength of the material involved and likely interactions that may occur between functional groups of the material and reactor gas must be carefully analysed. In biopharmaceutical areas, plasma treatment has been used to modify polymer membranes for various applications such as contact lenses, catheters, and dialysis membranes.

The treatment performed in this study was carried-out using air-plasma as the process gas in the reactor and was achieved using a benchtop Henniker Plasma machine (HPT-100), at a power of 100 W, 68 mbar and flow rate of 8 standard cubic centimeters per minute (SCCM). A treatment time of 90 seconds was used throughout the process, which was selected based upon an optimisation study carried out (data presented in chapter 3). It was realised that treatments above 90 seconds affected integrity of the membrane, making it not suitable for this study. Treatments were only undertaken on a single side of the membranes, as only modification on the surface directly in contact with drug was relevant in this study. Pieces of the membranes were cut into square forms sufficient enough to cover the diffusion area of the diffusion cell ($\sim 0.54 \text{ cm}^2$). The top right corner of the square shaped membranes that were cut, were marked, making it possible to identify plasma treated side, when used for further analysis. It is considered a pre-treatment method in this research; therefore, it was employed solely to replace PDMS surface methyl groups with hydroxyl groups, thereby forming a plasma-treated oxidised membrane, more susceptible for future chemical modifications.

A diagram illustrating a typical plasma treatment process is summarised in Figure 2.1.

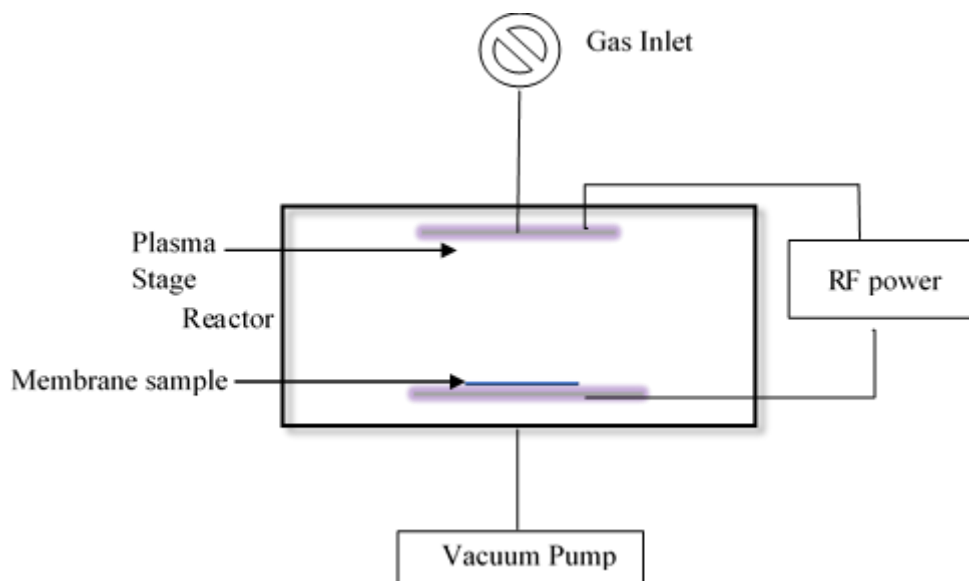


Figure 2. 1 Schematic representation of a typical Plasma generator

Oxygen containing plasma is widely employed for the surface oxidation of PDMS (Gunda, Singh, Norman, Kaur, & Mitra, 2014), however, it is known that oxygen species present in the reactor chamber can interact with the polymeric material to produce functional groups (Nehra, Kumar, & Dwivedi, 2008) such as C-O, C=O, O-C=O, C-O-O and CO₃ bonds at the membrane surface. Additionally, there is the likelihood of etching the polymer substrate, thereby giving rise to reactive volatile reaction products (Chan et al., 1996). These factors deemed this form of surface treatment unsuitable in this study.

Generally, nitrogen containing plasma is widely used to improve wettability and biocompatibility, whereas halogen containing plasmas (especially fluorine and chlorine) are largely used to promote etching in polymeric membranes. Air plasma treatment on the other hand, provides an easier and inexpensive alternative. This latter process operates using a similar mechanism with that employed using oxygen-based treatment. Energy from the plasma extracts hydrogen from methyl groups present on the membrane surface, thereby leaving an unstable methylene group (-CH₂) on the surface. The hydrogen removed further reacts with process air in the plasma chamber, or atmospheric oxygen to form a hydroxyl group (-OH). The hydroxyl

group formed, attacks and displaces the unstable methylene group that was left on the membrane. Consequently, a hydrolysed membrane surface can be achieved as a result of the plasma treatment. Practically, the hydrolysed surface becomes more suitable for further treatment, due to an increase in surface tension (Bodas, Khan-Malek, & Chemical, 2007), (Zhou, Ellis, & Voelcker, 2010) , (Goda, Konno, Takai, Moro, & Ishihara, 2006) .

The effectiveness of this process, alongside its ease, has attracted a lot of interest and consideration. The process (air plasma treatment of PDMS) is reported to be used as a pre-requisite in the formation of poly(vinylalcohol) coatings (Li, Wang, & Shen, 2012). It is also employed in the field of microfluidic devices (Sharma, Dhayal, Shivaprasad, & Jain, 2007), tissue engineering (Leclerc, Duval, Pezron, & Nadaud, 2009), biomolecule immobilisation (Hu, Ma, Zhang, & Wang, 2014) and lipid bilayer support systems (Kim & Jeong, 2011). More recently, in an attempt to modify PDMS membrane as an artificial skin mimic, the use of air plasma treatment has also been reported (Waters et al., 2017). The overall effect on the membrane, and how this change can contribute to altering drug permeation profiles through this membrane was also reported.

In addition to available literature, storage conditions and environmental effects that may contribute to leaching and an aging effect (reported problems often associated with this membrane), were carefully considered, monitored, reported, and controlled in this work.

2.3.1.2 Scanning Electron Microscopy

Scanning Electron Microscopy (SEM) is primarily a spectroscopic technique that uses a beam of electrons to scan the surface of materials, thereby, creating a 3-dimensional image of the material. The basic set-up of SEM involves a light source, a monochromator and lenses to focus the electron beam. Hence, a typical SEM has a fine beam of electrons generated by heating a filament. In the case of the SEM used in this study, a tungsten filament was used as the filament.

The principle of this technique is such that electron beams are accelerated towards an anode and focused using condensed lenses onto a very fine spot on the material, deflected with the help of the lenses to scan and create a surface image of the sample material.

When the electron beam hits the surface of the material, a variety of signals are generated as a result of interactions between the electron beam and atoms of the materials. These signals are mainly:

- Transmitted electrons (beam that passed through the sample)
- Secondary electrons (electrons obtained from the material itself)
- Backscattered electrons (electrons generated from interaction with nuclei of the atom in the material).

Other signals generated includes X-rays and heat, as summarised in Figure 2.2.

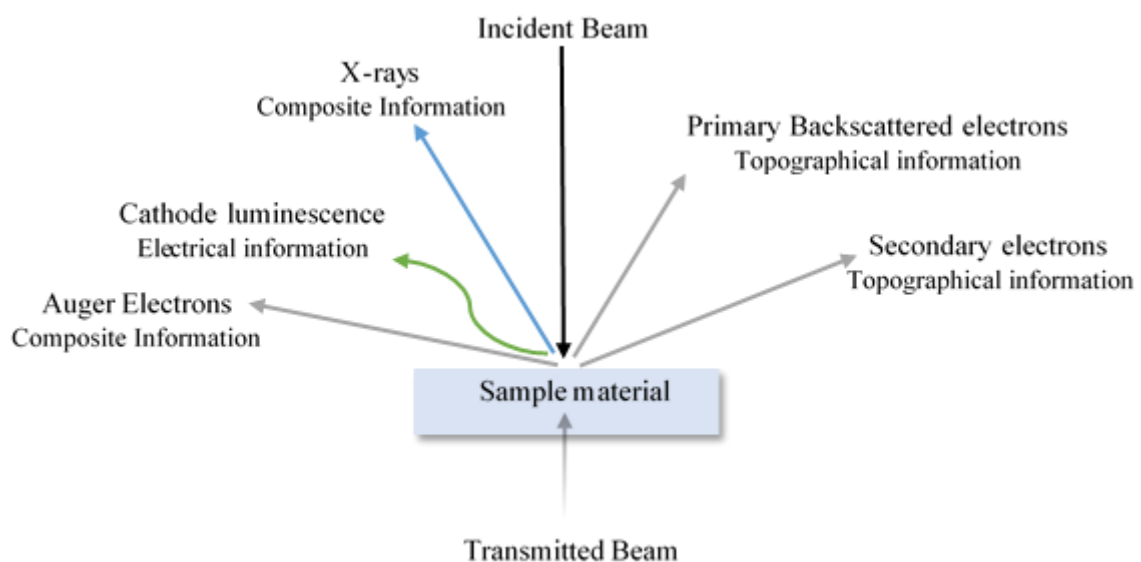


Figure 2. 2 Typical Incident beam interactions with sample material in SEM analysis, adapted with modifications from (Dehm, Howe, & Zweck, 2012)p 4.

Secondary electrons (SE) are released from the surface of the material to give a high-resolution image which is readily interpretable, and this is because of the small depth of penetration associated with this interaction. Back scattering electrons (BSE) on the other hand, are primary beam electrons reflected from atoms of the sample. The BSE give us information about different chemical phases in the sample, and their image resolution is lower compared to that obtained from SE, this phenomenon is associated with depth of penetration in the BSE. X-rays are produced as a result of in-elastic interactions between the primary beam and atoms of the sample material. The interaction results in shell transition which causes the emission of X-rays. The emitted X-rays have an energy characteristic that matches that of the parent, therefore, measurement and detection of these X-rays provides quantitative and qualitative analysis of the sample material, in an analysis referred to as elemental diffraction analysis (EDX) and can have a sampling depth of 1-2 microns.

In SEM analysis there is a continuous flow of electrons, which are deposited on the surface of the sample material. This may cause a reduction in image resolution. In inorganic samples, the SEM process can result in accumulation of charged materials on the surface without discharge which can also contribute to a reduction of the image quality. All these problems are overcome by coating the sample material with gold (as in the case of this study) or carbon. However, this process can cause obscuring of some materials due to possible electric field build-up in between the material surface and the coated layer.

In this research, SEM analysis was performed using a 6060LV JEOL SEM. Prior to the analysis, the non-metallic nature of the unmodified, plasma treated, and modified membranes made it necessary to coat them for effective conductivity using an 80/20 percent gold/palladium sputter coater, and the process was mostly for 40 seconds, using a quorum technologies SC7720 sputter coater. An Everhart-Thornley detector (ETD) was used. Images were obtained at a

stage distance of 15 mm for effective focus, and an acceleration voltage of 20 kV, for cross section observation.

2.3.1.3 Water Contact Angle analysis

Water contact angle (WCA) analysis is a key analysis in this project, as it informs changes that have occurred on the membrane surface in relation to its hydrophilicity. Static contact angle is defined as the measurable angle ($0 - 180^\circ$) that a liquid form when in contact with solid materials. Young's equation (Equation 2.1) tries to describe the contact angle of a liquid on a flat-homogeneous solid surface, by relating the surface tension with:

- the solid-vapor interface (γ_{sv}),
- the solid-liquid interface (γ_{sl}) and
- the liquid-vapor interface (γ_{lv}).

Hydrophilic surfaces have static contact angles in the range of $0^\circ - 90^\circ$, while hydrophobic surfaces display static contact angles between 90° and 180° . Surfaces with contact angles greater than 150° are considered super-hydrophobic (Ramirez-Canon, Miles, Cameron, & Mattia, 2013).

$$\cos \theta = \frac{\gamma_{sv} - \gamma_{sl}}{\gamma_{lv}} \quad \text{Equation 2.1}$$

Where γ_{sv} represents solid-vapor interface, γ_{sl} solid-liquid interface, γ_{lv} liquid-vapor interface and $\cos \theta$ = measured contact angle.

Young's equation depicted in Equation 2.1, also tries to explain behaviours of liquid on solid surfaces in relation to their contact angles. It describes that when $\gamma_{sv} = \gamma_{sl}$ then an angle of 90° is obtained, and liquids tend to coagulate on solid surfaces when $\gamma_{sv} < \gamma_{sl}$.

In this study, static contact angle (SCA) measurement (1 μ L drop size) was used to analyse hydrophilicity behaviours between various types of modified PDMS membranes. Analysis was carried out using a Kruss, Germany, machine equipped with an optical contact angle device, and the process was carried out using an automated dosing system, controlled from a computer operating dispensing syringe and a remote-controlled movable stage. The sessile method in air at room temperature with ultrapure water was used as the probe liquid. All measurements were obtained after three different point measurements within each membrane, with an error of $\pm 2^\circ$. In this study, super hydrophobic PDMS membrane showed a drastic change with characteristics of a hydrophilic membrane.

2.3.1.4 Ultraviolet – visible (UV - vis) spectrophotometry

UV-vis spectrophotometry was used to quantify the concentration of model compounds following permeation analysis.

This spectroscopic analysis uses a spectrometer that produces an incident light of a selected wavelength, followed by a photometer to measure the intensity of the light. In-between the light source and the photometer is where the cuvette (where the sample is placed) is positioned. The resultant intensity captured by the photometer delivers a signalled voltage on to a display device. The intensity of the signal displayed is an objective parameter resulting from net change of light intensity passing through the liquid sample in the cuvette. Therefore, as the concentration of the liquid sample changes, so does the amount of light absorbed by the liquid, thus resulting in changes in the signal displayed (Sommer, 2012).

A UV-visible spectrophotometer uses a light source usually from a tungsten lamp, which generates the visible region of the spectrum and a hydrogen or deuterium lamp to form the ultraviolet wavelengths. The ultraviolet region has a wavelength range of 200 – 400 nm and the visible region has 400 – 800 nm. The ultraviolet and visible light beams are usually

scattered or absorbed by atoms or molecules of substance present in the sample. Absorption spectra is achieved due to an energy transition between the bonding and antibonding outer electrons of the molecule. Therefore, since the absorption spectra is from 200 – 800 nm, it is not advisable to use solvents with very strong absorptions such as most organic solvents in sample preparations. Usually water, ethanol and mild buffers are used as reference solutions for this type of analysis.

Application of this spectroscopic technique to quantify the concentration of a substance in solution by means of its light absorption at appropriate wavelength is conceptualised using the Beer-Lambert law, which states that; when monochromatic light of a specific wavelength passes through a solution, there is usually a quantitative relationship between the solute concentration and intensity of the transmitted light (Commoner & Lipkin, 1949).

$$I = I_0 * 10^{-kcl} \quad \text{Equation 2.2}$$

Where I_0 (cm^2) = intensity of transmitted light using pure solvent, I (cm^2) = intensity of transmitted light when a coloured compound is added, and l = distance of light travel through the solution, in a concentration c , and at a constant k .

However, since the light path (l) in a UV – visible set-up remains constant, Equation 2.2 can be re-written as

$$\frac{I}{I_0} = 10^{-kc} = T \quad \text{Equation 2.3}$$

Where T = transmittance

A logarithmic relationship exists between the transmittance (T), and concentration of compound (I)

$$-\log T = \log (1/T) = kc = \text{Absorbance} \quad \text{Equation 2.4}$$

Since there is a direct relationship between absorbance and concentration, the concentration of a solute can therefore be determined using Equation 2.4. However, there are certain limitations with the law considering solutions can ionise at higher concentrations or solutes within a solution could precipitate to give turbid or cloudy suspensions that may alter absorbance, and consequently provide a wrong concentration profile. As such, it is important to note that the law is more accurate at low concentrations.

A combination of very little sample preparation and how it can be easily coupled with a flow-through system, makes it a suitable technique for the determination of model compound concentration in this research. However, considering different chemical modifications employed in modifying PDMS membrane, it was necessary to support the technique with high-performance liquid chromatography (HPLC), as discussed in Section 2.3.1.8.

2.3.1.5 Brunauer-Emmett-Teller Technique

The Brunauer-Emmett-Teller (BET) technique is a physical method used to study surface properties of materials. The method uses condensation or adsorption of a process gas, (usually N₂, Ar or CO₂) with known sizes onto the surface of sample material analysed. The quantity of gas adsorbed on the sample material, and sample pressure obtained, are measured at a constant temperature corresponding to the boiling point of the process gas used in the analysis, and this data is used to produce an adsorption-desorption isotherm and subsequently, porosity calculations.

This technique is used in this study to quantify changes that may occur as a result of modification processes as it relates to changes in permeation profile. Results obtained with the help of the technique, further helps to inform an opinion about the effect of modification on the membrane surface area, so that associated permeation changes can be attributed to chemical changes that may have occurred as a result of molecular interactions between atoms on the

membrane surface and the model compounds, and not as a result of physical change from the membrane.

The principles of BET rely on the ability of a monolayer gas formation on a given sample (the number of adsorbed molecules within the sample surface) and by fitting the experimental adsorption data into the BET equation, then the total surface area of given sample can be obtained. Hence, when a pre- and post-sample analysis are compared, resultant changes in surface area, can be easily identified.

$$\frac{P}{V(P_o - P)} = \frac{1}{V_m C} + \frac{C-1}{V_m C} \left(\frac{P}{P_o} \right) \quad \text{Equation 2.5}$$

In the BET equation depicted in Equation 2.5, P is the actual gas pressure, V = volume of gas absorbed by the material, P_o = saturation pressure of a given temperature, V_m = monolayer capacity, and C is a constant (representing enthalpy of adsorption). Specific surface is obtained using this equation by simply multiplying monolayer capacity with cross-sectional area of the individual molecule absorbed. However, application of the principle is based under the assumption that: the surface is flat and all sites on the surface are equivalent; only a monolayer is formed i.e. no lateral interactions between adsorbed molecules; an infinite layer can be formed and molecular adsorption energy is equal to the liquefaction energy except for molecules in the first layer (Kruk & Jaroniec, 2001).

In this study the process was carried out using a Micromeritics ASAP 2020 physisorption analyser (Figure 2.3). Samples were degassed at 50 °C under vacuum for 18 hours using nitrogen as the process gas. This step in the process helps remove unwanted contaminants (gases and vapours) from the membrane surface which may interfere with the experimental results and then conditioned with nitrogen as the processed gas for 6 hours. After outgassing,

surface area was determined using nitrogen vapour adsorption data (77 K) and were evaluated by the Brunauer-Emmett-Teller model.

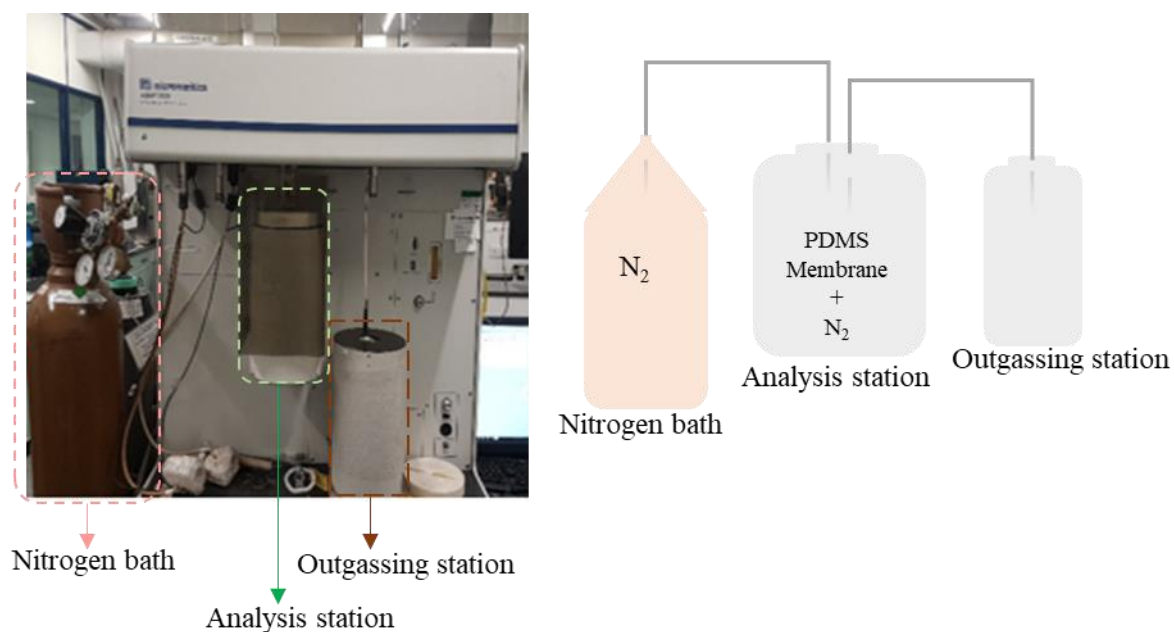


Figure 2. 3 A typical BET analyser (UoH Chemistry Lab, 2019)

2.3.1.6 Attenuated Total Reflectance-Fourier Transform Infra-red spectroscopy

Attenuated Total Reflectance-Fourier Transform Infra-red spectroscopy (ATR-FTIR) is another type of Fourier transform Infrared Spectroscopy (FTIR). FTIR, just like most spectroscopic techniques consists of a light source, monochromator and a detector. One of the main advantages of FTIR is its ability to analyse solid, liquid and gaseous substances with little or no sample preparation required.

The infrared (IR) technique generally involves sources of radiation (light sources), which are usually inert solids that are heated electrically to initiate thermal emission of radiation in the infrared region of the electromagnetic spectrum, and these beams are subsequently directed towards a monochromator which selectively allows the light to interact with the sample, hence, generating a spectrum captured by the detector, which ultimately gives subjective information

of the sample. However, while the working principle of infrared spectroscopy remains the same, there have been changes in the analytical set-up over the years.

The first type of IR was developed in the 1950s. Apart from the radiation source, it has an optical prism system made up of NaCl, which scans the sample material and produces spectrum results. IR produces light of different frequencies, but the monochromator installed in its system has a certain motor configuration which selectively opens as the emitted radiation reflects on it. As mirrors in the monochromator move, each wavelength of light within the emitted beam is periodically reflected at different modulated rates, such that each transmitted beam has a different spectrum. The resultant spectrum is captured by detectors, and this gives molecular information for the sample analysed. However, this type of IR has a narrow scan range and produces poor repeatability, which is why it is no longer in use today (Larsen, 2020).

The second generation produced in the 1960s includes an optical chopper that has a double beam design. The incident radiation from the IR source is directed towards this optical chopper (that is equipped with special mirror gratings and slits), and it splits the incident radiation into two. The analytical design in this type of IR machine is such that one of the split beams travels towards a sample compartment and the other towards a reference cell, for analytical comparison.

The incident beam that travels through the sample emits radiation, and the emitted radiation is directed towards a detector. The detectors are mostly classified as either quantum (photon) or thermal detectors. This additional optical splitter and monochromatic feature is the distinct feature compared to the first IR generation. There is a change between the incident beam travelling through the sample cell and the beam that travels through the reference cell, this change is considered an off-null signal (difference from reference signal), and this comparison

gives the final spectrum. This type of IR is called dispersion IR (Larsen, 2020) as shown in Figure 2.4.

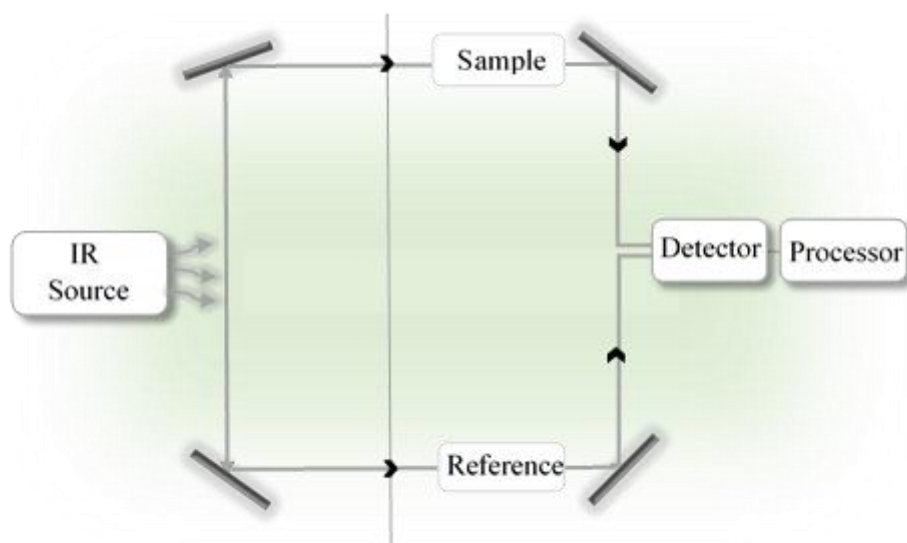


Figure 2. 4 Schematic representation of a Dispersive IR.

However, this type of IR has a low scan speed, low sensitivity and poor wavelength accuracy, giving rise to the third generation, i.e. 'Fourier Transform infrared spectrometer'(FTIR).

In FTIR, instead of juxtaposing data captured by detectors (emitted from a reference and sample cell), it requires a 'Michelson interferometer' which splits the IR radiation, allowing one path to run through the sample, and the other via a stationed mirror, and subsequently recombines the two emitted lights from both pathways. Consequently, measuring the change in intensity of these beams from different paths, with the help of an algorithm called the 'Fourier transform', which transforms the acquired spectrum into wavenumbers in cm^{-1} . This rendered the use of a reference beam obsolete (Perkins, 1986; Skoog, Holler, & Crouch, 2017). Consequently, broadening the application of IR spectroscopy.

The infrared region is divided into the near-infrared region ($12000 - 4000\text{cm}^{-1}$), mid-infrared region ($4000 - 200\text{ cm}^{-1}$) and far-infrared region ($50 - 1000\text{ cm}^{-1}$). However, in the case of this study it is within $4000 - 400\text{ cm}^{-1}$, partly because it falls within the absorption radiation range

of most organic and inorganic compounds, hence the most commonly used, and the research interest is less concerned with the fingerprint region ($> 400\text{ cm}^{-1}$) as quite distinct materials were used.

However, the nature of the membrane analysed in this study necessitated the use of Attenuated total reflectance (ATR)-FTIR spectroscopy. This type of FTIR has an additional ATR crystal strategically placed in the sample compartment area. The sample material is in contact with this crystal, and reflection between IR incident radiation and the ATR crystal produces a change in refractive indices between the two materials, resulting in a phenomenon called ‘evanescent wave’, and this wave extends into the sample. The phenomenon allows consolidation of IR radiation and gives a more robust interaction with the sample, as shown in Figure 2.5. This additional boost and consolidation of the IR radiation into a confined area provides a higher limit of detection in samples analysed (Griffiths & De Haseth, 2007; Smith, 2011).

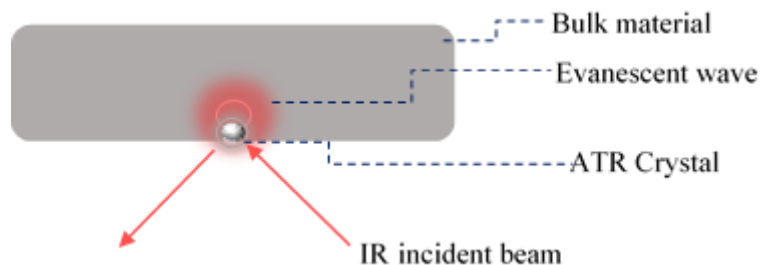


Figure 2. 5 Schematic illustration of ATR single bounce cell

In this study, comparative analysis specifically related to bond changes of modified and unmodified membranes was carried out using this technique. A Nicolet FTIR 380 machine was used, which was in attenuated total reflectance mode with a diamond crystal as the sensor. Omnic software was employed for data analysis and analysis wavelength was adjusted from $400 - 4000\text{ cm}^{-1}$. Bonds corresponding to prominent functional groups were identified in conformity with existing literature and were analysed. Limitations resulting from the position

of the sensor as shown in Figure 2.6, were addressed using other supporting techniques, such as optical microscopy.

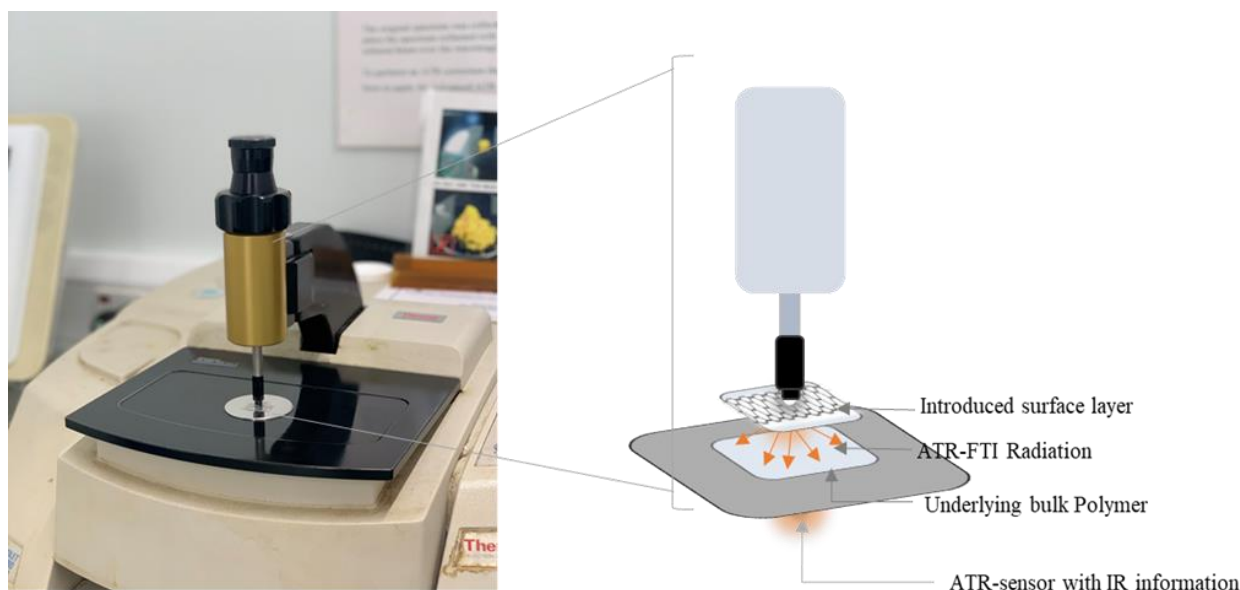


Figure 2. 6 Graphical and schematic representation of ATR-FTIR technique, illustrating working methods of the technique. (FTIR laboratory UoH, 2020)

2.3.1.7 Permeation Analysis

Permeation analysis using diffusion cells in a controlled hydrostatic and hydrodynamic donor and receptor compartment respectively, was experimentally performed in triplicate, for each model compound used. Each saturated solution of drug was prepared using pH 7.4 phosphate buffered saline. The buffer was prepared by dissolving 8.766 g of sodium chloride, 7.385 g of dipotassium phosphate and 1.034 g of dihydrogen potassium phosphate in 1 L of ultra-pure water (18.2 M Ω , Barnstead). pH adjustment was carried out using dilute concentrations of HCl and NaOH where necessary.

Saturated drug solutions were prepared by adding an excess amount of sample drug in 10 mL sample vials containing buffer. Sample vials containing a micro-size magnetic stirrer were mounted in a water bath maintained at ~32 °C for 24 hours, equipped with a magnetic stirrer

plate. This process is independent of the flow through measurement, as it is primarily aimed to acquire the saturated form of model drug intended for a given permeation analysis.

Following the process highlighted above, resulting solutions were filtered, and added via a syringe, into the donor compartments of the flow through system to avoid bubbles. Openings on the donor compartment were occluded to maintain constant temperature and prevent evaporation. The donor compartment was mounted on a specialised solid support designed to have a hollow internal feature, where pre-heated water of approximately 35.5 °C circulated through, to help maintain a stable temperature within the donor compartment. Samples passing through specialised tubes that connected the donor and receiver compartment were collected from the receptor arm at 30-minute intervals for 6 hours and analysed using UV-visible spectroscopy and HPLC. Diagrams to illustrate the analytical process are shown in Figures 2.7 and 2.8.

A standard calibration graph of each drug ($R^2 \geq 0.9$.) was used to calculate its resultant concentration after the experiment, covering the concentration range of the samples obtained in the permeation analysis.

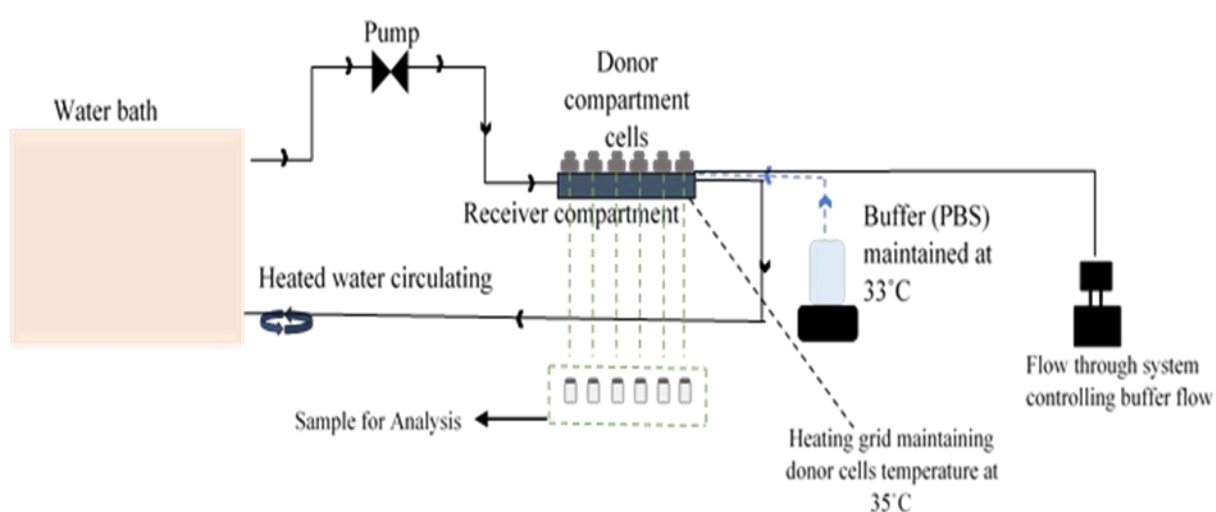


Figure 2. 7 Schematic representation of a flow-through system

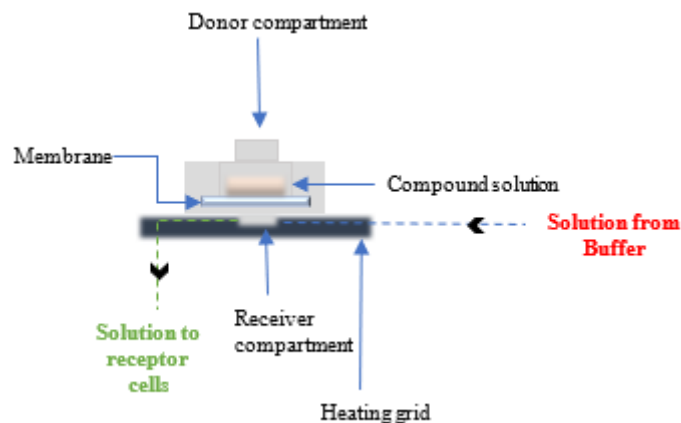


Figure 2. 8 Schematic representation of a diffusion cell used for permeation analysis

2.3.1.8 High Performance Liquid Chromatography

This is a relatively straightforward analytical technique which was also employed in this study. Its principle is simply based on the distribution of analyte (sample material), between a mobile phase (eluent) and a stationary phase (column). Depending on chemical structures of different entities that may be present in the analyte, movement of these entities are staggered while passing through a stationary phase (mainly due to differences in physicochemical properties such as polarities, and level of affinity to the stationary phase), conveyed by the mobile phase, in a specialised set-up present in a typical high-performance liquid chromatography (HPLC) system. These interactions between the stationary phase material and the eluents are distinct, and consequently determines the time needed for each entity to be eluted. In other words, different constituents of a sample are eluted at different times, and the time each component takes to pass through the column is termed as the ‘retention time’, and it serves as a fingerprint upon which these entities can be identified, and in addition achieving separation.

Upon analytes leaving the stationary phase of the HPLC, different types of detectors are used to qualify the eluents, and this different detector type forms the main basis upon which HPLC systems can be classified.

A typical HPLC set-up involves a solvent reservoir (mobile phase), a pump (which delivers the solvent at a high pressure and constant speed, to minimise noise), an injector valve (through which analytes are introduced to the system), a column (stationary phase), a detector (which produces a signal proportional to the amount of analyte emerging from the column, thus providing an avenue for quantitative analysis) and a data processing system.

In this study, a Shimadzu HPLC system, equipped with a pump, oven, an autosampler and a UV-visible detector was used. A stainless steel C18 column, and an aqueous solution of acetonitrile [80:20] as the mobile phase solution was also used.

The chromatographic conditions were established and are listed in Table 2.4.

Table 2. 4 Summary of HPLC experimental conditions

Parameter	Specification		
	System	Pump	Detector
Instrument	Shimadzu, Kyoto, Japan HPLC	Phenomex Luna 5 μ L C18 column (250mm \times 4.60 mm dimension)	UV-Vis detector
Analysis software	Lab solutions (LC-solutions), Shimadzu		
Eluent A (non -aqueous solution)	Acetonitrile		
Eluent B (aqueous solution)	Water		
Flow rate (mobile phase)	1 mL/min		
Injection volume	10 μ L		
Method of Elution	Isocratic (Constant flow of mobile phase solution)		
Column Temperature	30°C		
Column operational method	Reverse phase chromatography column		

2.3.1.9 Optical Microscopy

The need to observe in detail changes that may have occurred on the surface of sample material used in this research work following modifications prompted the use of optical microscopy.

Although the limiting magnifying power of optical microscopy is very much established compared to electron microscopy (X. Chen, Zheng, & Liu, 2011), the need to view a moderately enlarged form of the membrane sufficient enough to determine how grafted materials are physically attached and distributed on the material surface cannot be over-emphasised.

Although different types of imaging systems have been developed over the years, their basic concept remains the same. An optical imaging system requires objective lenses and an eyepiece. These objectives lenses simply magnify objects for the observer. When a sample material is placed in the space provided within the microscope, optical waves within the visible spectrum help generate an image of the sample, which is first cast on a focal plane. This image is magnified by an intermediate lens, which then reflects it on the eyepiece. The eyepiece also works as a magnifier, and subsequently a magnified and virtual image is provided for the observer. Spatial resolutions of any well-designed microscope are provided by the objective lens, and although the eye piece can serve as a magnifier itself, it cannot in principle help in increasing focus or improving resolution.

Resolutions in optical microscopy can be determined using the Rayleigh equation (Mertz, 2019; Tsujita, 1967)

$$\Delta r_o = 0.62\lambda/n \sin \alpha \quad \text{Equation 2.6}$$

Where Δr_o = minimum resolvable distance, λ = wavelength of the light source, n = refractive index between the lens and the object, and α = half angle aperture – half inclination of the lens to the objective points.

Optical microscopy can be divided into various types, including transmission and reflection (X. Chen et al., 2011). Transmission microscopy uses light that directly passes through a transmitted material, onto the sample, while, reflection microscopy has a light source

strategically installed inside the microscope, which illuminates non-transparent objects, and the reflected light is collected by the sample. The technique can also be classified based on observation methods such as, polarised light microscopy, dark field microscopy, and bright field microscopy. Although, bright field microscopy is sometimes employed, its dependence on an environmental light source and the fact that colourless materials are not visible using this technique, makes its use limited (Tatosian, Shuler, & Kim, 2005)

In this study optical microscopy analysis was carried out using a Keyence digital microscope VHX-2000 equipped with VH-z250R sensor, set at a multi-scan mode. Samples were placed in a sterilised glass plate to maintain a flat surface which enabled autofocus on the machine. The stage was also adjusted to a 20 mm working distance and x 250 magnification was maintained throughout the process. The machine was set to reflectance mode.

2.4 Conclusion

In summary, this chapter provides a list of materials and analytical methods utilised in this work, including justification for all the processes employed in this study. Using the techniques discussed, results and discussion arising from these experiments are subsequently presented in Chapters 3-5.

References

- Bodas, D., Khan-Malek, C. J. S., & Chemical, A. B. (2007). Hydrophilization and hydrophobic recovery of PDMS by oxygen plasma and chemical treatment—An SEM investigation. *Sensors and Actuators B: Chemical*, 123(1), 368-373.
- Botvay, A., Máthé, Á., & Pöpl, L. (1999). Nitration of polyethersulfone by ammonium nitrate and trifluoroacetic anhydride. *Polymer*, 40(17), 4965-4970.
- Chan, C.-M., Ko, T.-M., & Hiraoka, H. (1996). Polymer surface modification by plasmas and photons. *Surface science reports*, 24(1-2), 1-54.
- Chen, X., Zheng, B., & Liu, H. (2011). Optical and digital microscopic imaging techniques and applications in pathology. *Analytical Cellular Pathology*, 34(1, 2), 5-18.
- Commoner, B., & Lipkin, D. (1949). The application of the Beer-Lambert law to optically anisotropic systems. *Science*, 110(2845), 41-43.
- Dehm, G., Howe, J. M., & Zweck, J. (2012). *In-situ electron microscopy: applications in physics, chemistry and materials science*: 62(1), 193-203
- Goda, T., Konno, T., Takai, M., Moro, T., & Ishihara, K. J. B. (2006). Biomimetic phosphorylcholine polymer grafting from polydimethylsiloxane surface using photo-induced polymerization. *Biomaterials*, 27(30), 5151-5160.
- Griffiths, P. R., & De Haseth, J. A. (2007). *Fourier transform infrared spectrometry* (Vol. 171): John Wiley & Sons.
- Gunda, N. S. K., Singh, M., Norman, L., Kaur, K., & Mitra, S. K. (2014). Optimization and characterization of biomolecule immobilization on silicon substrates using (3-aminopropyl) triethoxysilane (APTES) and glutaraldehyde linker. *Applied Surface Science*, 305, 522-530.
- Hu, Y., Ma, B., Zhang, Y., & Wang, M. (2014). Small molecule—folic acid modification on nanopatterned PDMS and investigation on its surface property. *Biomedical microdevices*, 16(3), 487-497.
- Kim, H. T., & Jeong, O. C. J. M. E. (2011). PDMS surface modification using atmospheric pressure plasma. *Microelectron engineering* 88(8), 2281-2285.
- Kruk, M., & Jaroniec, M. (2001). Gas adsorption characterization of ordered organic–inorganic nanocomposite materials. *Chemistry of materials*, 13(10), 3169-3183.
- Larsen, D. (2020). Reimaging the Future of Chemistry Textbooks with LibreTexts pg 1844.
- Leclerc, E., Duval, J. L., Pezron, I., & Nadaud, F. (2009). Behaviors of liver and kidney explants from chicken embryos inside plasma treated PDMS microchannels. *Materials Science and Engineering: C*, 29(3), 861-868.
- Li, J., Wang, M., & Shen, Y. (2012). Chemical modification on top of nanotopography to enhance surface properties of PDMS. *Surface and Coatings Technology*, 206(8-9), 2161-2167.
- Mertz, J. (2019). *Introduction to optical microscopy*: Cambridge University Press.
- Nehra, V., Kumar, A., & Dwivedi, H. (2008). Atmospheric non-thermal plasma sources. *International Journal of Engineering*, 2(1), 53-68.
- Perkins, W. (1986). Fourier transform-infrared spectroscopy: Part I. Instrumentation. *Journal of Chemical Education*, 63(1), A5.
- Ramirez-Canon, A., Miles, D. O., Cameron, P. J., & Mattia, D. (2013). Zinc oxide nanostructured films produced via anodization: a rational design approach. *RSC advances*, 3(47), 25323-25330.
- Sharma, V., Dhayal, M., Shivaprasad, S., & Jain, S. (2007). Surface characterization of plasma-treated and PEG-grafted PDMS for micro fluidic applications. *Vacuum*, 81(9), 1094-1100.

- Skoog, D. A., Holler, F. J., & Crouch, S. R. (2017). *Principles of instrumental analysis*: Cengage learning.
- Smith, B. C. (2011). *Fundamentals of Fourier transform infrared spectroscopy*: CRC press.
- Sommer, L. (2012). *Analytical absorption spectrophotometry in the visible and ultraviolet: the principles*: Elsevier.
- Tatosian, D. A., Shuler, M. L., & Kim, D. (2005). Portable in situ fluorescence cytometry of microscale cell-based assays. *Optics letters*, 30(13), 1689-1691.
- Tsujita, J. (1967). LC Martin: The Theory oh the Microscope, Blackie and Son Ltd. London, 1966 488. *Journal of the Physical Society of Japan*, 22(6), 395.
- Yam, M. F., Mohammed, E.A.H., Ang, L. F., Pei, L., Darwis, Y., Mahmud, R., & Ahmad, M. (2012). A simple isocratic HPLC method for the simultaneous eupatorin, and 3'-hydroxy-5, 6, 7, 4'-tetramethoxyflavone in Orthosiphon stamineus extracts. *Journal of Acupuncture and Meridian Studies*, 5(4), 176-182
- Waters, L. J., Finch, C. V., Bhuiyan, A. M. H., Hemming, K., & Mitchell, J. C. (2017). Effect of plasma surface treatment of poly (dimethylsiloxane) on the permeation of pharmaceutical compounds. *Journal of pharmaceutical analysis*, 7(5), 338-342.
- Zhou, J., Ellis, A. V., & Voelcker, N. H. (2010). Recent developments in PDMS surface modification for microfluidic devices. *Electrophoresis*, 31(1), 2-16.

Chapter 3

Poly(dimethylsiloxane): Membrane optimisations and the chemical vapour deposit process

3.1. Introduction

It is known that the surface of PDMS membrane is non-porous, similar to human skin, and xenobiotics can only permeate through the membrane with the help of physicochemical interactions by atoms or molecules present on the surface of the membrane (as discussed in Chapter 1). However, the exact mechanism through which substances permeate membrane needs to be established and understood before any attempts to modify it can be undertaken.

In this study, to effectively compare any membrane to that of skin, an approach was undertaken of comparing permeation data through PDMS membrane with that of skin, i.e. by trying to mimic experimental conditions similar to the skin surface.

3.2. Results and Discussion

3.2.1. Standard PDMS membrane

3.2.1.1 Permeability Studies

Generally, two distinct approaches are employed in drug permeation analysis namely, a finite and infinite dose approach. The basic difference between the two approaches is such that the former requires a known and calculated drug concentration that can be changed and varied according to suitability of the intended experiment(s), while the latter employs a constant concentration usually from the saturated form of the drug in question (Neupane, Boddu, Renukuntla, Babu, & Tiwari, 2020). The infinite dose approach was adopted in this study, and this is simply to eliminate variations that may result from different drug concentrations and preparations in the analysis. In other words, variables were meant to remain as low as possible, making it easier to track and attribute changes resulting from surface membrane modifications. Hence, super saturated solutions (infinite doses) were prepared for all model compounds in this study and the approach was adopted throughout the research.

Standard permeation methodology was adopted (according to European Medicines Agency (EMA) Guidelines) for *in vitro* permeation studies with slight modifications: the system was allowed to equilibrate for 24 hours prior to analysis, the flow rate was adjusted to 100 rpm and the total experimental duration was 6 hours to cover the therapeutic window. These modifications were all adopted to more closely replicate the human system, for example equilibration was necessary to allow the donor compartment to attain 36 °C. Table 3.1 highlights the mean cumulative mass of drug compounds used in this chapter, and in an attempt to relate these values with solubility as it relates to permeation studies, the drugs biopharmaceutical classification is also presented alongside.

Table 3. 1 Cumulative mass of model drugs used in this chapter alongside their biopharmaceutical classification, which are: caffeine (CAF), lidocaine (LID), benzoic acid (BZA), ethyl paraben (EPB), benzocaine (BEN), salicylic acid (SAL), ibuprofen (IBU), diclofenac (DCF), ketoprofen (KPF), antipyrine (ANT), tetracaine (TTC), procaine hydrochloride (PRC), and pentoxifylline (PTX) permeated through standard PDMS membrane following permeation analysis (mean \pm standard deviation, rounded to whole numbers, $n = 3$).

Compounds	Mean cumulative mass permeated after 6 hours ($\mu\text{g}/\text{cm}^2$)	BCS*
CAF	72 ± 4	I**
LID	3351 ± 23	II**
BZA	4513 ± 18	III**
EPB	323 ± 09	**
BEN	2294 ± 16	II**
SAL	862 ± 06	I**
IBU	1176 ± 11	II**
DCF	134 ± 04	II**
KPF	85 ± 04	II**
ANT	313 ± 02	I**
TTC	1551 ± 11	II**
PRC	33 ± 01	**
PTX	79 ± 01	III**

*Biopharmaceutical classification

**Class

The concentration of model pharmaceutical compounds was calculated using equations obtained in their standard calibration plots ($R^2 = 0.99$) (Figure 3.1 and 3.2). These concentrations were subsequently integrated to give cumulative mass. However, the flow through system cells used in this work have a diffusion surface area < 1 (0.56 cm^2), for uniformity, all cumulative mass obtained herein, were adjusted to reflect cumulative mass/ cm^2 for effective comparisons.

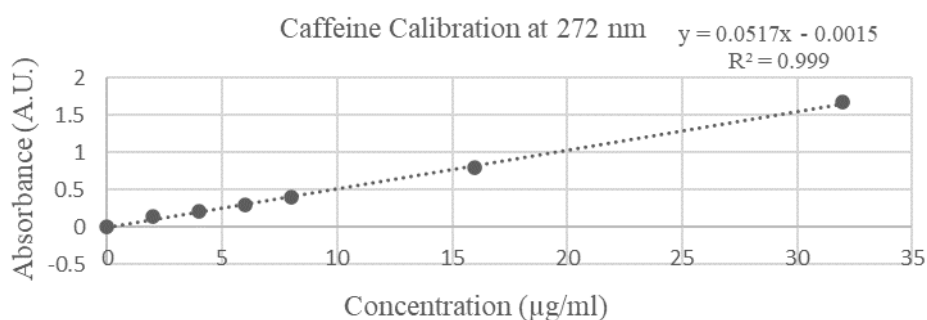


Figure 3. 1 Caffeine calibration at 272 nm

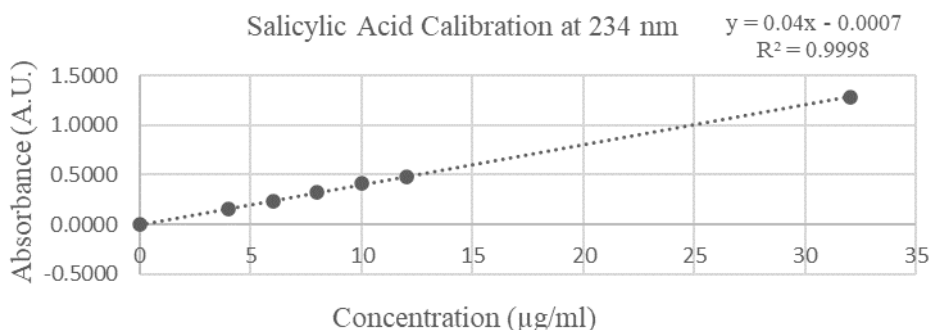


Figure 3. 2 Salicylic acid calibration at 234 nm

Interestingly following the permeation process, acceptable steady state was obtained (Figure 3.3 – 3.5), as all experiments undertaken with model compounds had regression values of $R^2 \geq 0.9$. At this stage of the research, it was possible to draw the following conclusions regarding the use of standard PDMS (N-PDMS) membrane for permeation analysis.

- ✓ The membrane is stable throughout the duration of the experiment (6 hours)

- ✓ The permeation profiles of compounds analysed are within an acceptable limit that can be modified to mimic permeation profiles through skin
- ✓ It is a selective permeable membrane, as each compound used gave a distinct permeation profile, as a result, a quantity-structure activity can be established, which will help in predicting its behaviour. In other words, selectivity, activity and stability were established.
- ✓ Steady state (J_{ss}) was obtained, and thus allowed application of Fick's law and the introduction of a physical factor (permeation coefficient K_p), which will allow a comparison to be made between experimental data, and that of human skin.

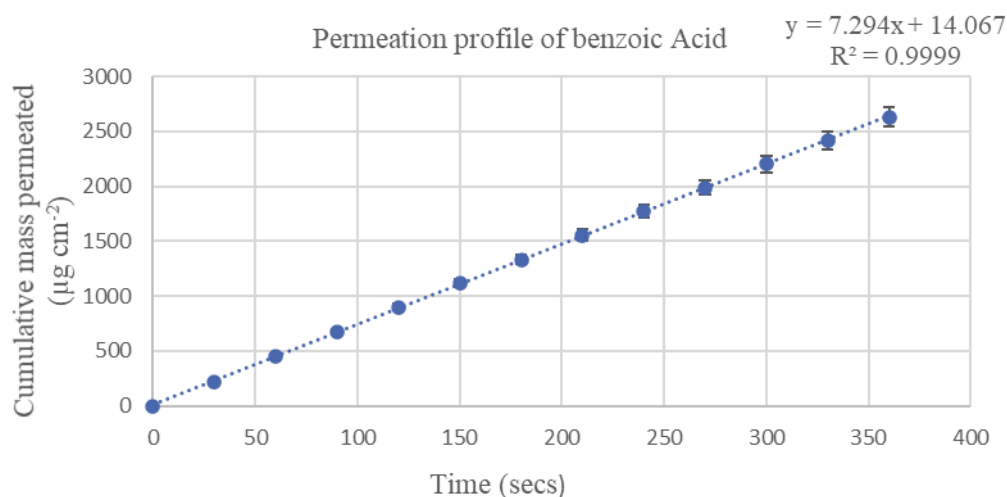


Figure 3. 3 Steady state flux of benzoic acid through standard PDMS

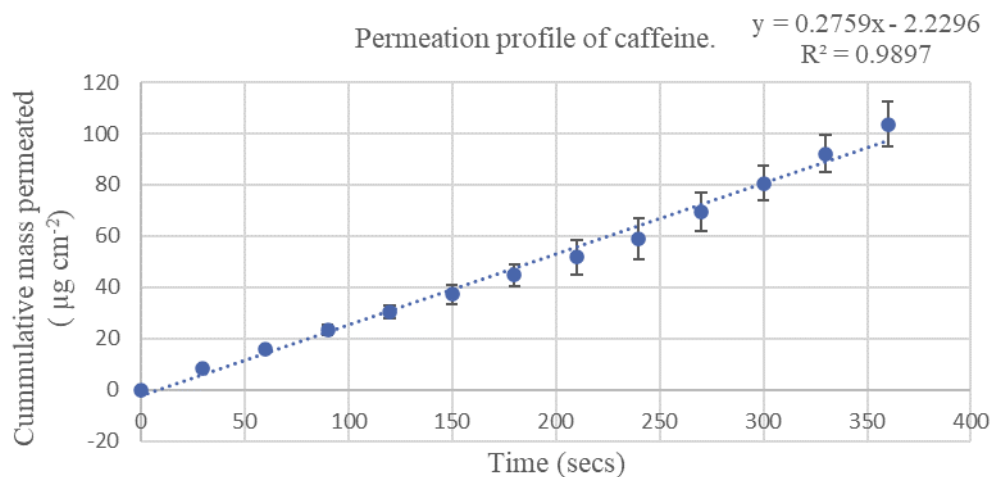


Figure 3. 4 Steady state flux of caffeine through standard PDMS

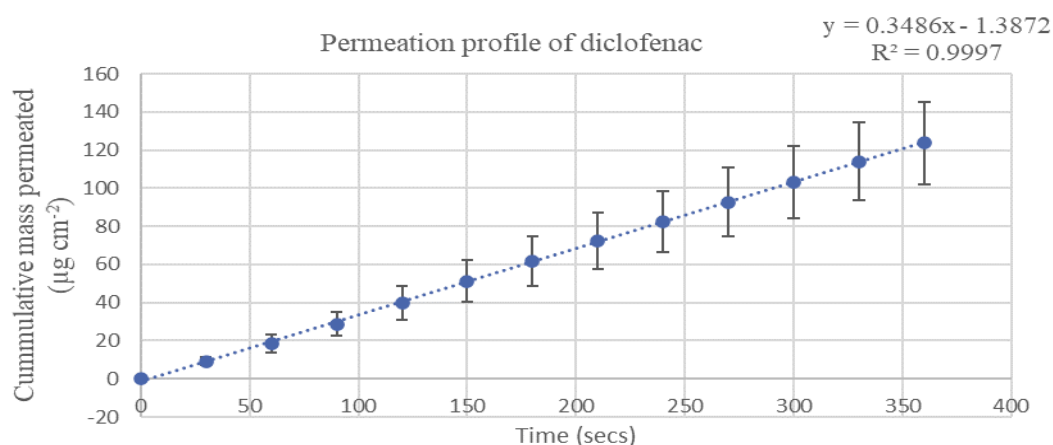


Figure 3. 5 Steady state flux of diclofenac through standard PDMS

3.2.2. Optimisation Processes

As stated in Chapter 1, the surface of PDMS membrane is made up of methyl groups, and to activate the surface atoms, a solventless process was adopted. The membrane was exposed to a series of plasma treatments to enable activation of its surface, before any further modifications were adopted. In this section of the work, these processes will be highlighted, along with confirmatory techniques.

3.2.2.1 Atmospheric Pressure Nonthermal Air Plasma Treatment of Poly(dimethylsiloxane)

Fundamentally, PDMS has a silicone-oxygen backbone, with a bond energy in the range of 350-470 kJ mol⁻¹. This high bond energy makes it stable thermally, with degradation occurring at about 350 °C (De Jaeger et al., 2008). The surface of the membrane is also embedded with methyl groups, making it relatively inert, consequently, making it challenging to chemically modify. It was seen in previous permeation analysis that compounds selectively pass through the membrane in relatively low amounts courtesy of the silicone-oxygen arrangements, and surface methyl groups. To modify this membrane therefore, it was necessary to create reactive sites, i.e. activate the membrane surface, to facilitate further modification.

PDMS used in this study was treated under plasma; energy from the plasma facilitates abstraction of hydrogen from methyl groups present on the membrane surface, thereby leaving an unstable methylene group (-CH₂). The hydrogen removed further reacts with air in the plasma chamber, or atmospheric oxygen to form a hydroxyl group (-OH). The hydroxyl group formed, attacks, and displaces the unstable methylene group that was left on the membrane surface. Consequently, a hydrolysed surface can be achieved because of the plasma treatment. Practically, the hydrolysed surface is suitable for further treatment, such as in the work of (Bodas, Khan-Malek, & Chemical, 2007), (Zhou, Ellis, & Voelcker, 2010), (Goda, Konno, Takai, Moro, & Ishihara, 2006) and (Waters, Finch, Bhuiyan, Hemming, & Mitchell, 2017). Although, there are other surface-activating methods, such as UV/irradiation (Schnyder et al., 2003), which employ the same mechanism in hydrolysing the PDMS surface, the solventless air plasma treatment method is more appropriate for this study and summarised in Figure 3.6.

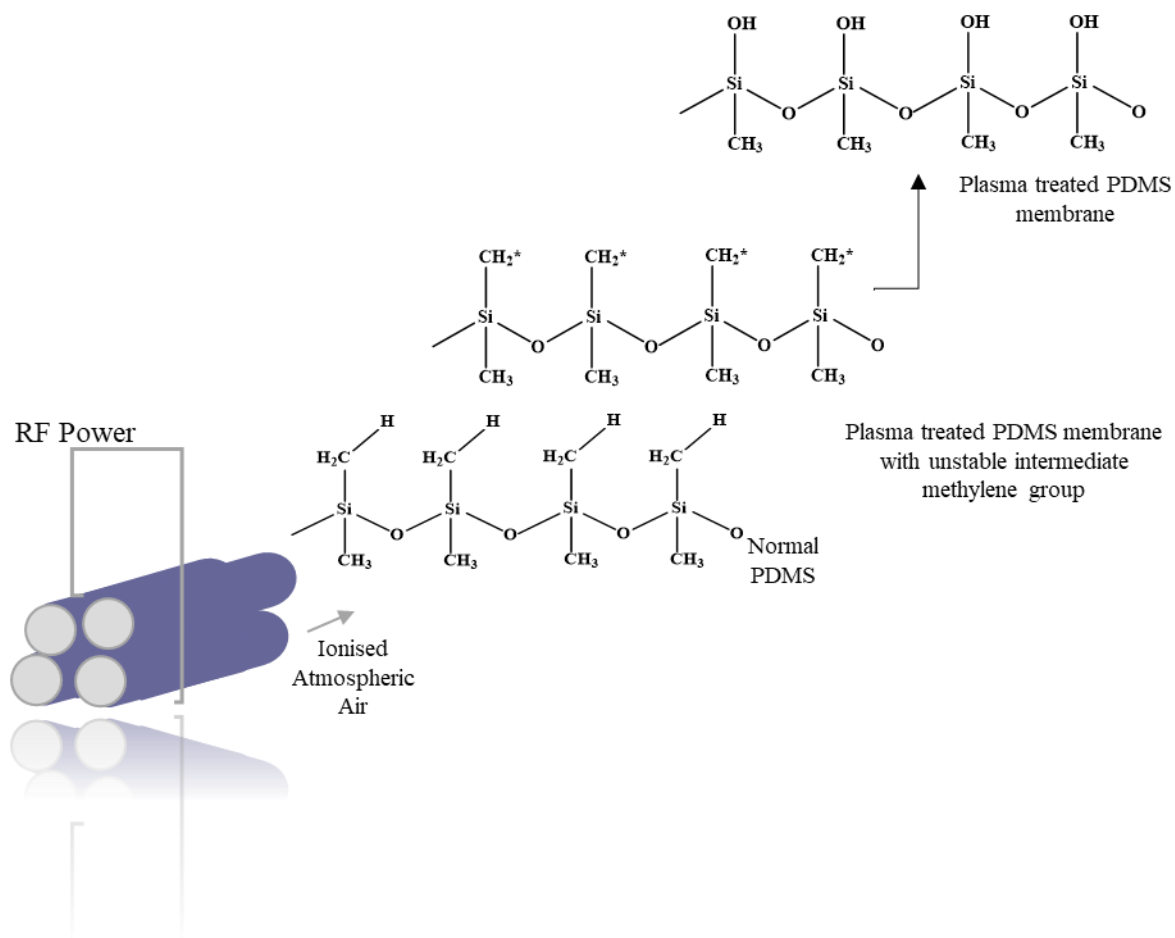


Figure 3. 6 Schematic representation of the plasma treatment mechanism employed in this study to modify the surface of PDMS membrane.

3.2.2.2 Scanning Electron Microscopy

Amongst the spectroscopic techniques employed in this study to visualise surface changes on the membrane is Scanning Electron Microscopy (SEM). Upon plasma treating the membrane, the following results were obtained using this analysis (Figures 3.7 and 3.8).

Plasma treatment – Parameters and Effects

This image represents the standard PDMS membrane surface (1-2 microns' depth). It visualises the surface of the membrane prior to any form of modification.

Similar to the description given by (Majeed et al., 2012), the membrane shows a smooth and homogeneous surface.

It is noteworthy to mention that the membrane was coated before carrying out the SEM analysis (Section 2.3.1.2). Additionally, the membrane was in 10 kV (accelerating voltage), and a working image distance of 15 mm.

Permeation results presented in Section 3.2.1.1 were carried out using this form of the membrane.

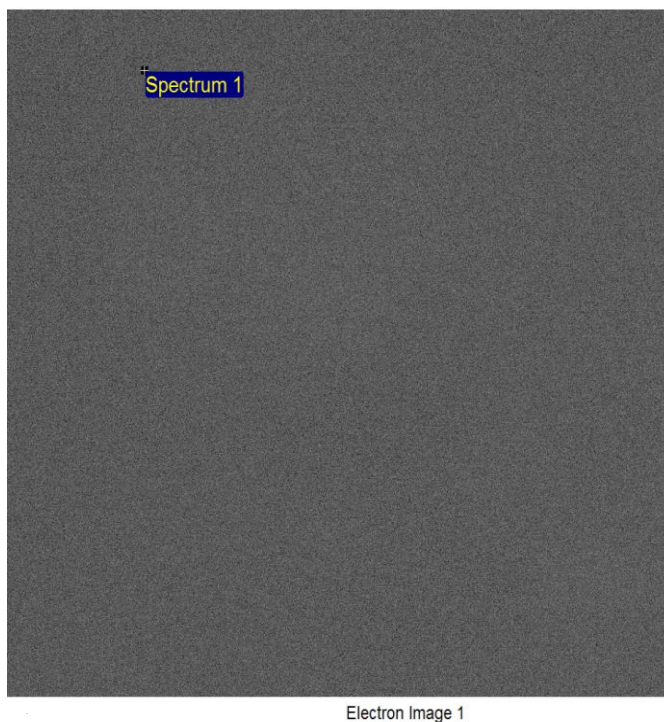


Figure 3. 7 SEM image of Standard PDMS prior to modification ($\times 500$)

Plasma treatment – Parameters and Effects

The image represents a plasma treated PDMS membrane surface (1-2 microns' depth). Comparing this image to Figure 3.7, one can easily see a striking difference between the two images.

This change can be easily presumed to arise from possible deformity following a thermal process although this is not the case as it could not have been from a thermal process. In this result it is believed that a chemical interaction has likely occurred from the plasma process, given rise to the striking difference between the two images (Figure 3.7 and 3.8).

The plasma parameters in this modification are air as the process gas, at 100 W, flow rate of 8 SCCM and a treatment time of 120 seconds.

NB. SEM parameters were kept constant throughout the study, for effective comparisons

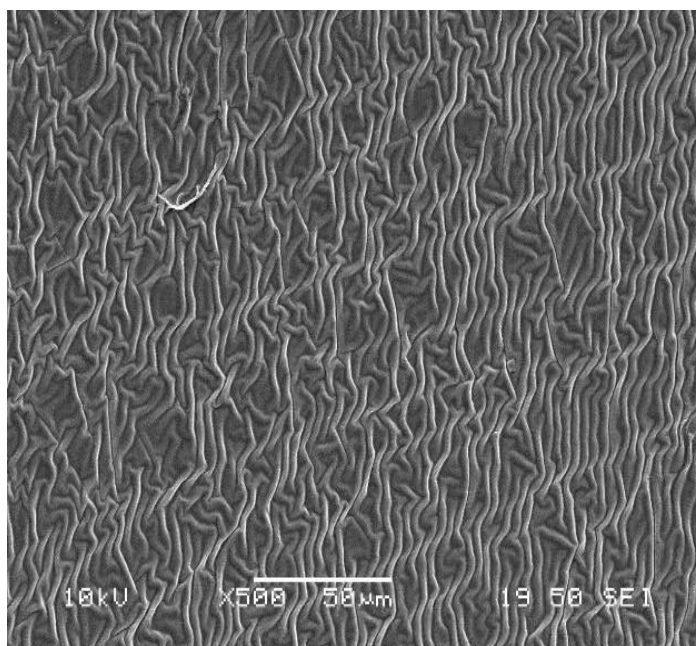


Figure 3. 8 SEM image of plasma treated PDMS (over cured) ($\times 500$)

Although, the above process seemed potentially successful from the SEM image, it presented a limitation in the overall aim of this study. Following the plasma treatment process, the membrane was used for permeation measurements, which resulted in over-absorption (results not shown). It became a disadvantage to this study especially how the plasma treated membrane was unable to maintain a concurrent permeation profile necessary for concordance after repeated runs ($n = 3$). It was concluded that the membrane must have been subjected to an excessive exposure time, as a result Si-O_x membrane bonds became compromised, resulting in possible crack formation or structural damage, that may have led to the undesirable increase in permeability. An optimised process was therefore chosen as shown in Figure 3.9.

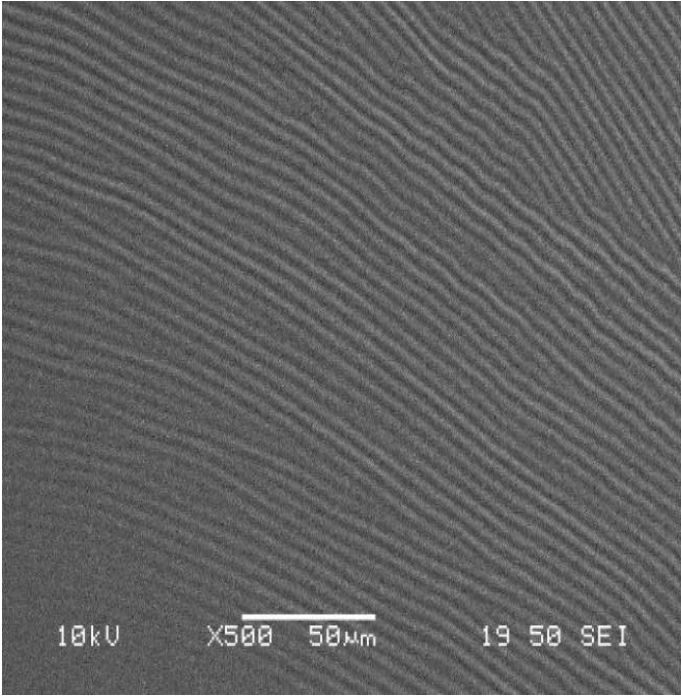
<p>Plasma treatment – Parameters and Effects</p>	
<p>An optimised plasma treated PDMS membrane surface (1-2 microns' depth).</p> <p>The plasma parameters used in the modification reported here remained similar to parameters presented in Figure 3.8. except for the treatment time, that was reduced from 120 seconds to 90 seconds.</p> <p>The image presented shows a change, sufficient enough to suggest a response to the plasma treatment without necessarily compromising the membranes physical structure.</p> <p>The wrinkly-like effect seen in this study has also been similarly reported (Kaczorowski, Szymanski, Batory, & Niedzielski, 2015).</p>	

Figure 3. 9 SEM image of plasma treated PDMS (optimised) ($\times 500$)

Following the process described in Figure 3.9, the membrane was also subjected to permeation analysis, in order to evaluate the effect of plasma treatment in relation to its permeation profile. Results of this analysis are presented in Table 3.2 and Figure 3.10 that shows graphical representation of the permeation profiles.

The wrinkling effect observed following plasma treatment has been previously reported and attributed to an effect arisen from possibly oxidation of a silicon surface, which can result in elasticity contrast and increased mechanical strain between the surface of the material and its remaining bulk (Cordeiro, Zschoche, Janke, Nitschke, & Werner, 2009; Lee, Hong, Park, Lee, & Kim, 2017; Nania, Matar, & Cabral, 2015).

Table 3. 2Cumulative mass of caffeine (CAF), lidocaine (LID), ethyl paraben (EPB), benzocaine (BEN), salicylic acid (SAL), ibuprofen (IBU), diclofenac (DCF), and ketoprofen (KPF) permeated through standard PDMS membrane and plasma treated PDMS membrane following permeation analysis (mean \pm standard deviation, rounded to whole numbers, $n = 3$), presented for comparison.

Compounds	Membrane type	Mean cumulative mass permeated after 6 hours ($\mu\text{g}/\text{cm}^2$)	BCS
CAF	Normal PDMS	72 ± 4	I
	Plasma treated PDMS	74 ± 6	
LID	Normal PDMS	3351 ± 23	II
	Plasma treated PDMS	3362 ± 31	
EPB	Normal PDMS	323 ± 09	II
	Plasma treated PDMS	327 ± 04	
SAL	Normal PDMS	862 ± 06	I
	Plasma treated PDMS	890 ± 11	
IBU	Normal PDMS	1176 ± 11	II
	Plasma treated PDMS	1076 ± 07	
DCF	Normal PDMS	134 ± 04	II
	Plasma treated PDMS	134 ± 02	

BCS = Biopharmaceutical classification system

Biopharmaceutical classification (BCS) refers to an experimental model that measures permeability of compounds in relation to their solubility. It is essential to consider and take cognisance of the BCS concept, as any physiochemical properties of drug that may influence rate of permeation needs to be established prior to modification. Hence, any change can be appropriately and effectively considered as resulting from the modification process, and to what extent is that change. Furthermore, in an attempt to predict behaviour of other drug

compounds independent of this study, the BCS can further help in establishing a model for these predictions, as drugs within the same BCS can be grouped and analysed.

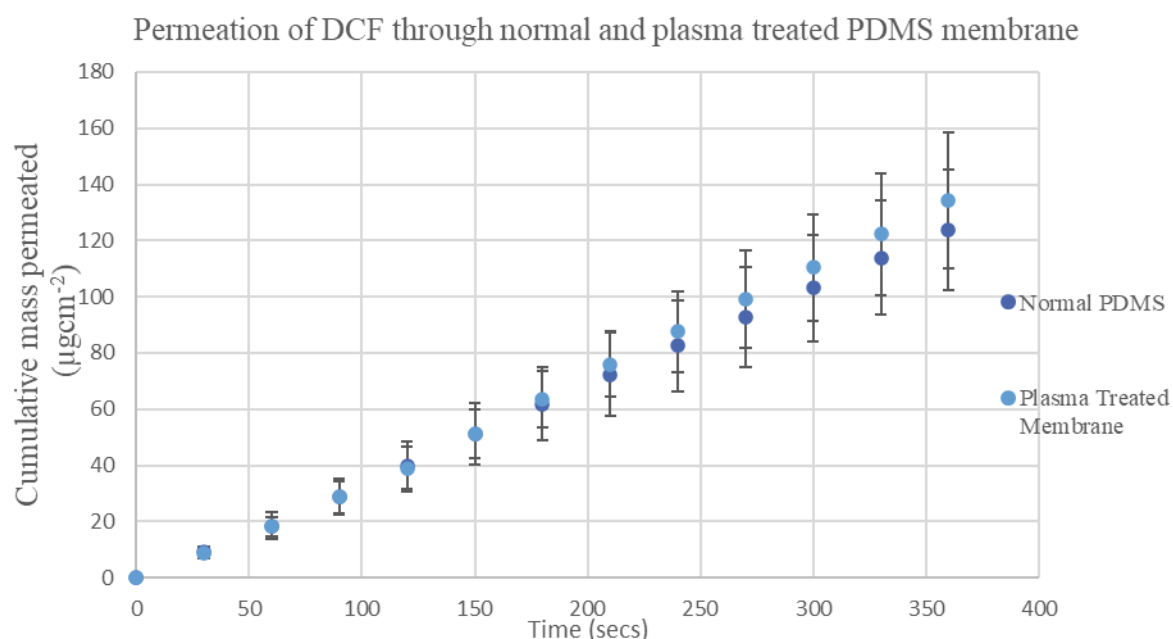


Figure 3. 10 Steady state flux of diclofenac through standard and plasma treated PDMS membrane.

Permeation measurement using the optimised form of the plasma treated membrane shows a reduction effect when comparing its value with that of the normal membrane. What this process shows is that the parameters used in this plasma process produced energy sufficient enough to bring about changes observed using SEM, without compromising the nature of the membrane, meaning the much-needed selectivity and stability of the membrane remained intact. Hence the optimised version was more appropriate for further investigation.

3.2.2.3 Water Contact Angle analysis

Static contact angle measurements in this analysis served as a supporting technique to augment the findings visualised from SEM images following the plasma process carried out on the membrane, as shown in Figure 3.11.

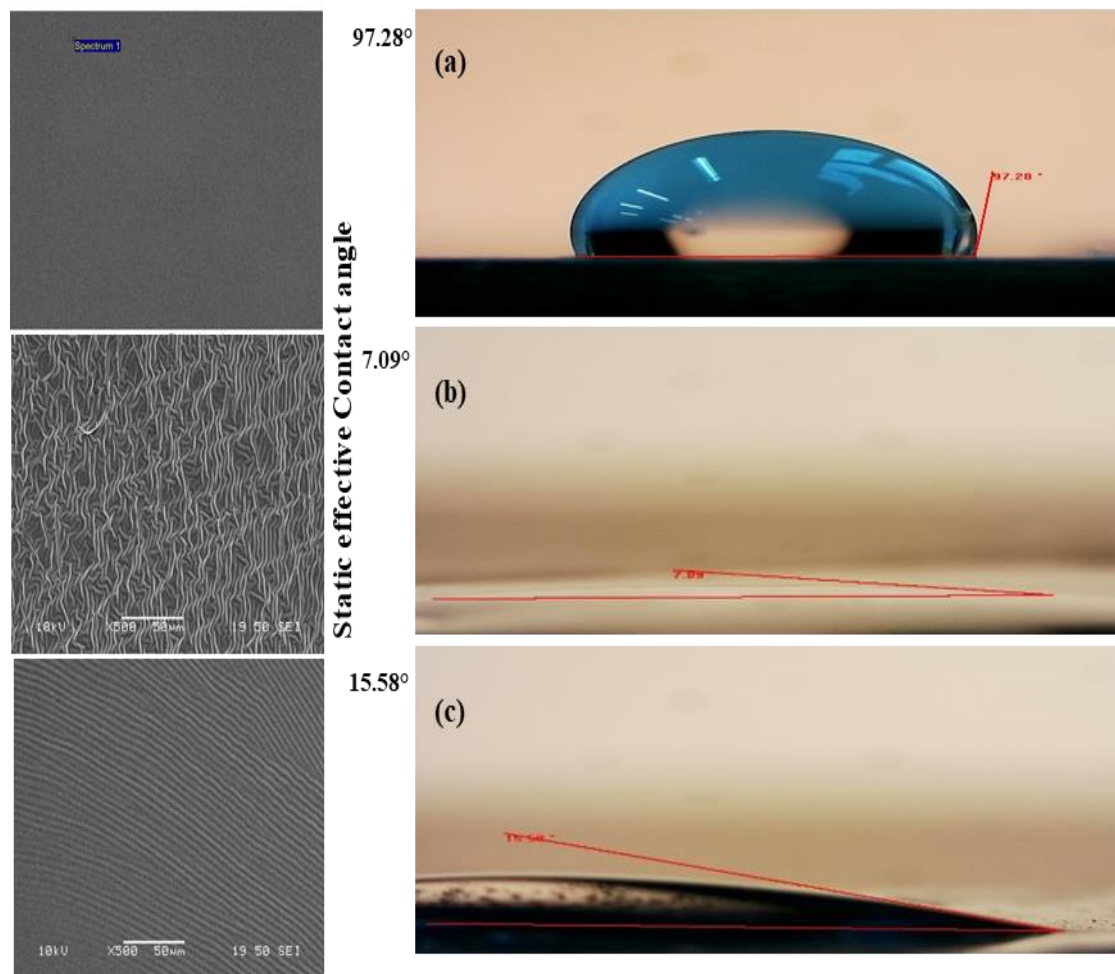


Figure 3. 11 SEM of normal (a), plasma treated (b) (over cured) and optimised (c), PDMS membranes (left), alongside their respective water contact angle measurements (right).

Although it is presumed that the atomic entities between normal and plasma treated PDMS membrane differs on the surface, the bulk material remains the same, as such the membrane surfaces remained a flat and homogeneous surface, and by extension, Young's postulates can be applied. Therefore, for wettability analysis, standard PDMS membrane showed static effective contact angles (SEC- angles) of $97.28^\circ (\pm 1^\circ)$. This shows that the membrane was hydrophobic (contact angle ≥ 90) (Ramirez-Canon, Miles, Cameron, & Mattia, 2013), and also in line with a description given by (Ou et al., 2013).

However, following treatment of the membrane with plasma, SEC angles of the resultant membrane reduced from 93.28 ° to 7.09 ° (Figure 3.11). According to Young's description this newly modified material can be considered a hydrophilic membrane. More crucial to this study is how these changes can be attributed to the earlier proposal that the new surface might contain hydroxyl groups (-OH) which can easily increase affinity with water molecules (-H₂O) therefore, increasing hydrophilicity. This result emphasises the importance of altering the PDMS surface in order to achieve an increased propensity of a chemical interaction.

It appears that the nano-ridged like structures in Figure 3.11b can be as a result of over-curing the membrane, and as such can lead to a compromise in the membrane integrity, therefore, parameters used in the treatment were optimised, SEC angles of the newly formed membrane (Figure 3.11c) were obtained with an average value of 15.58 °.

Within this study it was possible to say with certainty that the modified membrane will be more reactive and susceptible for modification, as has been reported in other studies. It can conclude that the increased wettability on the PDMS membrane surface can lead to an increase in its reactivity (Karakoy, Gultepe, Pandey, Khashab, & Gracias, 2014). However, although the results were ideal, and in good agreement with literature, it was difficult to say with certainty that liquids dropped on the plasma treated membranes cannot be trapped in the ridge-like interstices. This could be an issue as it could lead to trapped air and hence form a solid-air-liquid interface, resulting in a small degree of uncertainty with reported contact angles of treated membranes.

3.2.2.4 Attenuated Total Reflectance-Fourier Transform Infra-red spectroscopy

ATR-FTIR analysis was undertaken with results presented in Table 3.3. The technique was used to analyse standard membrane as well as plasma treated membrane for confirmation of the existing bonds and detection of any new bond formation. A comparison was necessary to

effectively detect any change that might occur as a result of the modification process. Surface methyl groups were confirmed by symmetrical stretching vibrations at 2962.4 and 29632 cm^{-1} for untreated and treated membranes respectively. Asymmetric deformations of methyl groups for treated membranes were also observed at 1411.9 cm^{-1} . Symmetric deformation of methyl groups for untreated and treated membranes was at 1257.1 and 1257.8 cm^{-1} respectively. Peaks from stretching vibrations at 1004.7, and 1005.7 cm^{-1} were attributed to Si-O-Si bonds, for untreated and treated membranes respectively. This analysis in a way serves as a quality control for PDMS membrane as results obtained were in close agreement with reported works by (Bodas & Khan-Malek, 2006; Kim & Jeong, 2011).

O-SiCH₃ were confirmed by peaks at 784.4 and 783.7 cm^{-1} , the presence of C-SiCH₃ groups were confirmed by 669.8 and 669.8 cm^{-1} for untreated and treated membranes respectively.

There was an expectation that the technique might detect the newly proposed hydroxyl group (-OH) on the plasma treated membrane. However, the plasma process was a surface treatment, hence chemical changes were limited to membrane surface, consequently, penetration depth of the spectroscopic technique wasn't suitable at this stage for detection of this surface change.

Table 3. 3 ATR-FTIR Assignment of standard and plasma-treated PDMS membrane

Assignment	ν_{\max} (cm ⁻¹)	
	Normal PDMS	Plasma treated PDMS
ν_s (CH ₃)	2962.4	2962.0
δ_{as} (CH ₃)	1411	1411.9
δ_s (CH ₃)	1257.1	1257.8
Si-O-Si	1004.7	1005.7
Si-O	481	477
O-SiCH ₃	784.6	783.7
C-SiCH ₃	669.8	669.8
C – OH	N/A	N/A

3.2.3. Glycerol Attachments on Plasma treated Poly(dimethylsiloxane) membrane

3.2.3.1. Introduction

Glycerol (1,2,3- propanetriol) is a colourless, odourless and viscous liquid (Pagliaro & Rossi, 2008), and it is one of the most versatile chemical substances known to man (Lourhraz & El Asli, 2018). It has a melting point of 18.2 °C and a boiling point of 290 °C, it is completely soluble in water and alcohols, slightly soluble in many common solvents such as ether and dioxane, and insoluble in hydrocarbons. Combination of its high flexibility, possibility of intramolecular hydrogen bonds formation and intermolecular solvation all due to its hydroxyl groups, makes it suitable for the intended process.

The idea of attaching glycerol to the plasma treated membrane surface was partly coined from behaviour of the plasma treated membrane when it was subjected to permeation analysis as reported in Table 3.2. In that analysis, a slight change in permeation profile of this treated membrane when compared to its standard form was observed. More interestingly, the plasma

treated membrane was able to maintain its initial selectivity throughout the process. It was then proposed that an additional layer made up of primarily hydroxyl groups (similar to plasma treated surface) could form a basis for a more detailed insight on how the membrane surface worked. This would not only solidify the earlier proposal about the nature of the membrane surface but will also allow the formation of an additional layer (as proposed in Figure 3.6). Such a membrane could lead to a decrease in permeation by simply filling possible voids created by the plasma treatment, and forming a more tightly packed membrane, helping to achieve the aim of this study.

It is a known fact that attachment of materials on inorganic polymer surfaces remains a challenging task (Gill & Ballesteros, 1998), despite the considerable research that has been focused on the field. This study involves applying a technique that was first introduced in 1973 by Horning's group, known as atmospheric pressure ionisation (API), later renamed atmospheric pressure chemical ionisation (APCI) (Horning, Horning, Carroll, Dzidic, & Stillwell, 1973). The technique works by introducing a sample solution via a sample injection port which interacts with a high-pressured stream of pre-heated carrier gas (usually nitrogen), released from a separate gas inlet valve, resulting in the formation of micro-droplets of the sample. Subsequently, ionisation of this micro-droplet can occur when in contact with high voltage discharge (corona discharge) (Dass, 2007). The principle of this technique can be exemplified by the working system of an electronic cigarette (e-cig) (Liu, 2015), that comprises of an atomiser, which is a chamber comprising of specialised coils that are powered by a battery source and can provide the needed voltage to heat and drive the atomisation of sample solutions present in e-cigarettes.

This methodology was extended to functionalised siloxane in this study. The advantage was simply that it can improve reactivity of the precursor sample (glycerol) significantly, due to the

increase in ionisation efficiency caused by the high pressure used in the method, leading to more gas phase collisions, a principle that has been previously reported (Watson & Sparkman, 2007), in other words, adopting the chemical vapour deposit methodology.

3.2.3.2. Glycerol coat method

Glycerol (10 mL) was introduced into a reactor which was equipped with a coil, heated by a battery source, all enclosed in a compartment considered as the atomisation unit. The reactor contained a 3.7-volt battery capacity and 2.4Ω atomiser, capable of producing about 5.5 watts of power. This power was strong enough to vaporise the glycerol.

Freshly plasma treated PDMS of square sizes sufficient to cover the effective area of diffusion cells used in permeation analysis ($\approx 0.56 \text{ cm}^2$) were used in the process. The membranes were placed at a close distance to the exit point of the glycerol. The process lasted for 3 hours and at this stage a comparative measurement of the residual glycerol indicated 3 mLs was used in the process. The temperature of the reactor was kept at about 50°C to support the condensation reaction. After the modification process, in trying to address an unwanted leaching effect attributed to the PDMS membrane (Bodas & Khan-Malek, 2007) and creating a more homogeneous surface, the coated membrane surface was exposed to a nitrogen atmosphere for 10 minutes this can also help in preserving the membrane from unwanted interaction with atmospheric air. A diagram to illustrate this process is shown in Figure 3.12 and the associated chemical modification in Figure 3.13.

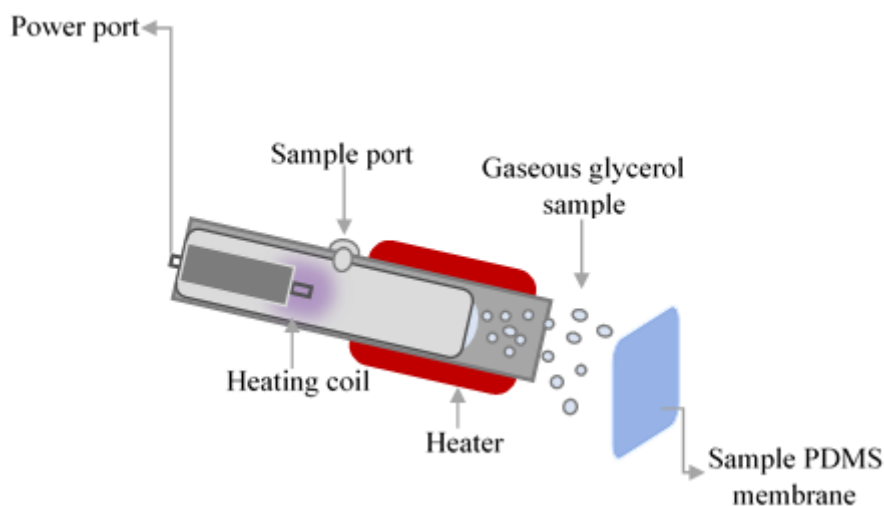


Figure 3.12 Schematic representation of chemical vapour deposit procedure - technique inspired by the atmospheric pressure chemical ionisation (APCI) process.

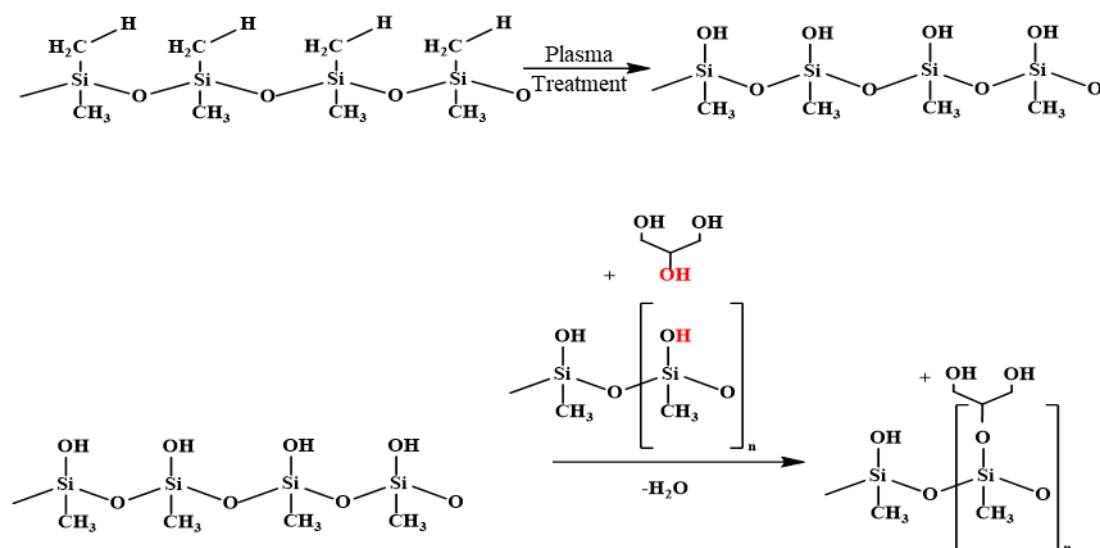


Figure 3.13 Proposed reaction process of chemical vapour deposit of glycerol on plasma treated PDMS membrane.

The chemical vapour deposit method is a tool in improving dispersion of various sample materials on surfaces or inner matrices of polymer materials, thereby improving some of their surface or bulk properties (Javanbakht, Raphael, & Tavares, 2016; Uznanski et al., 2018;

Volcke et al., 2010; Zhang et al., 2018). The process can be grouped mechanistically into two categories (Majeed et al., 2012) viz-a-viz: (a) binding of functional groups on a π -conjugated skeleton via covalent attachment or (b) physical adsorption from a variety of functional molecular interactions via a non-covalent bond (Hwang et al., 2011). The overall mechanism for silane bond formation depicted in Figure 3.13, has been reviewed in detail by (Pape & Plueddemann, 1991; Plueddemann; Tesoro & Wu, 1991). Alkoxysilanes undergo hydrolysis by both acid- and base-catalysed mechanisms, and in contrast with chlorosilanes and acetoxysilanes, products from alkoxysilane hydrolysis do not propagate hydrolysis reactions. In other words, these products are stable when in contact with water. The same factors which influence hydrolysis of alkoxysilanes also influence condensation of silanols with other silanols or alkoxy precursors (Arkles, Steinmetz, Zazyczny, Mehta, & Technology, 1992). In other words, the proposed modified membrane can be stable enough to undergo permeation analysis and is therefore a potential advantageous modification of PDMS.

3.2.3.3 Scanning Electron Microscopy of modified PDMS membrane

Following the modification process presented in Section 3.2.3.2, modified membrane was analysed using SEM analysis with the results displayed in Figure 3.14. The experimental technique was kept the same as previously reported in Section 3.2.2.2 for effective comparison.

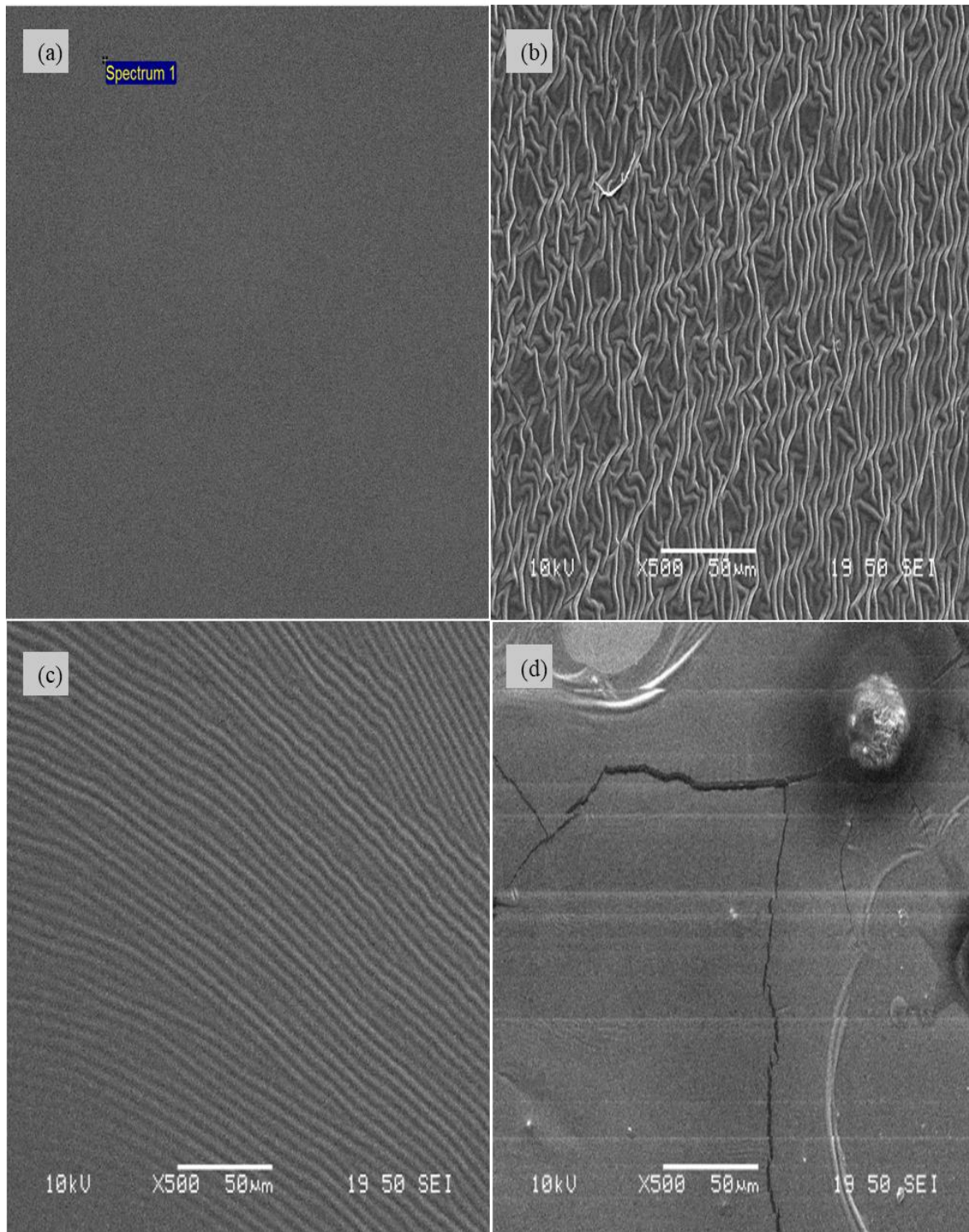


Figure 3. 14 SEM of standard (a), plasma treated (over cured and optimised (b) and (c) respectively) and modified (d) PDMS membranes.

In Figure. 3.14 (d) above, a notable change in the membrane surface can be visualised, compared to standard and plasma treated membranes. A rather smooth deposited layer can

easily be attributed to the modified membrane from the SEM image. A presumed crack can also be seen from the image, which may be possible from the nature of the deposited glycerol. However, structural integrity of the membrane was not compromised as the process was a mild technique and was more technically ascertained using permeation analysis. The presumed crack was attributed to a discontinuous layer resulting from the glycerol coat. Spots seen on the membrane surface were possibly also because of coalescing small particles that were deposited on the membrane following the process.

3.2.3.4 Water Contact Angle analysis

WCA analysis was undertaken, and results presented in Figure 3.15, alongside different degrees of membrane treatments for effective comparison.

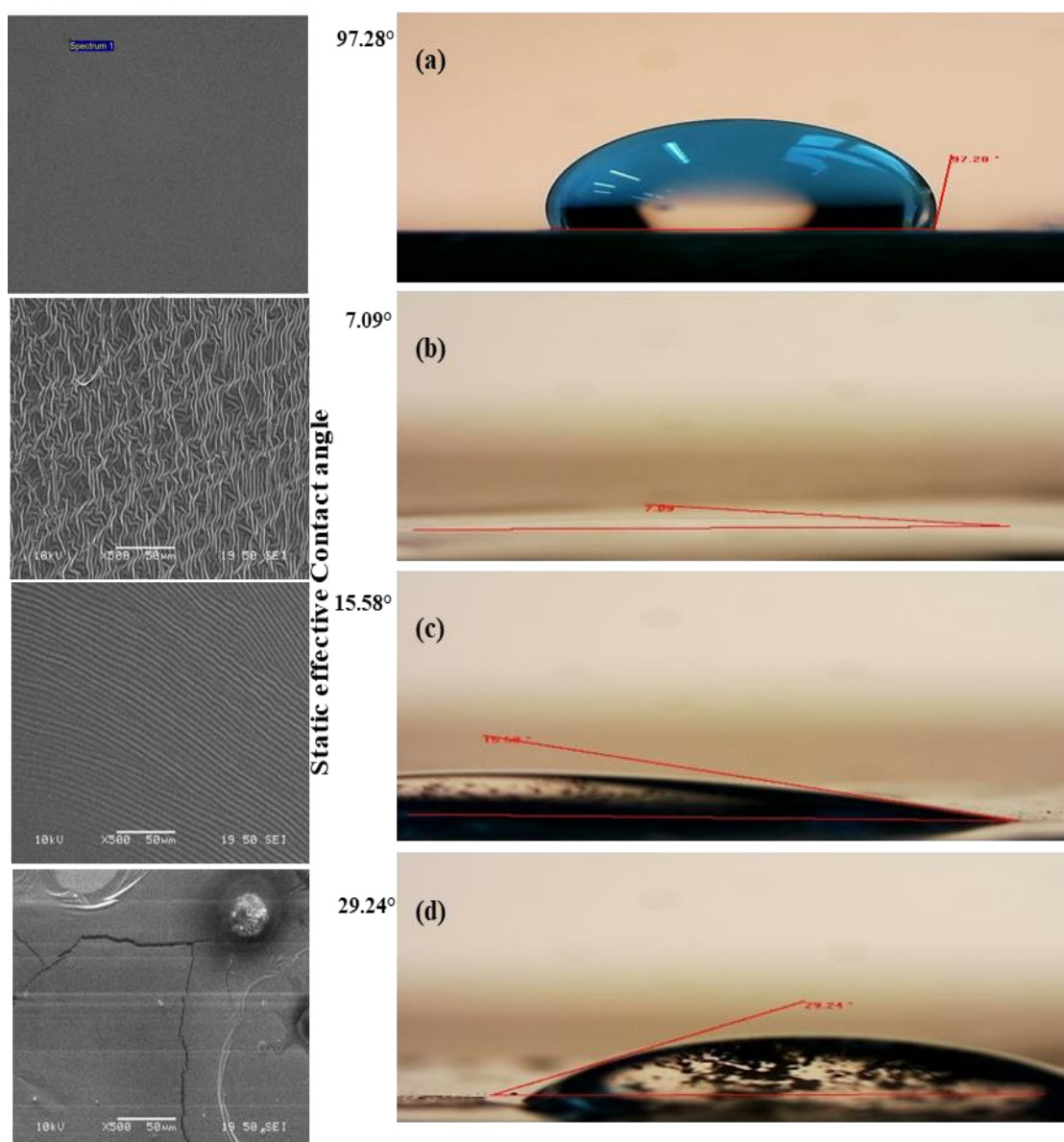


Figure 3.15 SEM of standard (a), plasma treated (b) (over cured) and optimised (c) and modified (d) PDMS membranes (left), alongside their respective water contact angle measurements (right) ($\times 500$).

Due to a similar proposed hydroxyl group on the surface of the membranes (plasma treated membrane and membrane coated with glycerol Figure 3.15), a decrease in WCA was primarily envisaged. Moreover, the water-soluble nature of the coated material (glycerol) was another reason why it was assumed that contact angle would decrease following the modification process. However, the coated membrane had an increased contact angle compared to the

plasma treated membrane i.e. from 15.58 ° to 29.24 °. However, it is important to note that an additional layer resulting from the coat was achieved, which explains its smoother surface, and possibly, the increase in contact angle. In other words, a correlation between surface smoothness and hydrophobicity takes precedence, and this is also in line with previous work by (Majeed et al., 2012).

3.2.3.5 Permeation Analysis

Permeation analysis using diffusion cells (as described earlier) was performed using seven pharmaceutical compounds namely, caffeine, diclofenac, ibuprofen, benzoic acid, ethyl paraben, butyl paraben and salicylic acid. Each saturated solution of drug was prepared using pH 7.4 phosphate buffered saline. The buffer was prepared by dissolving 8.766 g of sodium chloride, 7.385 g of dipotassium phosphate and 1.034 g of dihydrogen potassium phosphate in 1 L of ultra-pure water (18.2 MΩ, Barnstead). pH adjustment was carried out using dilute concentrations of HCl and NaOH as necessary.

Saturated drug solutions were prepared by adding an excess amount of drug in 10 mL sample vials containing buffer. The sample vial containing a micro size magnetic stirrer was mounted in a water bath maintained at ~32 °C for 24 hours, equipped with a magnetic stirrer plate. The resulting solution was filtered, and added via a syringe, in the donor compartment to avoid bubbles. Openings were occluded to maintain constant temperature and prevent evaporation. Samples were collected from the receptor arm at 30-minute intervals for 6 hours and analysed using UV-vis spectroscopy.

A standard calibration graph of each drug ($R^2 \geq 0.9$.) was used to calculate its resultant concentration after the experiment, covering the concentration range of the samples obtained in the permeation analysis. It bears mentioning that freshly prepared serial drug concentrations for calibration graph purposes were prepared each time an analysis was carried out, instead of

using the same graph for all analysis involving a particular drug. This is in line with standard operating procedures as contained in the Accreditation of laboratory competence (ISO/IEC 17025). However, the Act allows usage of a concentration standard (1000 ppm in the case of this study, unless defined otherwise) more than once, from which a series of calibration standards should be prepared daily and valid for only one batch run. In line with that, the concentration standard for stable drugs (such as caffeine) were stored under a controlled environment and sometimes used more than once.

The resultant permeation data is summarised in Table 3.4.

Table 3. 4 Cumulative mass of caffeine (CAF), and salicylic acid (SAL), permeated through normal, plasma treated and modified PDMS membrane alongside their Permeation coefficient (K_p) values, compared with literature values, following permeation analysis (mean \pm standard deviation, rounded to whole numbers, $n = 3$).

Compounds (Absorbance)	Cumulative mass ($\mu\text{g}/\text{cm}^2$)			Permeation coefficient (K_p) values ($K_p \times 10^{-4}$ (cm/min))			Literature values	Reference
	Normal PDMS	Plasma treated PDMS	Modified PDMS	Normal PDMS	Plasma treated PDMS	Modified PDMS		
Caffeine (272)	72 ± 4	74 ± 6	79.5 ± 4	0.13	0.13	0.15	0.1	(Uchida et al., 2015)
Salicylic Acid (234)	862.4 ± 06	890 ± 11	975.2 ± 6	2.82	2.91	3.14	2.4	(Degim, Pugh, & Hadgraft, 1998)

An infinite dose approach was employed in this permeation analysis. This approach was adopted to ensure an accurate comparison could be made between experimental and *in-vivo* permeation coefficient (K_p) values obtained from literature using human tissue. Baba *et al* reported this approach as a vital measure for evaluating permeation of *in vitro* models (Baba, Takahara, & Mamitsuka, 2015).

Two different compounds were presented herein, partly because they cover a distinct range of therapeutic classes i.e. keratolytic agents, and central nervous system stimulants, and because they presented interesting results compared with the previous membrane permeation data.

K_p values of the compounds (Table 3.7) indicates significant differences between standard and modified membranes. Values regarding drugs interacting with the membrane prior to modification were necessary as they would be essential to compare any change that might occur when analysing drug permeation through treated membrane.

Results obtained from salicylic acid indicated a 9.6 % increase in K_p value after treatment. Although, the supposed increase in hydrophilic groups on the surface of the treated membrane can serve as a rate limiting step for drugs (Bhuiyan & Waters, 2017), thus resulting in low permeation, the relatively high log P value (2.06) (Chemspider) of salicylic acid meant that the drug is lipophilic in nature, hence is less affected by an increase in hydrophilicity of the membrane. Moreover, contact angle measurements indicated an increase in contact area of the treated membrane hence, resulting in more affinity of drug to the membrane, which can also serve as a potential factor for an increased permeation value.

However, in the case of caffeine, K_p values remained similar for the treated vs. untreated, although, with a slight increase in cumulative mass of compounds permeated through modified membrane. This observed increase might be because of the hydrophilic nature of caffeine (log P - 0.13).

3.2.3.6 Sequential silanisation alongside PDMS-PEG BCP Co-Polymerisation

PDMS silicon membrane, 0.3 mm thickness with approximately 0.6 cm² size was utilised in this process. The membrane was plasma-treated then cured with 1 mL dimethylphenylsilanol. The process was a wet process, and the reaction was carried out in an ethanolic medium (~ 5 mL). PDMS-PEG BCP curing agent was also added to the reactor (~ 1 mL). The entire reaction process lasted for 2 hours.

Subsequently, the membrane formed was placed on an aluminium foil covered glass plate and introduced in an oven adjusted to 50 °C for 24 hours to completely cure and evaporate any excessive solution from the product and to further drive the process.

3.3. Conclusion

It is widely accepted that the surface of human skin comprises of tightly packed materials that only allow substances to selectively permeate through them via physicochemical interactions. It is based on this understanding that it becomes necessary to try and understand the working principle of PDMS, in order to effectively provide it as an alternative to human skin. This membrane has already shown promising indicators to replace skin from its very low permeability and selectivity. Moreover, the membrane has limited ethical criticism, legal constraints and has heightened availability which are all added advantages. However, it still shows an over-estimation of permeation when compared with human skin.

In this chapter PDMS membrane was studied in detail and attempts were made to modify it. The inert nature of the membrane surface was overcome following atmospheric pressure nonthermal air plasma treatment and in line with reported literature, methyl groups present on the membrane surface were considered to be replaced with hydroxyl groups. Two analytical techniques, namely scanning electron microscopy (SEM) and static water contact angle (WCA) measurements were used to confirm this modification. Following plasma treatment, the resultant membrane was subjected to permeation analysis with a clear difference between plasma treated membrane and PDMS membrane. Following this success, an attempt was made

to further saturate the surface of the membrane with similar functional groups achieved via plasma treatment i.e., hydroxyl groups. It was proposed that an additional layer comprising of the same group can reduce permeation of the membrane and at the same time maintain its already established selectivity.

A selection of model drugs indicated a considerable difference between plasma treated membrane and the modified membrane, indicating a successful modification process. However, it was clear that a heterogeneous surface is needed to effectively mimic the skin surface, being the skin a heterogeneous layer itself, rather than having a surface comprising mainly of hydroxyl groups, rendering it a homogenous layer.

Optimised parameters in surface treatment of the membrane achieved in this chapter, which increased the membrane chemical reactivity and compatibility, introduced a plethora of opportunities for a more robust modification process, some of which are presented in Chapters 4 and 5.

References

- Arkles, B., Steinmetz, J., Zazyczny, J., Mehta, P. J. J. o. A. S., & Technology. (1992). Factors contributing to the stability of alkoxysilanes in aqueous solution. *Jornal of Adhesion Science and technology* 6(1), 193-206.
- Baba, H., Takahara, J.-i., & Mamitsuka, H. (2015). In silico predictions of human skin permeability using nonlinear quantitative structure–property relationship models. *Pharmaceutical research*, 32(7), 2360-2371.
- Bhuiyan, A., & Waters, L. J. (2017). Permeation of pharmaceutical compounds through silicone membrane in the presence of surfactants. *Colloids and Surfaces A: Physicochemical and Engineering Aspects*, 516, 121-128.
- Bodas, D., & Khan-Malek, C. (2007). Hydrophilization and hydrophobic recovery of PDMS by oxygen plasma and chemical treatment—An SEM investigation. *Sensors and Actuators B: Chemical*, 123(1), 368-373.
- Bodas, D., & Khan-Malek, C. J. M. e. (2006). Formation of more stable hydrophilic surfaces of PDMS by plasma and chemical treatments. *Microelectronic engineering* 83(4-9), 1277-1279.
- Bodas, D., Khan-Malek, C. J. S., & Chemical, A. B. (2007). Hydrophilization and hydrophobic recovery of PDMS by oxygen plasma and chemical treatment—An SEM investigation. *Sensors and Actuators B: Chemical* 123(1), 368-373.
- Cordeiro, A. L., Zschoche, S., Janke, A., Nitschke, M., & Werner, C. (2009). Functionalization of poly (dimethylsiloxane) surfaces with maleic anhydride copolymer films. *Langmuir*, 25(3), 1509-1517.
- Dass, C. (2007). *Fundamentals of contemporary mass spectrometry* (Vol. 16): John Wiley & Sons.
- De Jaeger, R., Mazzah, A., Gengembre, L., Frere, M., Jama, C., Milani, R., . . . Gleria, M. (2008). Surface functionalization with phosphazenes. V. Surface modification of plasma-treated polyamide 6 with fluorinated alcohols and azobenzene derivatives through chlorinated phosphazene intermediates. *Journal of Applied Polymer Science*, 108(5), 3191-3199.
- Degim, I. T., Pugh, W. J., & Hadgraft, J. (1998). Skin permeability data: anomalous results. *International journal of pharmaceutics*, 170(1), 129-133.
- Gill, I., & Ballesteros, A. (1998). Encapsulation of biologicals within silicate, siloxane, and hybrid sol–gel polymers: an efficient and generic approach. *Journal of the American Chemical Society*, 120(34), 8587-8598.
- Goda, T., Konno, T., Takai, M., Moro, T., & Ishihara, K. J. B. (2006). Biomimetic phosphorylcholine polymer grafting from polydimethylsiloxane surface using photo-induced polymerization. *Biomaterials* 27(30), 5151-5160.
- Horning, E., Horning, M., Carroll, D., Dzidic, I., & Stillwell, R. (1973). New picogram detection system based on a mass spectrometer with an external ionization source at atmospheric pressure. *Analytical Chemistry*, 45(6), 936-943.
- Hwang, J., Jang, J., Hong, K., Kim, K. N., Han, J. H., Shin, K., & Park, C. E. (2011). Poly (3-hexylthiophene) wrapped carbon nanotube/poly (dimethylsiloxane) composites for use in finger-sensing piezoresistive pressure sensors. *Carbon*, 49(1), 106-110.
- Javanbakht, T., Raphael, W., & Tavares, J. R. (2016). Physicochemical properties of cellulose nanocrystals treated by photo-initiated chemical vapour deposition (PICVD). *The Canadian Journal of Chemical Engineering*, 94(6), 1135-1139.
- Kaczorowski, W., Szymanski, W., Batory, D., & Niedzielski, P. (2015). Effect of plasma treatment on the surface properties of polydimethylsiloxane. *Journal of Applied Polymer Science*, 132(11).

- Karakoy, M., Gultepe, E., Pandey, S., Khashab, M. A., & Gracias, D. H. (2014). Silane surface modification for improved bioadhesion of esophageal stents. *Applied Surface Science*, 311, 684-689.
- Kim, H. T., & Jeong, O. C. J. M. E. (2011). PDMS surface modification using atmospheric pressure plasma. *Microelectronic engineering* 88(8), 2281-2285.
- Lee, J. S., Hong, H., Park, S. J., Lee, S. J., & Kim, D. S. (2017). A simple fabrication process for stepwise gradient wrinkle pattern with spatially-controlled wavelength based on sequential oxygen plasma treatment. *Microelectronic Engineering*, 176, 101-105.
- Liu, Q. (2015). Electronic cigarette and method for electronic cigarette extinguishment. In: Google Patents.
- Lourhraz, K., & El Asli, A. (2018). VALORIZATION OF BIODIESEL WASTE.
- Majeed, S., Filiz, V., Shishatskiy, S., Wind, J., Abetz, C., & Abetz, V. (2012). Pyrene-POSS nanohybrid as a dispersant for carbon nanotubes in solvents of various polarities: its synthesis and application in the preparation of a composite membrane. *Nanoscale research letters*, 7(1), 296.
- Nania, M., Matar, O. K., & Cabral, J. T. (2015). Frontal vitrification of PDMS using air plasma and consequences for surface wrinkling. *Soft Matter*, 11(15), 3067-3075.
- Neupane, R., Boddu, S. H., Renukuntla, J., Babu, R. J., & Tiwari, A. K. (2020). Alternatives to biological skin in permeation studies: Current trends and possibilities. *Pharmaceutics*, 12(2), 152.
- Ou, J., Hu, W., Xue, M., Wang, F., Li, W. J. A. a. m., & interfaces. (2013). One-step solution immersion process to fabricate superhydrophobic surfaces on light alloys. *ACS applied materials & interfaces* 5(20), 9867-9871.
- Pagliaro, M., & Rossi, M. (2008). *The future of glycerol*.
- Pape, P. G., & Plueddemann, E. P. (1991). Methods for improving the performance of silane coupling agents. *Journal of adhesion science and technology*, 5(10), 831-842.
- Plueddemann, E. Silane coupling agents, 1982. *Plenum Press, New York*.
- Ramirez-Canon, A., Miles, D. O., Cameron, P. J., & Mattia, D. (2013). Zinc oxide nanostructured films produced via anodization: a rational design approach. *RSC advances*, 3(47), 25323-25330.
- Schnyder, B., Lippert, T., Kötz, R., Wokaun, A., Graubner, V.-M., & Nuyken, O. (2003). UV-irradiation induced modification of PDMS films investigated by XPS and spectroscopic ellipsometry. *Surface Science*, 532, 1067-1071.
- Tesoro, G., & Wu, Y. (1991). Silane coupling agents: the role of the organofunctional group. *Journal of adhesion science and technology*, 5(10), 771-784.
- Uchida, T., Kadhum, W. R., Kanai, S., Todo, H., Oshizaka, T., & Sugibayashi, K. (2015). Prediction of skin permeation by chemical compounds using the artificial membrane, Strat-M™. *European Journal of Pharmaceutical Sciences*, 67, 113-118.
- Uznanski, P., Glebocki, B., Walkiewicz-Pietrzykowska, A., Zakrzewska, J., Wrobel, A. M., Balcerzak, J., & Tyczkowski, J. (2018). Surface modification of silicon oxycarbide films produced by remote hydrogen microwave plasma chemical vapour deposition from tetramethyldisiloxane precursor. *Surface and Coatings Technology*, 350, 686-698.
- Volcke, C., Gandhiraman, R., Gubala, V., Raj, J., Cummins, T., Fonder, G., . . . Daniels, S. (2010). Reactive amine surfaces for biosensor applications, prepared by plasma-enhanced chemical vapour modification of polyolefin materials. *Biosensors and Bioelectronics*, 25(8), 1875-1880.
- Waters, L. J., Finch, C. V., Bhuiyan, A. M. H., Hemming, K., & Mitchell, J. C. (2017). Effect of plasma surface treatment of poly (dimethylsiloxane) on the permeation of pharmaceutical compounds. *Journal of Pharmaceutical Analysis*, 7(5), 338-342.

- Watson, J. T., & Sparkman, O. D. (2007). *Introduction to mass spectrometry: instrumentation, applications, and strategies for data interpretation*: John Wiley & Sons.
- Zhang, T., Liao, Z., Sandonas, L. M., Dianat, A., Liu, X., Xiao, P., . . . Zschech, E. (2018). Polymerization driven monomer passage through monolayer chemical vapour deposition graphene. *Nature communications*, 9(1), 1-9.
- Zhou, J., Ellis, A. V., & Voelcker, N. H. (2010). Recent developments in PDMS surface modification for microfluidic devices. *Electrophoresis*, 31(1), 2-16.

Chapter 4
Sequential Silanisation Processes for the modification of Plasma-treated
Poly(dimethylsiloxane)

4.1. Introduction

In the previous chapter it was demonstrated that PDMS could be modified to contain hydroxyl groups instead of methyl groups on its surface, and this modification renders it more reactive chemically. Following that process, glycerol material was attached on the plasma treated membrane surface following a condensation process, in an attempt to further treat the membrane. It was concluded that a more robust surface, preferably comprising of heterogeneous entities could possibly bring about a more desired outcome, in terms of a skin mimic system.

The aim of this chapter is to identify and study different functionality that is compatible with plasma treated PDMS membrane, capable of driving effects strong enough to result in permeation profile changes. More specifically, chemical group functionalities well-suited with plasma treated PDMS membrane were considered, namely: alkyl, phenyl, embedded polar groups, pentafluoro phenyl, alkylcyano derivatives and other groups were incorporated on the polymer surfaces, with the aim of altering surface properties of the membrane.

These compounds were selected on the basis of their physicochemical properties which makes them distinct and suitable for this purpose. For example, alkyl derivatives are known to separate analytes base on their degree of hydrophobicity and log P values, phenyl derivatives based on π - π bond interactions and embedded polar groups due to their unique binding property as a result of heightened affinity and selectivity with surface silanol groups. This is the reason these compounds are already used as stationary phases in HPLC techniques.

4.2. Sequential Silanisation using Dimethylphenylsilanol.

4.2.1. Background

Dimethylphenylsilanol (DMPS) is an alkoxysilane, primarily selected to impart its reported lipophilic properties to the already established hydrophilic PDMS surface, such that a Si-O-Si bond attachment is achieved between the polymer substrate and the DMPS reagent, via a silanisation process. Organosilicon compounds, such as DMPS utilised in this study, have been previously reported to impart lipophilic properties on hydrophilic aliphatic silanes, and these modified forms are then adopted for chromatographic purposes (Virtanen, Kinnunen, & Kulo, 1988).

The surface modification process represents an important tool for the preparation of a large variety of differently functionalised solid inorganic polymer membranes, incorporating a variety of functional groups. Specifically, in this study, several criteria, such as the high yields obtained under mild reaction conditions, compatibility of different functional groups, no required catalytic activation and the absence of by-products (Lummerstorfer & Hoffmann, 2004), are all advantageous for the intended process.

Essentially, the silanisation process, i.e. coating hydrolysed surfaces with an organofunctional alkoxysilane molecule thereby forming a Si-O-Si bond via covalent attachment, was investigated in this study. The aim was to achieve an alkoxysilane functionalised PDMS membrane.

It is also paramount to mention that alkoxysilanes have been widely accepted to constitute a stable membrane, mostly attributed to the presence of the Si-O-Si bond (Arkles, Steinmetz, Zazyczny, Mehta, & Technology, 1992). This desired stability forms part of the reason this process was considered in this study.

4.2.2. Silanisation method

In this study, the approach reported by (Sui et al., 2006) was adopted, i.e. hydroxyl groups present from both reactants (DMPS and plasma treated membrane) were reactable, consequently, a condensation reaction could occur which may lead to attachment of the silane reagent on the membrane surface, thereby, creating a Si-O-Si bond.

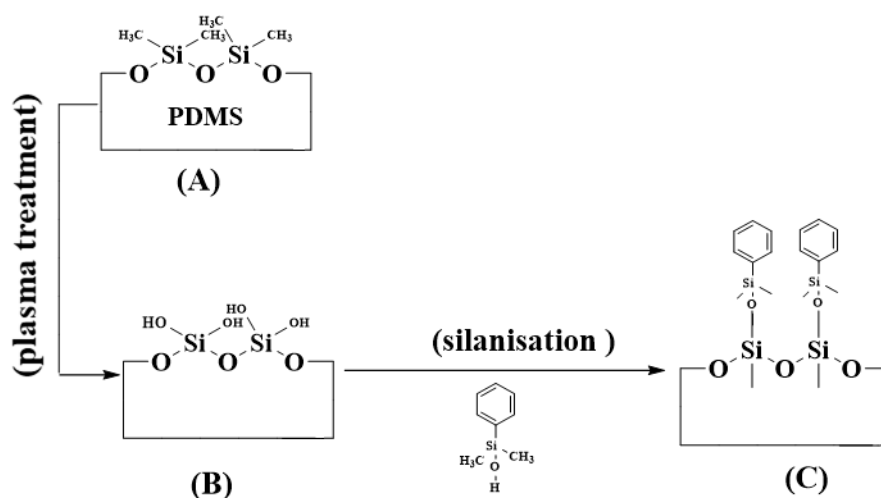


Figure 4. 1 Proposed reaction scheme (A) Un-modified membrane (B) Plasma-treated membrane (C) Modified membrane.

The general mechanism depicted in Figure 4.1 for silane bond formation was carried out in an acid-catalysed medium. Ethanol was used as solvent in the process to enhance an even distribution of the silane reagent, thereby reducing the likelihood of steric hinderance. To maintain an acidic environment (which can improve the condensation process) the measured pH (~ 8) was lowered by adding 1-2 drops of dilute hydrochloric acid thereby adjusting it to approximately pH 5.5. Approximately 1 mL of the silanising reagent (DMPS) was introduced into the reactor already containing 5 mL ethanol, using a glass pipette. This stage of the reaction lasted for 30 minutes and the temperature was maintained at 40 °C.

Although the reaction was a wet process (solution based), it was primarily aimed to achieve passivation of the PDMS surface mainly from the silane reagent, hence, after the initial

reaction, membranes from the reactor were collected, placed on aluminium foil and conditioned in a vacuum desiccator to promote formation of a silane monolayer. This process lasted for 15 minutes. Subsequently, membranes were placed on a glass plate covered with aluminium foil and introduced into an oven at 120 °C for 15 minutes to completely cure and evaporate any excessive solution from the product and to further drive the process.

The resultant membrane was dried under a nitrogen atmosphere, in line with the reported process (Ou, Hu, Xue, Wang, & Li, 2013), which was an additional step to ensure physical dryness i.e. removal of solvent, complete condensation and to create a relatively stable surface.

All parameters used in this process such as water content, solvent utilised, age of solution, time required in each stage of the reaction, applied temperature to mention but a few were carefully ascertained prior to commencing the reaction and in some instances optimised. This was necessary as integrity of the membrane needs to be intact in order to achieve the overall aim of this research.

Recovery also is an important aspect of any chemical reaction, for environmental reasons and to reduce cost as well. In addition, there was concern as to whether the silane may choose to react with the solvent used (ethanol) instead of the PDMS membrane. Fractional distillation was employed in this regard because of the close boiling points that exist between DMPS and ethanol (62 °C and 78 °C respectively) (Pubchem). Two separated fractions obtained were further analysed using FTIR, the resultant peaks obtained from the separate fractions were cross matched with their initial spectra (prior to the reaction) and were found to be similar. This finding further implies a well-tailored silanisation process between the silane reagents and the membrane.

4.2.3. Scanning Electron Microscopy of modified DMPS-PDMS membrane

It should be noted that changes such as the one depicted in Section 4.2.2. ought to be strong enough to bring about visible differences between modified and un-modified membranes. It was in line with this understanding that proposed DMPS-PDMS membrane was first and foremost observed using SEM. However, to critically appraise the entire modification process, SEM analysis was carried out in a stepwise manner. Firstly, prior to conditioning of modified membrane under nitrogen, SEM data was acquired then again following the silanisation process and curing of the membrane, and finally at the end of the process a separate SEM image was acquired. This was completed to track changes that might occur at every step of the process and summarised in Figure 4.2.

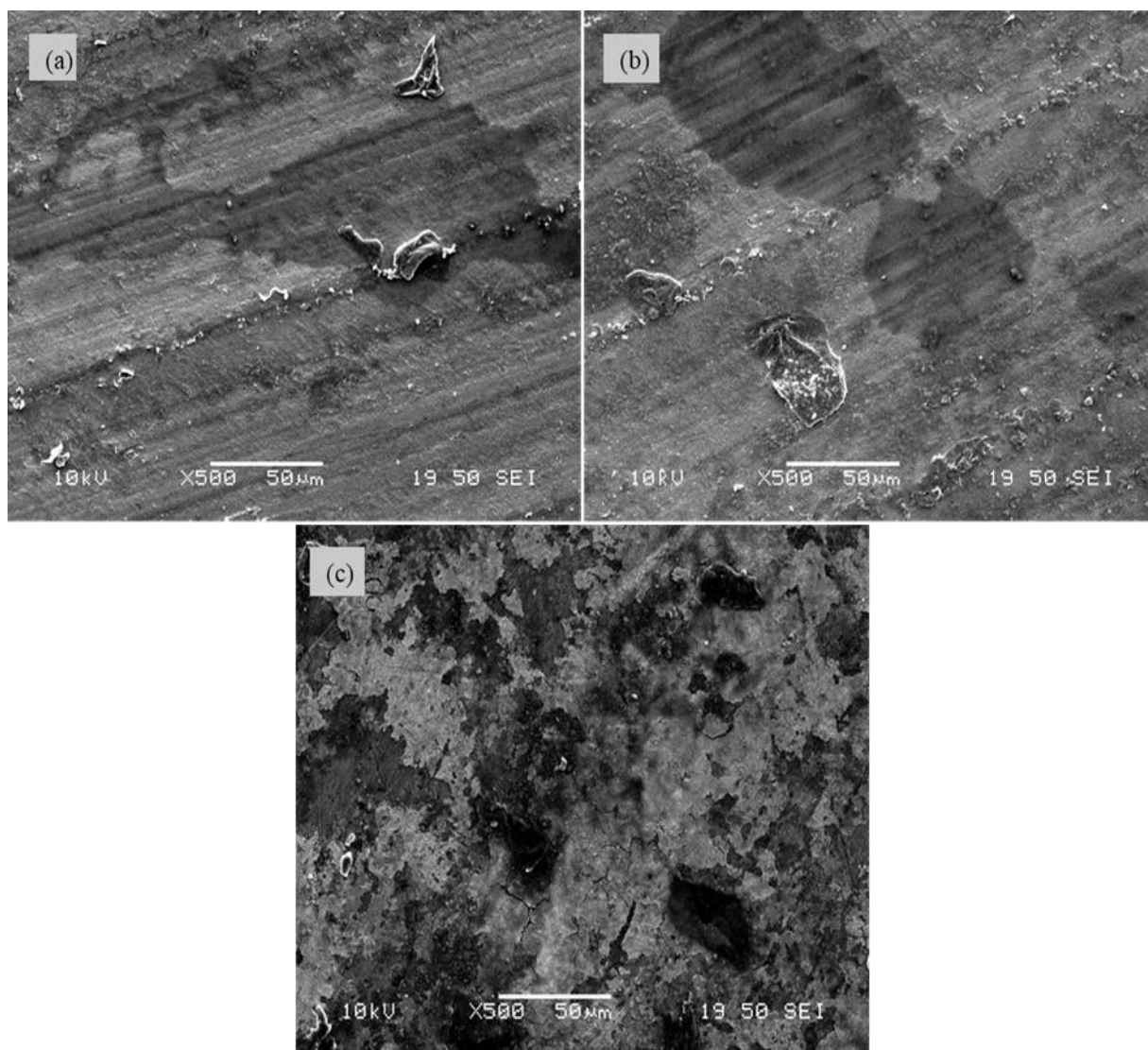


Figure 4. 2 SEM of DMPS-PDMS modified membranes with images (a), (b) and (c), representing the silanisation stage of the membrane modification process $\times 500$ magnification

Based upon the images in Figure 4.2 (a and b) it can be seen that there are some tiny particle-like features on the membrane surface, this could be monolith as a result of membrane transfer from the reactor onto the aluminium foil they were placed on, before being introduced to the oven. However, these are probably only loosely attached to the membrane, hence would not present any serious concern when considering the membrane for permeation analysis.

The modified membrane was subsequently conditioned under nitrogen atmosphere, to improve the stability of the membrane given its inert nature, as shown in Figure 4.3.

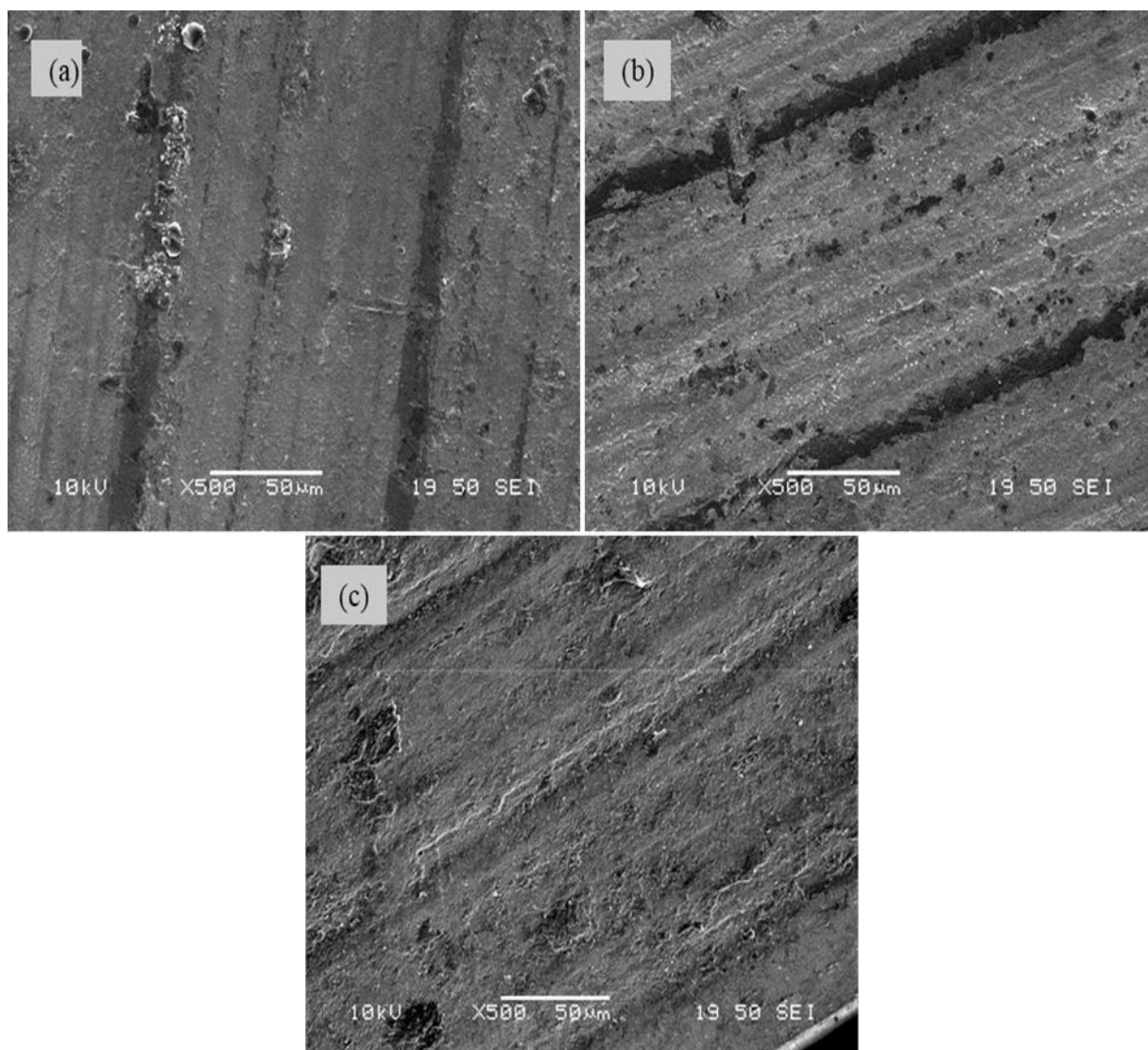


Figure 4. 3 SEM of DMPS-PDMS modified membranes, following exposure to nitrogen with images (a), (b) and (c), representing different samples of membrane $\times 500$ magnification

For comparative purposes, a selection SEM images of membrane surfaces is displayed in Figure 4.4.

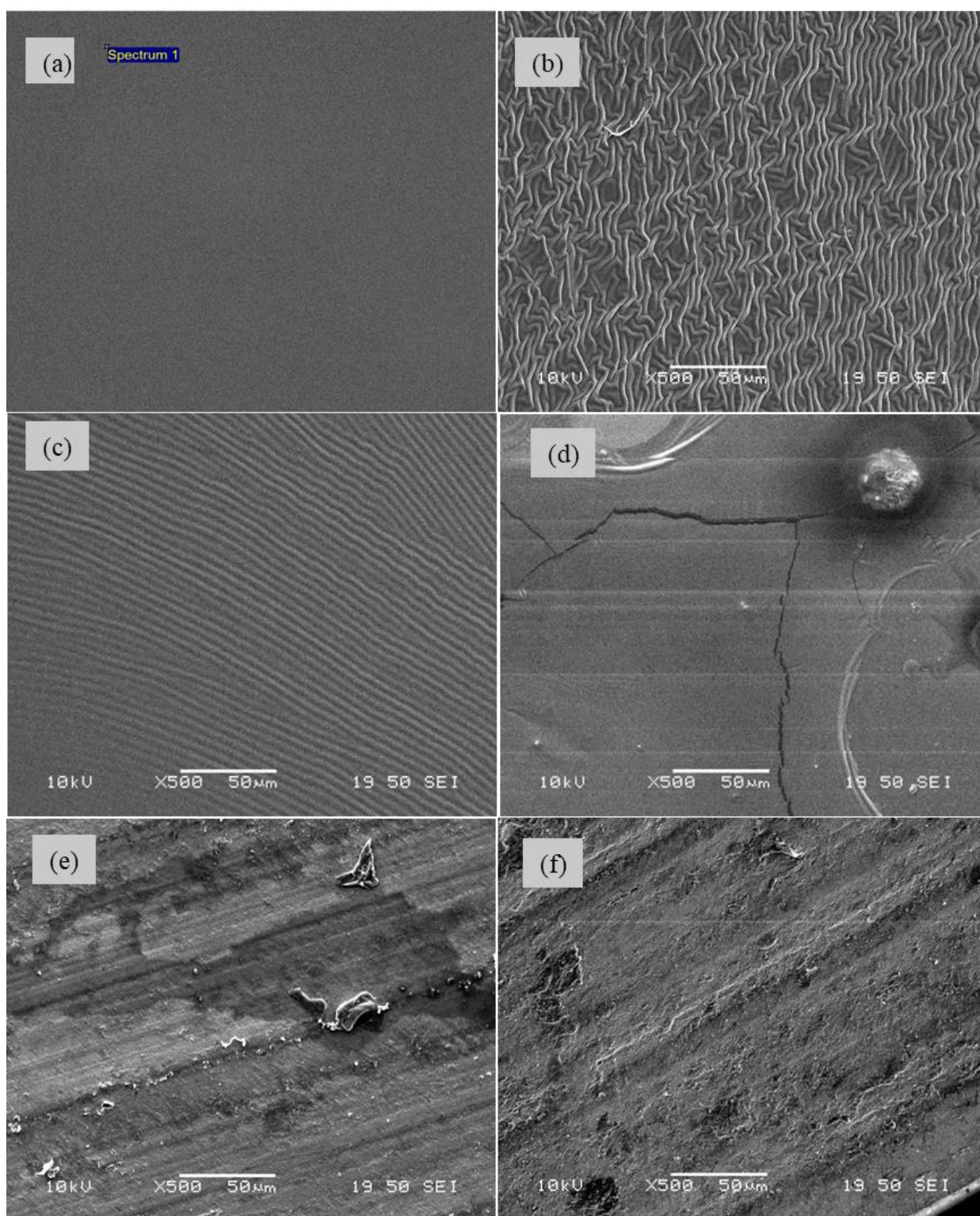


Figure 4. 4 Comparative SEM images of PDMS, normal membrane (a) plasma treated (over cured) (b), plasma treated (optimised) (c), glycerol-coated (d), DMPS modified (e), and DMPS-modified (conditioned under nitrogen atmosphere) (f) -PDMS membranes, respectively $\times 500$ magnification.

Following different modification processes established thus far in this study, a comparative SEM analysis becomes necessary at this stage to track changes with ease. Specifically, in relation to this chapter, there is not much difference between Figure 4.4 (e) and (f). However, Figure 4.4 (e) shows some dark patches on the membrane surface which was attributed to remaining moisture content that may be present on the observed sample. Following the membrane being conditioned under nitrogen (Figure 4.4 (e)), it can be visualised that these dark patches have disappeared, and the membrane appeared more even and homogeneous, indicating a rather stable surface layer formation.

4.2.4. Attenuated Total Reflectance-Fourier Transform Infra-red spectroscopy

ATR-FTIR analysis was undertaken on the modified membranes with results presented in Table 4.1.

Table 4. 1 ATR-FTIR assignment of PDMS pre- and post-modification.

Assignment	$\nu_{\max} (\text{cm}^{-1})$		
	PDMS	Plasma treated PDMS	D - PDMS
$\nu_s (\text{CH}_3)$	2962.4	2962.0	2962.3
$\delta_{\text{as}} (\text{CH}_3)$	1411	1411.9	1412.1
$\delta_s (\text{CH}_3)$	1257.1	1257.8	1257.2
Si-O	478	475	477
O-SiCH ₃	784.6	783.7	783.1
C-SiCH ₃	669.8	669.8	699.3
C – OH	N/A	N/A	N/A

ATR-FTIR was used to analyse un-modified membrane, modified membrane as well as plasma treated membrane for confirmation of the existing bonds and detection of any new bond

formation. A comparison was necessary to effectively assess any change that might occur as a result of the modification process.

It is paramount to realise that this method detects bond formations and not chemical entities, and only a small fraction of the surface is analysed compared with the effective area utilised for the overall permeation analysis process.

A notable finding achieved was a decrease in peak intensity attributed to the Si-O backbone bond when comparing spectra representing plasma treatment and chemically modified membranes, this increase in intensity observed in the chemically modified membrane points to a significant resolve that can be attributed to the formation of alkoxysilanes.

However, there were limitations when trying to ascertain aromatic overtones which theoretically were supposed to emerge after chemically modifying the membrane. This challenge could be as a result of the detector positioned deep inside the membrane matrix, possibly surpassing surface groups. Hence, other surface techniques were employed at a later stage of the analysis to address this concern.

Methyl groups were confirmed by symmetrical stretching vibrations at 2962.4, 2963.0 and 2962.3 cm^{-1} for un-modified, plasma treated and modified membranes respectively. Despite plasma treatment, the presence of methyl groups on the plasma treated membrane was seen and were attributed to underlying methyl groups, because only the membrane surface was targeted with the plasma treatment. Therefore, ATR-FTIR analysis was confirmed as having the ability to detect bond signals embedded within the polymer matrix.

Asymmetric deformations of methyl groups from the membranes were also observed at approximately 1411 cm^{-1} , and symmetric deformation of methyl groups for modified, un-modified and plasma treated membranes were at 1257.2, 1257.1 and 1257.8 cm^{-1} respectively. Peaks from stretching vibrations at 1004.5, 1004.7, and 1005.7 cm^{-1} were attributed to Si-O-Si

bonds, it is of paramount importance to note an increase in intensity of this peak from modified membrane, which further suggests the occurrence of the alkoxylation. The presence of O-SiCH₃ was confirmed by peaks at 783.1, 784.4 and 783.7 cm⁻¹, the presence of C-SiCH₃ groups were confirmed with peaks at 699.3, 669.8 and 669.8 cm⁻¹. Peaks from un-modified membrane were in close agreement with those from literature, (Bodas & Khan-Malek, 2006), (Kim & Jeong, 2011), especially for the modified membrane which was anticipated.

These characteristic changes in intensity and new peak formations observed using the ATR-FTIR technique (prior to and following membrane modification) confirmed the suitability of the technique to detect such changes had occurred.

4.2.5. Permeation analysis (Waters & Sabo, 2020)

Compounds ranging from different therapeutic classes such as anaesthetics, non-steroidal anti-inflammatories (NSAID), keratolytic agents, xanthine, and some anti-microbial or preservative compounds used in producing cosmetics were employed as model compounds to analyse permeation profiles through DMPS-PDMS modified membrane, as presented in Table 4.2.

Relevant physicochemical properties of these compounds are also presented to help consider a more logical, robust and informed conclusion as to what factor(s) really contribute or influence any change that may occur in the permeation pattern of the newly developed membrane. Moreover, these physicochemical parameters are also essential in developing any predictive model.

Table 4. 2 A summary of log P, molecular weight, hydrogen bond donor (HBD), hydrogen bond acceptor (HBA) count, polar surface area (PSA), and log D of compounds i.e., antipyrine (ATP), benzocaine (BEN), caffeine (CAF), diclofenac (DF), ethyl paraben (EP), ibuprofen (IBU), ketoprofen (KTF), lidocaine (LID), pentoxifylline (PXF), procaine hydrochloride (PCN), salicylic acid (SA), and tetracaine (TTC).

	Cmpds	log P	Mol.wght (g/mol)	CMP (µg/cm²) N-PDMS	CMP (µg/cm²) D-PDMS	HBD	HBA	PSA (Å²)	log D (pH 7.4)
1.	DF	4.98	296.14	123.8	617.5	2	3	49	1.37
2.	KTF	3.29	254.28	85.7	169.8	1	3	54	0.06
3.	EP	2.76	166.17	323.7	573.7	1	3	47	2.48
4.	BEN	2.2	165.19	2294.8	3787.9	1	3	52	1.83
5.	IBU	3.5	206.28	1176.2	2006.3	1	2	37	0.45
6.	PCN	2.14	272.77	33.4	56.8	2	4	56	0.29
7.	LID	1.81	234.34	3351.3	5048.7	1	2	36	1.26
8.	TTC	3.54	264.36	1551.0	2832.8	1	4	42	2.26
9.	ATP	1.18	188.23	313.3	450.1	0	2	24	0.74
10.	SA	1.96	138.12	862.4	1196.4	2	3	58	-0.77
11.	CAF	-0.24	194.19	72.0	87.5	0	3	58	-
12.	PXF	0.08	278.31	79.5	74.6	0	4	76	0.54

* Mol.wght – Molecular weight

* CMP (µg/cm²) N-PDMS – Cumulative mass permeated (µg/cm²) of normal PDMS membrane

* CMP (µg/cm²) D-PDMS - Cumulative mass permeated (µg/cm²) of DMPS modified PDMS membrane

* Mol.wght – Molecular weight

* log D – Distribution coefficient

* PSA – Polar surface area

* HBD - Hydrogen bond donor

* HBA – Hydrogen bond acceptor

- log P *source* DrugBank (Uniformly considered for linearity of data)
NB. The value of log P can be different depending on the source and often can be different according to methods used in obtaining the results

Following permeation analysis through PDMS membrane and modified DMPS-PDMS membrane (Figure 4.5), differences were observed between the membranes.

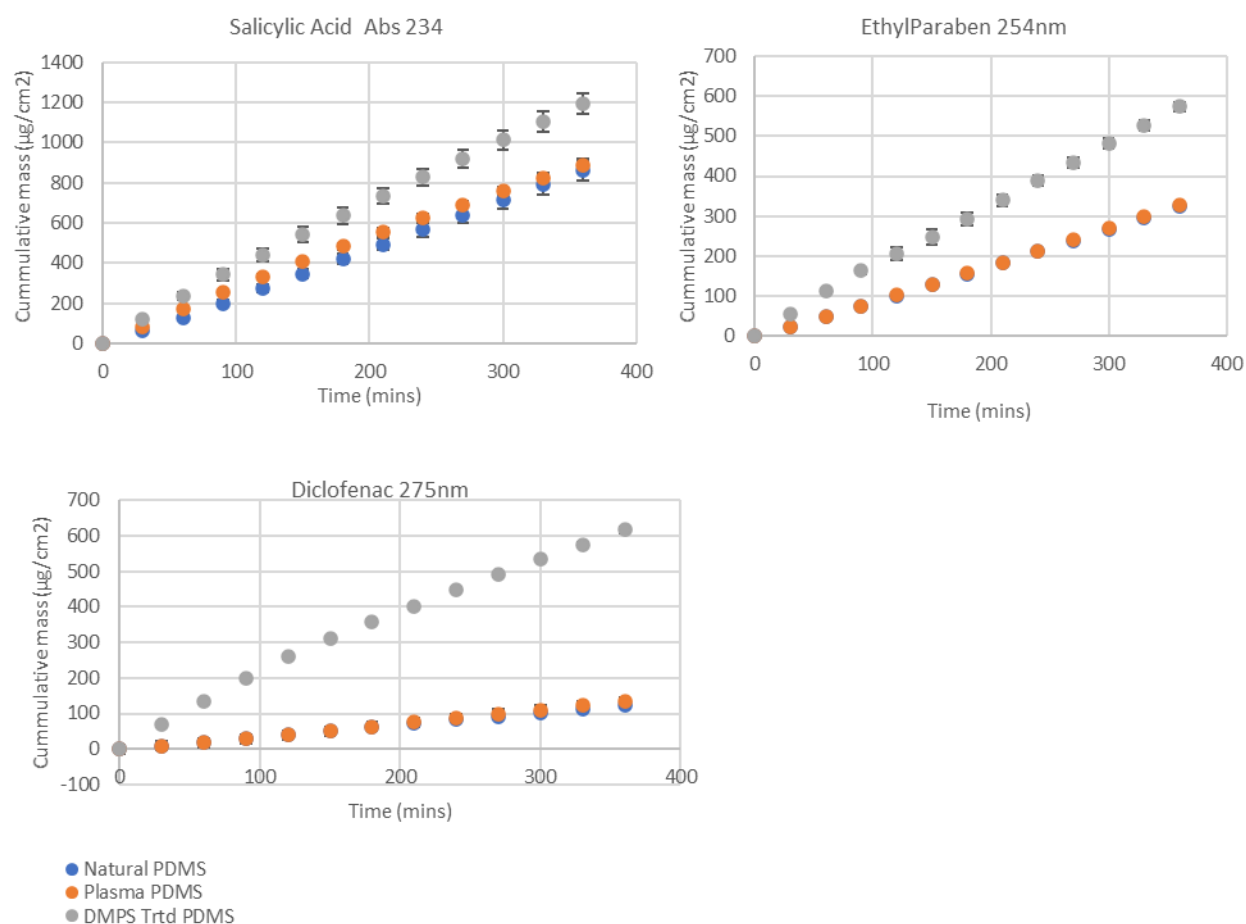


Figure 4. 5 Comparative steady state flux of salicylic acid, ethyl paraben and diclofenac through PDMS, Plasma Treated, and DMPS modified membranes

For ease of comparison Table 4.2 was compiled to instead consider the percentage increase observed following permeation studies, specifically between PDMS membrane and DMPS-PDMS membrane. These values are presented in Table 4.3.

Table 4. 3 Percentage increase (% incr.) of compounds i.e., antipyrine (ATP), benzocaine (BEN), caffeine (CAF), diclofenac (DF), ethyl paraben (EP), ibuprofen (IBU), ketoprofen (KTF), lidocaine (LID), pentoxifylline (PXF), procaine hydrochloride (PCN), salicylic acid (SA), and tetracaine (TTC), that permeated through normal and DMPS PDMS membranes

	Compounds	% Incr.
1.	DF	398 ± 7.8
2.	KTF	98 ± 6.1
3.	EP	77 ± 3.9
4.	BEN	65 ± 3.1
5.	IBU	70 ± 3.2
6.	PCN	70 ± 2.3
7.	LID	50 ± 2.5
8.	TTC	82 ± 5.4
9.	ATP	43 ± 2.8
10.	SA	38 ± 2.1
11.	CAF	21 ± 3.0
12.	PXF	-6 ± 0.1

* % Incr – Percentage Increase

- log P *source* DrugBank (Uniformly considered for linearity of data)
NB. The value of log P can be different depending on the source and often can be different according to methods used in obtaining the results

Percentage increase represents the percentage difference in cumulative mass ($\mu\text{g}/\text{cm}^2$) permeated over a 6-hour period (Table 4.3) between modified and un-modified membrane, and was calculated according to Equation 4.1:

$$\text{Mean percentage increase} = \left(\frac{\text{cumulative mass}^{\text{modified}} - \text{cumulative mass}^{\text{un-modified}}}{\text{cumulative mass}^{\text{un-modified}}} \right) \times 100$$

Equation 4.1

The increases observed in Table 4.3 indicate that even though the modification was only on the membrane surface, the overall effect on membrane permeation was quite significant. The manner in which Table 4.3 was presented is to enable easy correlation between percentage increases with respective physical parameters of the compounds.

Lipophilicity of compounds often expressed as log P, is a distribution co-efficient and represents relative ratios of a compound in an organic and aqueous solvent at the standard physiological pH of 7.4 (Arnott & Planey, 2012). The parameter is crucial in determining ADMET (absorption, distribution, metabolism, excretion and toxicity) and more specifically, it is also reported to influence extent of permeation in epidermal tissues and synthetic lipophilic membranes (Baba, Takahara, & Mamitsuka, 2015), (R. O. Potts & R. H. J. P. r. Guy, 1992; Zhang et al., 2012). Lipophilicity has various pharmacokinetic implications such as the way and manner compounds are distributed via biological tissues and accordingly is paramount in predicting how these distributions can be predicted (Hou, Wang, Zhang, Wang, & Xu, 2006; Testa, Crivori, Reist, & Carrupt, 2000). Hence, it was amongst the physical parameters considered for analysis of this result.

It was found that compounds with comparatively high log P values tended to have a greater permeation percentage increase when compared with their corresponding permeation profile for PDMS membrane. In other words, a linearity was achieved between compounds having high log P values and percentage increase in permeation profiles. Therefore, it is not surprising for diclofenac - having the highest log P value of 4.51 (Reymond, Awale, Probst, & Capecchi, 2019), (amongst the compounds used), displayed the highest percentage increase. In agreement with this theory, caffeine and pentoxifylline displayed a similar correlation, as having the

lowest log P values also had the lowest percentage increases. Overall a linear correlation was obtained when comparing literature log P values with percentage increase ($R^2 = 0.9$).

Extent of the effect achieved in terms of permeation profile change amongst standard PDMS membrane and its modified forms can be exemplified in a graphical representation as seen in Figure 4.6.

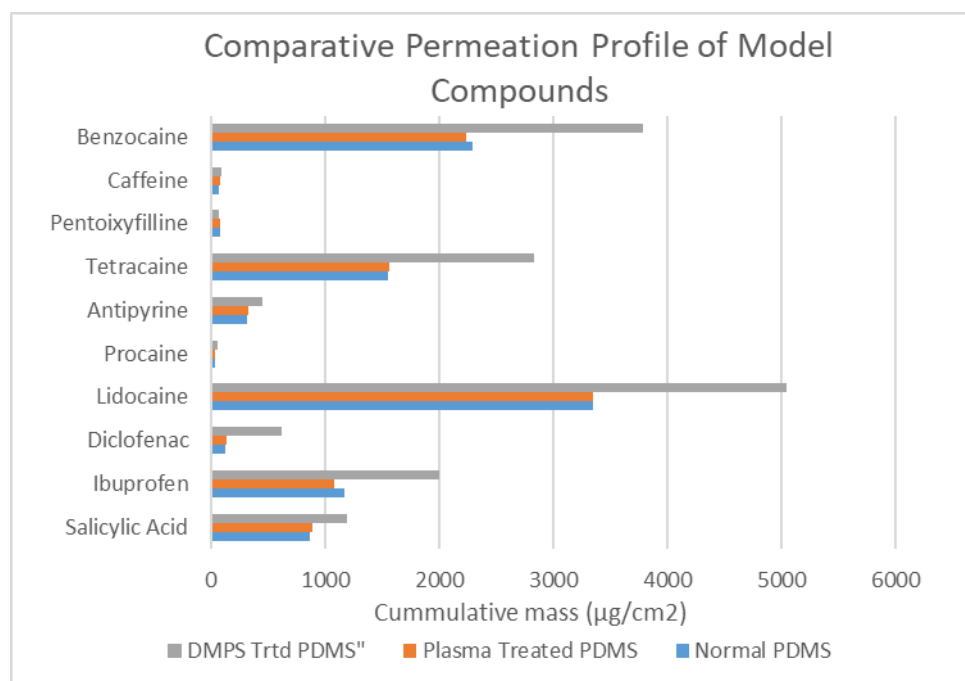


Figure 4. 6 Comparative permeation profiles of model compounds, permeated through PDMS, Plasma Treated, and DMPS modified membranes

Another quite interesting phenomenon was how the compounds appeared to behave partially according to their pharmaceutical classes (in terms of percentage increase), even when these compounds have a relatively substantial variety of log P values. It could be observed that the anaesthetics i.e. benzocaine (log P 2.2, 65 % increase), tetracaine (log P 3.54, 82 % increase) and procaine (log P 2.14, 70 % increase), behaved in a similar manner. In other words, these compounds probably interacted similarly with the surface of the modified membrane.

In summary, it has been established that there is a clear relationship between higher log P values and an increase in comparative permeation for the model compounds analysed across the modified membrane, as summarised in Figure 4.7.

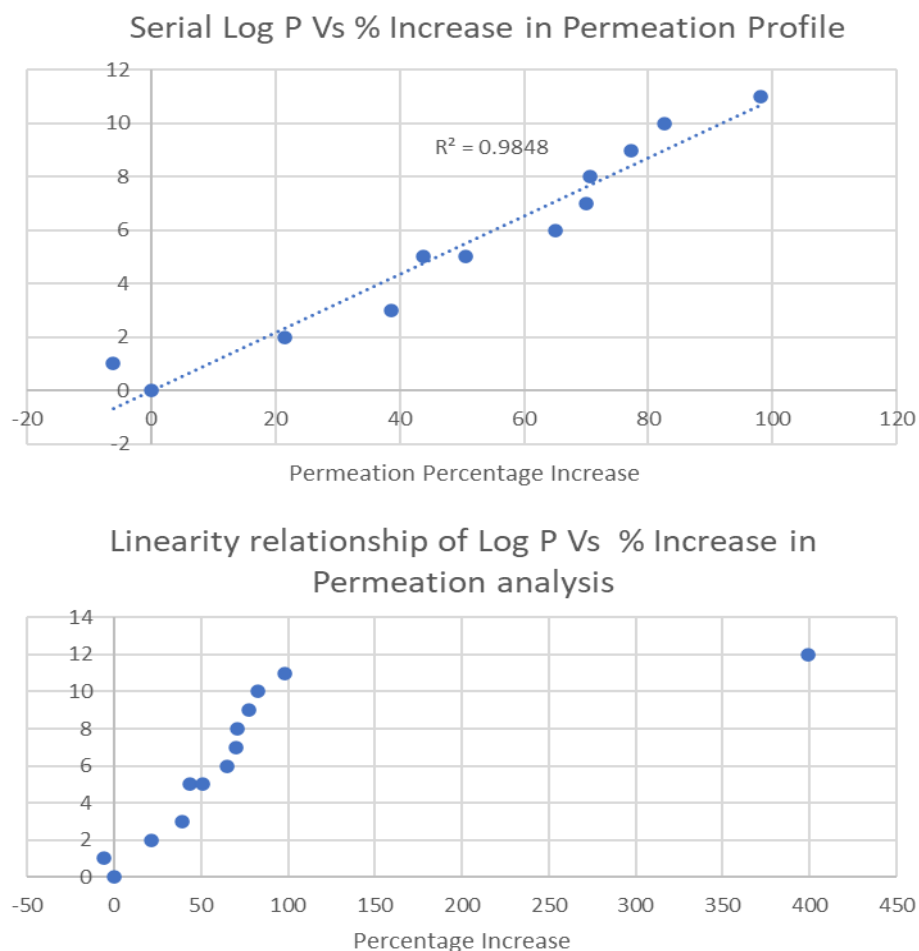


Figure 4. 7 Graphical representation of serially arranged log P values, in descending order, versus percentage increases in permeation profile (obtained between PDMS and modified PDMS)

It was additionally observed that an inverse relationship existed between log P value and the amount of cumulative mass permeated in ($\mu\text{g}/\text{cm}^2$) (CMP), amongst model compounds with similar chemical functionalities. For instance, this was seen for compounds with basic amino groups (Figure 4.8) i.e. lidocaine (log P 1.81, CMP 3351 $\mu\text{g}/\text{cm}^2$), benzocaine (log P 2.2, CMP

2294 $\mu\text{g}/\text{cm}^2$) and tetracaine (log P 3.54, CMP 1551 $\mu\text{g}/\text{cm}^2$) have shown a decrease in cumulative mass permeated over 6 hours, as their log P values tend to increase.

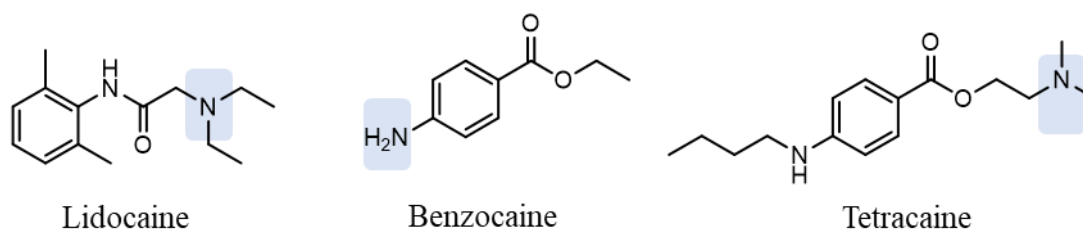


Figure 4. 8 Structural representation of lidocaine, benzocaine and tetracaine highlighting their similar functional groups

This phenomenon, however, was not surprising as Moss *et al* have reported a similar behaviour exhibited when using human skin (Moss, Gullick, & Wilkinson, 2016). The surface of human skin comprises of a disproportionate heterogeneous mixture which is largely lipophilic. Therefore, lipophilic compounds are considered more favoured in terms of transdermal permeation. However, there is a flipside when it comes to compounds having high log P values ($\log P > 2$), as they tend to get retained in this route, discouraged against permeating-out in a timely manner. In other words, there is poor clearance of these compounds out of the route into the underlying layer. It is therefore understood that compounds with log P values between $1 < \log P < 3$, are the most suitable for transdermal drug delivery (Moss et al., 2016). This could be the explanation for the decreased cumulative permeation profile observed in some of the model compounds as their log P values tend to increase, when comparing data for PDMS membrane against the modified form of the membrane. This further shows a similarity in behaviour between the modified membrane and human skin. Similarly, caffeine and pentoxifylline (both xanthines) were also observed to show a similar trend.

A study carried out by Bhuiyan *et al*, 2017, reported that the introduction of hydrophilic groups onto the surface of PDMS via physical adsorption can reduce the permeation of pharmaceutical

compounds through the membrane, this phenomenon, the authors added, was as a result of ‘reduced partitioning of the permeant into the membrane’ (Bhuiyan, Waters, 2017). It was based on this understanding that some researchers have hypothesised a correlation between polar surface area (PSA) and permeation profile of PDMS membrane. The hypothesis was such that, ‘partitioning of compounds with high polar surface area may be less affected by the introduction of polar functionalities on PDMS membrane, conversely, compounds with low polar surface area, will display low partitioning into the outermost hydrophilic polymer layers’. This theory wasn’t entirely the case in this analysis, as it was observed that although the partitioning effect can be very crucial in permeation of pharmaceutical compounds via PDMS, it was less influenced by PSA of the compounds, but rather, it was more likely influenced by the newly formed additional surface layer, as little or no correlation was drawn between PSA and permeation profile.

4.2.7.1 Comparison with Human Skin Data

The cumulative amount of drug permeated through PDMS membrane and that of the modified membrane, were converted to permeation co-efficient values (K_p), and these values were compared to values representing human skin, obtainable from literature. K_p were scrutinised on the basis of tissue type, and physicochemical parameters used in the experiments, for effective comparisons and summarised in Table 4.4.

Table 4. 4 Cumulative mass ($\mu\text{g}/\text{cm}^2$), and permeation coefficient (K_p) $\times 10^{-4}$ cm/min) values of lidocaine (LID), ketoprofen (KTF), salicylic acid (SA), ethyl paraben (EP), ibuprofen (IBU), diclofenac (DF), procaine hydrochloride (PCN), antipyrine (ATP), pentoxifylline (PXF), tetracaine (TTC), caffeine (CAF) and benzocaine (BEN) permeated through N-PDMS and D-PDMS, alongside some K_p literature values.

	Cmpds	Log P	CMP ($\mu\text{g}/\text{cm}^2$)		$(K_p) \times 10^{-4}$ (cm/min)		
			N-PDMS	D-PDMS	N-PDMS	D-PDMS	Literature
1	LID	1.81	3351.3	5048.6	8.2	12.6	4.2 (Miki et al., 2015b)
2	KTF	3.29	85.7	169.7	0.08	0.3	1.17 (Zhang et al., 2012)
3	SA	1.96	862.4	1196.4	2.8	3.8	2.3 (Degim, Pugh, & Hadgraft, 1998)
4	EP	2.76	304.9	573.6	3.2	5.9	2.3 (Uchida et al., 2015)
5	IBU	3.5	1176.2	2006.3	6.4	10.6	0.56 (Zhang et al., 2012)
6	DF	4.98	134.2	617.4	0.5	2.4	-
7	PCN	2.14	33.3	56.7	0.001	0.01	-
8	ATP	1.18	313	450	0.7	1	-
9	PXF	0.08	79.4	74.6	0.04	0.04	-
10	TTC	3.54	1551	2832.6			-
11	CAF	-0.24	72	87.5	0.1	0.1	0.1 (Uchida et al., 2015)
12	BEN	2.2	2294.8	3787.9	3.4	5.8	-

* Mol.wght – Molecular weight

* CMP ($\mu\text{g}/\text{cm}^2$) N-PDMS – Cumulative mass permeated ($\mu\text{g}/\text{cm}^2$) of normal PDMS membrane

* CMP ($\mu\text{g}/\text{cm}^2$) D-PDMS - Cumulative mass permeated ($\mu\text{g}/\text{cm}^2$) of DMPS modified PDMS membrane

* K_p – Permeation coefficient (Flux) in micrograms per centimetre squared ($\mu\text{g}/\text{cm}^2$).

- log P *source* DrugBank (Uniformly considered for linearity of data)
NB. The value of log P can be different depending on the source and often can be different according to methods used in obtaining the results

To effectively compare data with that of human skin, an additional physical parameter for total amount of drug permeated through the membrane over 6 hours i.e. K_p , was introduced and is represented in micrograms per centimetre squared ($\mu\text{g}/\text{cm}^2$).

From Table 4.4, a considerable difference was obtained when trying to compare values from modified membrane alongside standard literature, using the descriptive factor (K_p), considering the literature values originated from skin data. It is obvious that a reduced value from modified membrane would constitute a better skin mimic system. However, a regular increased pattern corresponding to certain drug properties, or a robust predicted behaviour of the modified membrane if achieved would constitute a good skin replacement, irrespective of the increase in permeation.

Overall, a plausible change in surface morphology of DMPS-PDMS was achieved in terms of its permeation profile. Difficulty in measuring permeation of some hydrophilic compounds (Miki et al., 2015a) such as caffeine, pentoxifylline and antipyrine when using PDMS has also been overcome following the silanisation process, however, it is apparent that a lipophilic layer has been achieved rather than a heterogeneous layer, resulting in over-estimation, particularly for lipophilic compounds.

4.2.6. Brunauer-Emmett-Teller Technique

Having established a modified layer that results in a change in permeation profile (Table 4.4), it was necessary to ascertain if this change is as a result of surface interaction only, or the integrity of the membrane has been affected during the modification process. Brunauer-Emmett-Teller Technique (BET) was used to determine porosity of the polymer material. More specifically, it was used to comparatively determine if there was any change regarding porosity between un-modified and modified membranes.

Un-modified membrane was seen to have zero porosity ($0 \text{ m}^2/\text{g}$) indicating the membranes were non-porous, and in conformity with its true nature. Similar results were obtained by (Nakade, Ichihashi, Ogawa, & technology, 2005), when analysing PDMS samples. The non-porous nature of the membrane makes it a good candidate for this study and was the reason it is considered a possible analogue for skin and hence, substances could only permeate through the membrane. Therefore, it is vital to ensure that this feature is maintained throughout the process of modification rather than creating a membrane that allows compounds to freely pass through a porous structure.

Interestingly, the same value ($0 \text{ m}^2/\text{g}$) was obtained when analysing the modified membrane, thus confirming that the increase in permeation is attributed to selective permeation and not porosity. It can, therefore, be confirmed that the chemical modification process has not compromised the membrane integrity and concerns arising from a mere physical modification were addressed with the help of this technique. Data acquired for this analysis are displayed in Appendix II.

4.2.7. Optical Microscopy

Optical microscopy was utilised to characterise the membranes studied through surface observation, as shown in Figure 4.9.

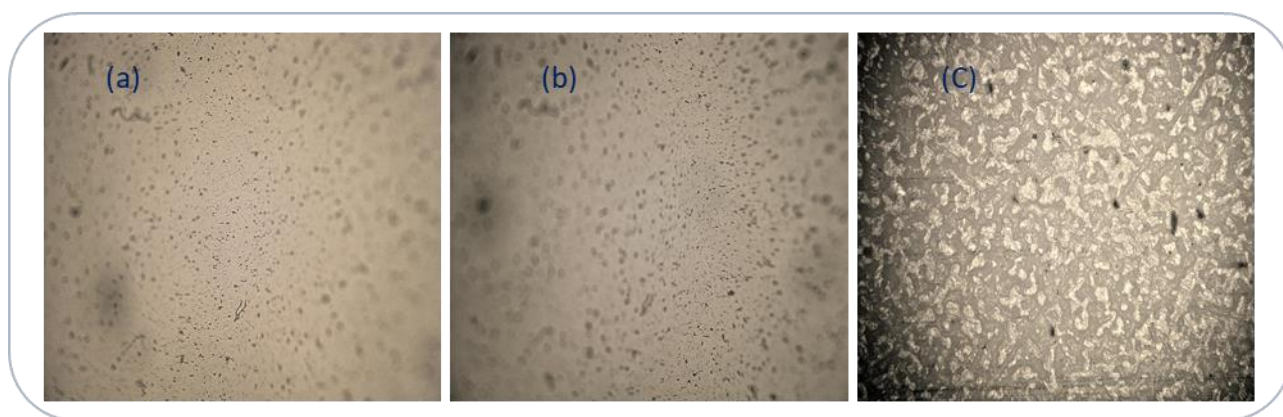


Figure 4. 9 Optical microscopy images for (A) PDMS, (B) plasma treated PDMS, and (C) D-PDMS at x 250 magnification

The surface appearance between different modified membranes could be seen following magnification. In Figure 4.4 (a) and (b) little difference could be observed, this shows that there was little or no physical change following the initial plasma treatment and the integrity of the membrane was not compromised.

This finding is confirmed when considering the results achieved from permeation analysis (Table 4.4) indicating cumulative mass of drugs permeated over 6 hours shows no considerable difference between un-modified and plasma treated membranes.

In contrast, a reasonable physical difference could be seen from the modified membrane, in comparison with the plasma treated and un-modified membranes, Figure 4.4 (a), (b), and (c) respectively. An increase in surface roughness and the presence of discontinuous patches can be seen in Figure 4.4 (c), which are attributed to the chemical treatment undergone by the modified membrane. However, no physical alteration or damage within the membrane that

might result in an increase in porosity could be seen from the image presented. These un-even patches which must be attributed to the chemical modification process, may have been part of the explanation for the detection difficulties experienced in ATR-FTIR analysis (Figure 4.10).

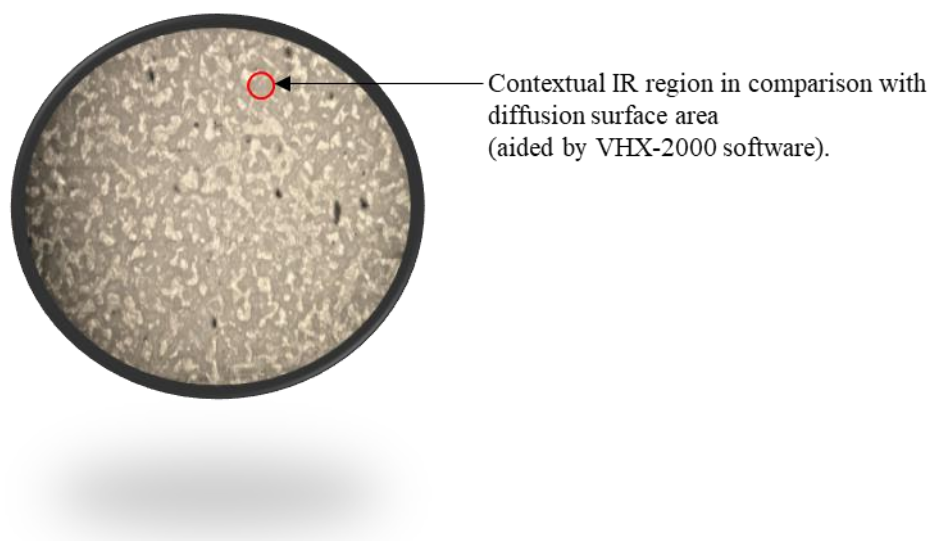


Figure 4. 10 Optical microscopy image of D-PDMS at x 250 magnification, illustrating the ATR-FTIR effective analysis area.

4.3. Sequential Silanisation using Tertbutyldimethylsiloxane

Utilisation of tertbutyldimethylsiloxane (TBDMS) was inspired by the work of Potts and Guy (R. O. Potts & R. H. Guy, 1992). In their pioneering work, they describe an increase in molecular weight, or molecular volume, to negatively influence the permeation coefficient. In other words, an increase in carbon chain length can be concomitant in reducing permeation through sample membrane.

However, following the silanisation process (method not presented), the resultant modified membrane, i.e. TBDMS modified – PDMS (T-PDMS), was found to have an increased percutaneous absorption profile when compared with plasma treated PDMS membrane. This result was somewhat unsurprising as an additional layer on the surface of the membrane was more likely to be formed in contrast to a heterogeneous layer, which is similar to skin. Interestingly, Cronin *et al* reported findings relating polymeric systems with ‘alternating hydrophobic and hydrophilic layers’ to provide a more robust system in terms of skin mimics, rather than two distinct layers (Cronin, Dearden, Gupta, & Moss, 1998).

Additionally, Addicks *et al* presented a finding that entails the permeation of alkyl 4-aminobenzoate through silicon membranes (Addicks, Flynn, & Weiner, 1987), as seen in Figure 4.11.

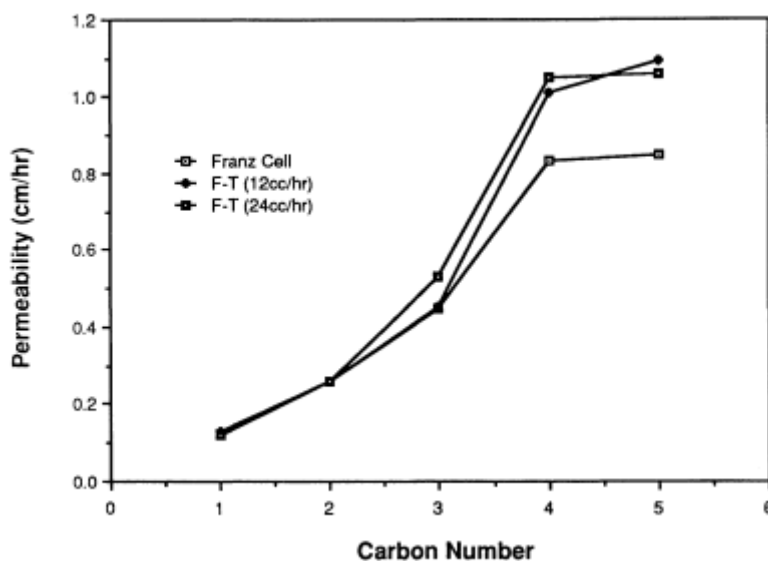


Figure 4. 11 Permeability coefficient of alkyl 4-aminobenzoate permeated via silicon membrane. Adopted from Addicks *et al*, 1987.

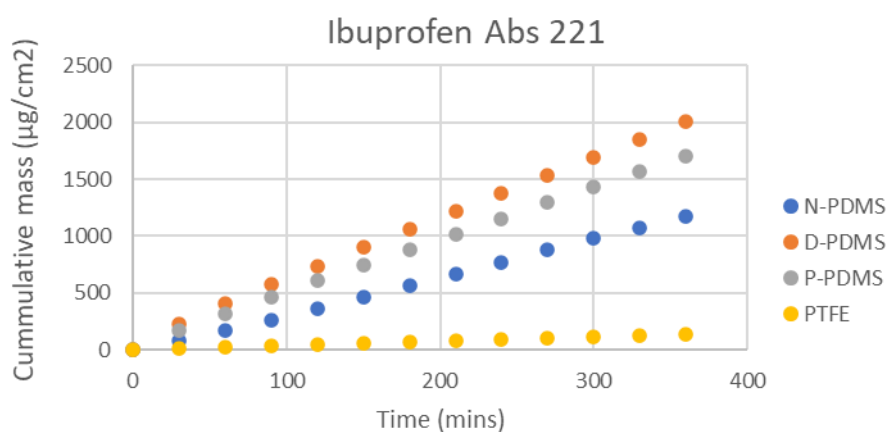
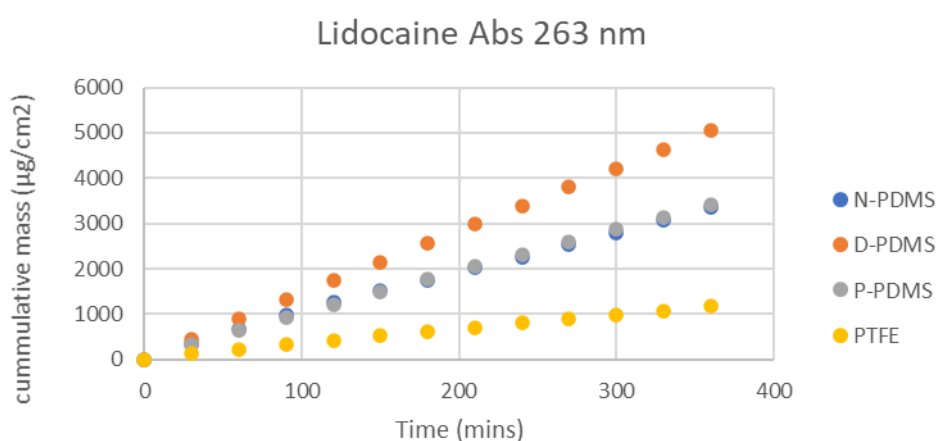
Figure 4.11 displays how an increase in carbon chain lengths in silicon membranes can lead to an increase in diffusion coefficient. However, it was proposed in the work that ‘as chain length increases, a plateau is reached, where rate of diffusion is no longer predominantly controlled by the membrane material itself, instead by an aqueous diffusion layer formed’. Following this work, it was considered that an additional layer made up of TBDMS was formed on the surface of the plasma treated membrane, hence instead of achieving an additional carbon chain membrane, a covalently attached layer was formed on the PDMS surface, and therefore, the rate of diffusion was primarily controlled by the additional layer formed.

4.4. Sequential Silanisation using Perfluorophenylsilanol

In this study the electronegativity of fluorine groups present in the pre-cursor reagent (perfluorophenylsilanol) was aimed to bring about a substantial change in the surface chemistry of PDMS. It was envisaged that this change could possibly be significant enough to alter permeation profiles through the membrane, in comparison with unmodified PDMS.

4.4.1. Comparative permeation profile between Perfluorophenylsilanol treated PDMS and PDMS membrane

Following the modification process, permeation analysis was carried out on perfluorophenylsilanol treated PDMS membrane (P-PDMS) and compared with PDMS membrane, as displayed in Figure 4.12.



N-PDMS – Normal Poly(dimethylsiloxane)
D-PDMS – Dimethylphenylsiloxane treated Poly(dimethylsiloxane)
P-PDMS – Perfluorophenylsilanol treated Poly(dimethylsiloxane)
PTFE – Polytetrafluoroethylene membrane

Figure 4. 12 Comparative steady state flux of lidocaine and ibuprofen compounds through PDMS, DMPS and Perfluorophenylsilanol modified PDMS membranes, alongside PTFE

From Figure 4.12 it can be seen that the newly formed membrane differs from the standard PDMS membrane, however, changes observed were somewhere in between permeation profiles of D-PDMS and standard PDMS. Therefore, this result was not distinct enough to necessitate further pursuit related to the primary aim of this study.

4.5. Conclusion

A series of modification processes have been depicted in this study, as summarised in Figure 4.13.

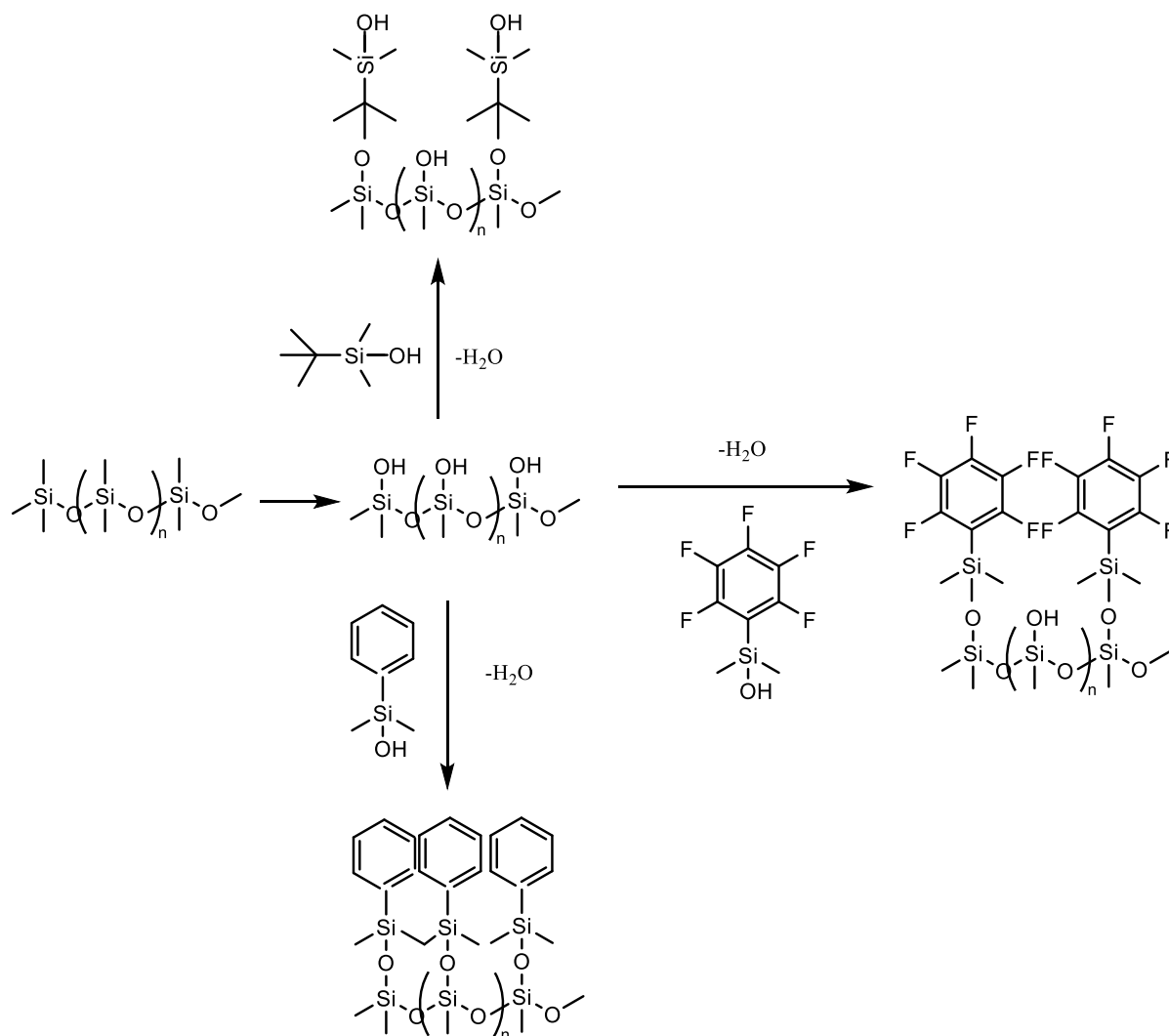


Figure 4. 13 Summary of silanisation processes employed in this study

DMPS-PDMS modified membrane has shown the most desirable change in permeation profile of model compounds analysed. More importantly, a similarity was established between behaviours of these model compounds permeated via the modified membrane, with permeation behaviours of compounds exhibited by skin. With the help of some spectroscopic techniques, it was also established that indeed an additional layer had been deposited on the surface of PDMS via a silanisation reaction, and the process was strong enough to last for 6 hours. This

positively indicates the initial stability of the membrane, along with a stable activity throughout the process.

A good correlation ($R = 0.9$) has also been established between a physicochemical parameter ($\log P$) with a comparative percentage increase between modified and unmodified PDMS membranes. This is to say a robust membrane capable of establishing a defined pattern has been achieved, and by extension, it could form the basis for a predictive model. Furthermore, the modified membrane was able to provide a novel achievement, by allowing the analysis of hydrophilic compounds such as the xanthines used in this study, which before now has been reported as a constraint for silicon membranes in permeation analysis, especially PDMS. The hydrophobic nature of the membrane was the main reason behind this constraint and changes observed in permeation profiles through DMPS-PDMS modified membrane confirm the proposed establishment of an additional layer.

Instead of an emulsified layer impregnated within the membrane matrix, it was believed that an additional layer was formed on the membrane surface, which then proceeded to serve as the rate determining factor for permeation flux. In other words, it provided a lipophilic partition that increased the affinity of lipophilic compounds towards the surface of the membrane, thereby increasing their permeation. This understanding has therefore paved an informed idea on how to create membranes with heterogenous surfaces which will better mimic skin in terms of permeation measurement instead of two distinct layers.

References

- Addicks, W. J., Flynn, G. L., & Weiner, N. (1987). Validation of a flow-through diffusion cell for use in transdermal research. *Pharmaceutical research*, 4(4), 337-341.
- Arkles, B., Steinmetz, J., Zazyczny, J., Mehta, P. J. J. o. A. S., & Technology. (1992). Factors contributing to the stability of alkoxysilanes in aqueous solution. *Journal of Adhesion science and technology* 6(1), 193-206.
- Arnott, J. A., & Planey, S. L. (2012). The influence of lipophilicity in drug discovery and design. *Expert opinion on drug discovery*, 7(10), 863-875.
- Baba, H., Takahara, J.-i., & Mamitsuka, H. (2015). In silico predictions of human skin permeability using nonlinear quantitative structure–property relationship models. *Pharmaceutical research*, 32(7), 2360-2371.
- Bhuiyan, A., Waters, L. J. J. C., Physicochemical, S. A., & Aspects, E. (2017). Permeation of pharmaceutical compounds through silicone membrane in the presence of surfactants. *Physicochemical and Engineering Aspects* 516, 121-128.
- Bodas, D., & Khan-Malek, C. J. M. e. (2006). Formation of more stable hydrophilic surfaces of PDMS by plasma and chemical treatments. *Microelectronic Engineering* 83(4-9), 1277-1279.
- Cronin, M., Dearden, J., Gupta, R., & Moss, G. (1998). An investigation of the mechanism of flux across polydimethylsiloxane membranes by use of quantitative structure-permeability relationships. *Journal of pharmacy and pharmacology*, 50(2), 143-152.
- Degim, I. T., Pugh, W. J., & Hadgraft, J. (1998). Skin permeability data: anomalous results. *International journal of pharmaceutics*, 170(1), 129-133.
- Hou, T., Wang, J., Zhang, W., Wang, W., & Xu, X. (2006). Recent advances in computational prediction of drug absorption and permeability in drug discovery. *Current medicinal chemistry*, 13(22), 2653-2667.
- Kim, H. T., & Jeong, O. C. J. M. E. (2011). PDMS surface modification using atmospheric pressure plasma. *Microelectronic Engineering* 88(8), 2281-2285.
- Lummerstorfer, T., & Hoffmann, H. (2004). Click chemistry on surfaces: 1, 3-dipolar cycloaddition reactions of azide-terminated monolayers on silica. *The Journal of Physical Chemistry B*, 108(13), 3963-3966.
- Miki, R., Ichitsuka, Y., Yamada, T., Kimura, S., Egawa, Y., Seki, T., . . . Morimoto, Y. (2015a). Development of a membrane impregnated with a poly (dimethylsiloxane)/poly (ethylene glycol) copolymer for a high-throughput screening of the permeability of drugs, cosmetics, and other chemicals across the human skin. *European Journal of Pharmaceutical Sciences*, 66, 41-49.
- Miki, R., Ichitsuka, Y., Yamada, T., Kimura, S., Egawa, Y., Seki, T., . . . Morimoto, Y. J. E. J. o. P. S. (2015b). Development of a membrane impregnated with a poly (dimethylsiloxane)/poly (ethylene glycol) copolymer for a high-throughput screening of the permeability of drugs, cosmetics, and other chemicals across the human skin. *European Journal of Pharmaceutical science* 66, 41-49.
- Moss, G. P., Gullick, D. R., & Wilkinson, S. C. (2016). *Predictive Methods in Percutaneous Absorption*: Springer.
- Nakade, M., Ichihashi, K., Ogawa, M. J. J. o. s.-g. s., & technology. (2005). Preparation of titania/PDMS hybrid films and the conversion to porous materials. *Journal of sol-gel science and technology* 36(3), 257-264.
- Ou, J., Hu, W., Xue, M., Wang, F., & Li, W. (2013). One-step solution immersion process to fabricate superhydrophobic surfaces on light alloys. *ACS applied materials & interfaces*, 5(20), 9867-9871.

- Potts, R. O., & Guy, R. H. (1992). Predicting skin permeability. *Pharmaceutical research*, 9(5), 663-669.
- Potts, R. O., & Guy, R. H. J. P. r. (1992). Predicting skin permeability. *Pharmaceutical research* 9(5), 663-669.
- Reymond, J., Awale, M., Probst, D., & Capecchi, A. (2019). PubChem and ChEMBL Beyond Lipinski. *Molecular informatics* 38(5), 1900016
- Sui, G., Wang, J., Lee, C.-C., Lu, W., Lee, S. P., Leyton, J. V., . . . Tseng, H.-R. (2006). Solution-phase surface modification in intact poly (dimethylsiloxane) microfluidic channels. *Analytical Chemistry*, 78(15), 5543-5551.
- Testa, B., Crivori, P., Reist, M., & Carrupt, P.-A. (2000). The influence of lipophilicity on the pharmacokinetic behavior of drugs: Concepts and examples. *Perspectives in Drug Discovery and Design*, 19(1), 179-211.
- Uchida, T., Kadhum, W. R., Kanai, S., Todo, H., Oshizaka, T., & Sugibayashi, K. (2015). Prediction of skin permeation by chemical compounds using the artificial membrane, Strat-M™. *European Journal of Pharmaceutical Sciences*, 67, 113-118.
- Virtanen, J. A., Kinnunen, P. K., & Kulo, A. E. (1988). Surface treatment agents and polymers comprising substituted phenyl silanes and siloxanes. In: Google Patents.
- Waters, L. J., & Sabo, S. (2020). Permeation of pharmaceutical compounds through silanised poly (dimethylsiloxane). *Journal of pharmaceutical sciences*, 109(6), 2033-2037
- Zhang, K., Chen, M., Scriba, G. K., Abraham, M. H., Fahr, A., & Liu, X. (2012). Human Skin Permeation of Neutral Species and Ionic Species: Extended Linear Free Energy Relationship Analyses. *Journal of pharmaceutical sciences*, 101(6), 2034-2044.

Chapter 5

Development of a Smart Poly(dimethylsiloxane) alternative for permeation analysis

5.1 Introduction

Having presented a modified PDMS membrane in Chapters 3 and 4 that predominantly comprises of a hydrophilic and lipophilic surface layer respectively, it is proposed, that a modified PDMS polymer membrane that has a heterogeneous layer comprising of both hydrophilic and lipophilic regions, reigns supreme in mimicking human skin for prediction of percutaneous absorption. In order to effectively achieve this proposed idea, the concept of smart polymerisation is considered in this chapter.

Smart polymers or ‘stimuli responsive polymers’, are polymers that can reversely respond to physicochemical effects. These effects can be changes in temperature or pH (Majcen, Mohsen, Snowden, Mitchell, & Voncina, 2018), light intensity and the presence of biological molecules at a macroscopic level, often characterised by swelling, group rearrangements, collapse or sol-to-gel transitions, depending on the physical state of the chains (Maria Rosa Aguilar, Elvira, Gallardo, Vázquez, & Román, 2007; María Rosa Aguilar & San Román, 2019). The idea of creating a smart polymer for percutaneous permeation analysis is coined from the hydrophobic nature of PDMS. Hydrophobic and lipophilic terms are often used interchangeably, probably because most hydrophobic substances are also lipophilic. However, it is important to note that certain materials, such as fluorocarbons and silicones, are an exception to this stereotype.

Results presented in Chapter 4 indicate that PDMS membrane does not encourage the adsorption of lipophilic compounds, to the extent that rather deliberate attempts need to be made towards achieving a permeable surface. However, it is quite understandable that the hydrophobic nature of PDMS makes it difficult to introduce aqueous substances on its surface (Hu et al., 2002). These combined effects exhibited by the membrane need to be harmonised to achieve the overall aim of this research.

5.2. Smart PDMS membrane

5.2.1. Background

An alternative approach that involves grafting a smart co-polymer layer incorporated on modified Dimethylphenylsilanol-Poly(dimethylsiloxane) (D-PDMS) membrane was proposed. In this approach, an amphiphilic poly(dimethylsiloxane) and poly(ethyleneglycol) block co-polymer PDMS-PEG BCP, was identified, partly due to the hydrophilic nature of PEG co-polymer. This co-polymerisation graft approach has been previously reported in some related studies. For instance, PEG has been grafted with polyacrylonitrile (PAN) (Asatekin, Kang, Elimelech, & Mayes, 2007; Asatekin & Mayes, 2009; Kang, Asatekin, Mayes, & Elimelech, 2007) and poly(vinylidene fluoride) (Kaner, Rubakh, & Asatekin, 2017), which enabled the resultant filtration membranes to have excellent fouling resistance.

Other studies that specifically reported the use of a PDMS-based additive namely PDMS-PEG BCP, have also been reported, which in part, motivated the selection of this additive. Yao *et al* reported in their work that the addition of PDMS-PEG BCP improved surface hydrophilicity of PDMS membrane, reducing water contact angle to $21.5 - 90.8^\circ$ from 112° , thereby increasing its hydrophilicity (Yao & Fang, 2012). Similarly, another study was carried out using the same additive, primarily to address stability and hydrophobic recovery often associated with the membrane. It was also reported in the study that PDMS-PEG BCP segregates when in contact with water, creating a surface re-arrangement with the PEG positioned on the membrane surface. In other words, PEG which is far more hydrophilic than PDMS, forces a displacement reaction within the PDMS-PEG BCP matrix when in contact with water (Gökaltun, Kang, Yarmush, Usta, & Asatekin, 2019). While these studies and other similar approaches have increased hydrophilicity, stability and smart re-orientation of PDMS-PEG BCP, their broader use in biopharmaceutical areas such as drug delivery and controlled drug release is limited.

This approach has not been utilised to produce a membrane for the purpose of predicting percutaneous absorption prior to this study.

5.2.2. D-PDMS - PDMS-PEG BCP method

From earlier modification (Section 4.2.2), it was possible to establish a modified form of PDMS that had a lipophilic surface i.e. D-PDMS. This established form of the membrane was then cured and grafted with PDMS-PEG BCP.

Commercially available PDMS-PEG BCP comprises of 60-70 % PEG and anchors on the PDMS base. The material is linked to D-PDMS with the help of a plasma treatment process, enabled by existing protocols with no added steps. Based on available literature, and earlier studies carried-out, it was proposed that this new form of modified PDMS will rather have a multi-layered structure which will selectively control permeation on the basis of the hydro-lipophilicity parameter. In other words, this newly modified PDMS membrane will act as a smart polymer by selectively re-orienting upon contact with foreign substances, primarily on the basis of their polarity (Figures 5.1 and 5.2).

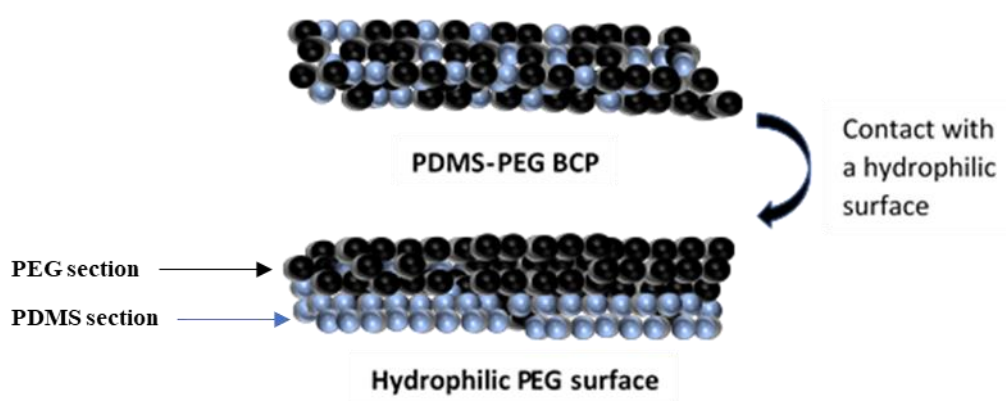


Figure 5. 1 Schematic representation of proposed surface re-arrangement exhibited by PDMS-PEG BCP, when in contact with hydrophilic materials.

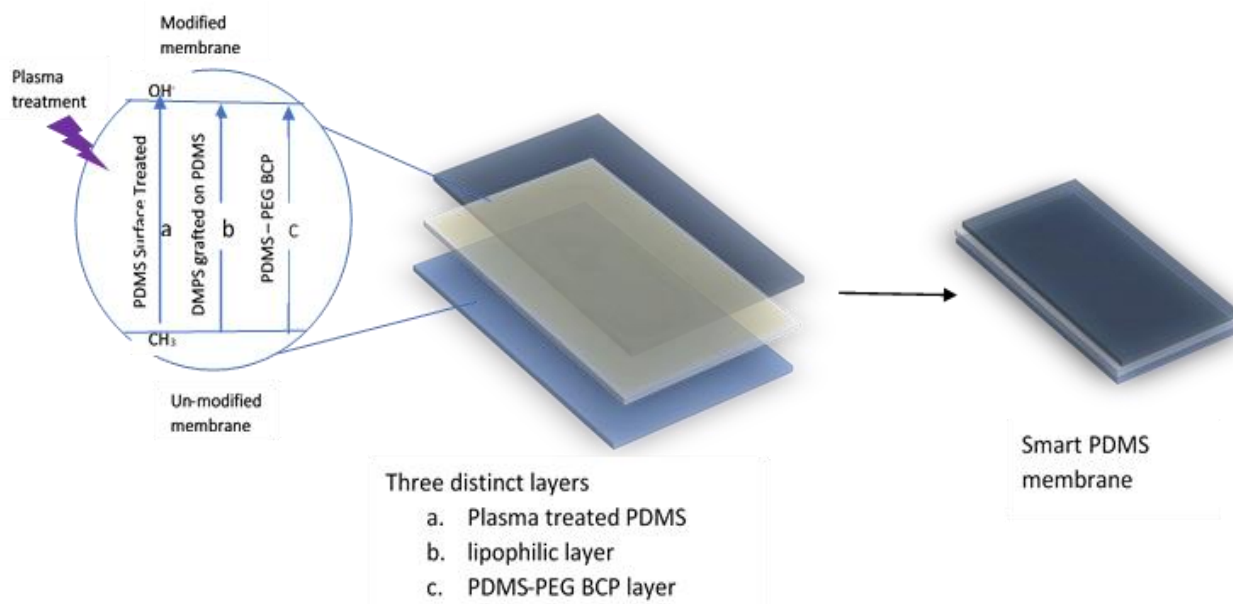


Figure 5. 2 Schematic illustration of distinct layers present in the formation of smart-PDMS membrane proposed in this study.

5.2.2.1 Schematic representation and process methodology

PDMS silicon membrane, 0.3 mm thickness with approximately 0.6 cm^2 size was utilised in this process. The membrane was plasma-treated then cured with 1 mL dimethylphenylsilanol. The process was a wet process, and the reaction was carried out in an ethanolic medium ($\sim 5 \text{ mL}$). PDMS-PEG BCP curing agent was also added to the reactor ($\sim 1 \text{ mL}$). The entire reaction process lasted for 2 hours.

Subsequently, the membrane formed was placed on an aluminium foil covered glass plate and introduced in an oven adjusted to 50°C for 24 hours to completely cure and evaporate any excessive solution from the product and to further drive the process.

The overall methodology is displayed in Figure 5.3.

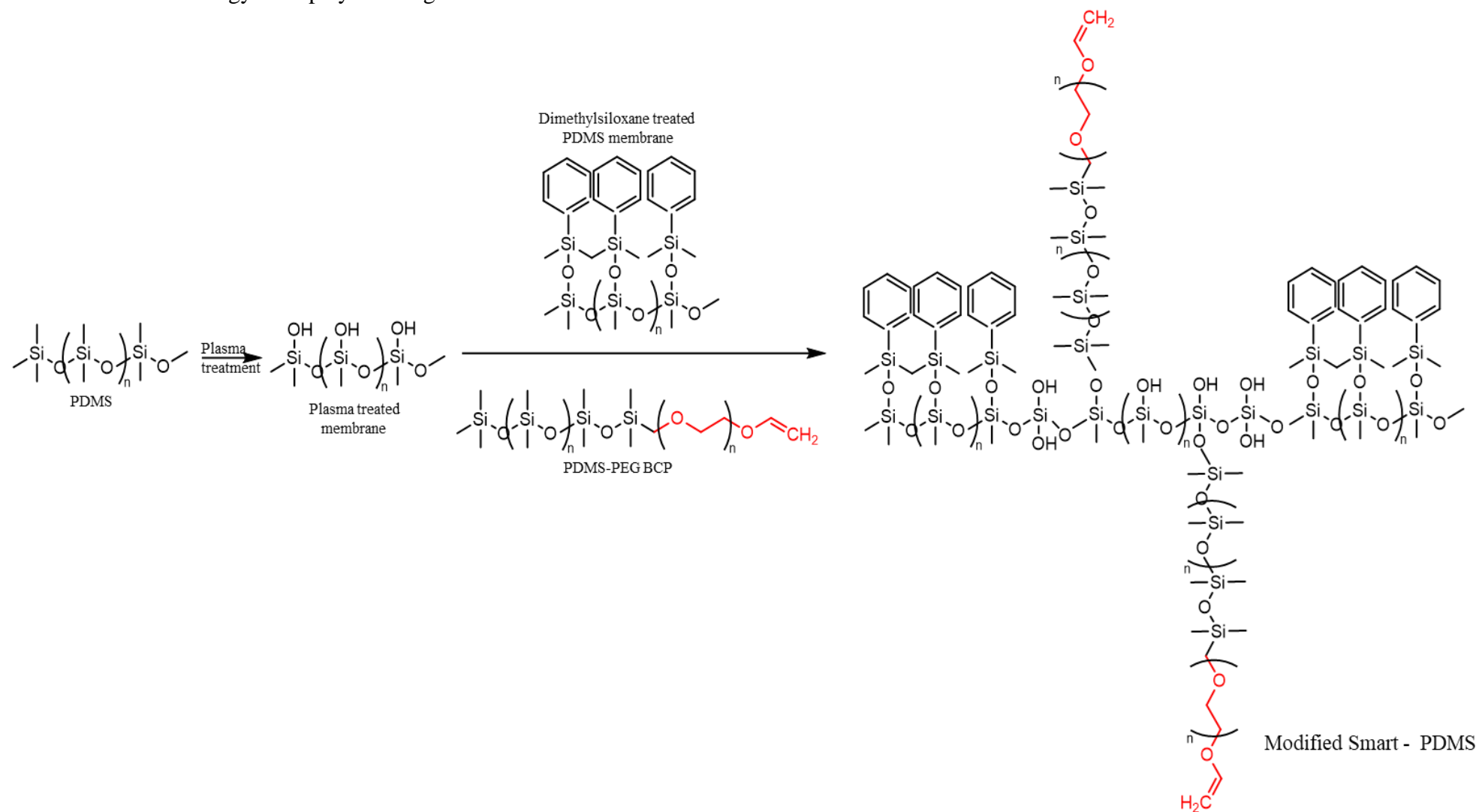


Figure 5. 3 Proposed reaction scheme in the development of a smart-PDMS membrane

5.2.3. Attenuated Total Reflectance-Fourier Transform Infra-red spectroscopy

ATR-FTIR analysis was undertaken with results presented in Table 5.1 and Figure 5. 4.

Table 5. 1 ATR-FTIR assignment of PDMS pre- and post-modification.

Assignment	ν_{\max} (cm ⁻¹)		
	PDMS	PDMS-PEG BCP	Smart - PDMS
ν_s (CH ₃)	2982.4	2990.1	2991
δ_{as} (CH ₃)	1416.2	1419	1412.1
δ_s (CH ₃)	1272.7	1277.5	1278.1
ν_s (CH ₃)	-	2874.9	2883.6
Si-O-Si	-	-	1097.6
Si-O	478	-	475
O-SiCH ₃	771.2	778.2	783.1
C-SiCH ₃	680.3	677.7	680.6

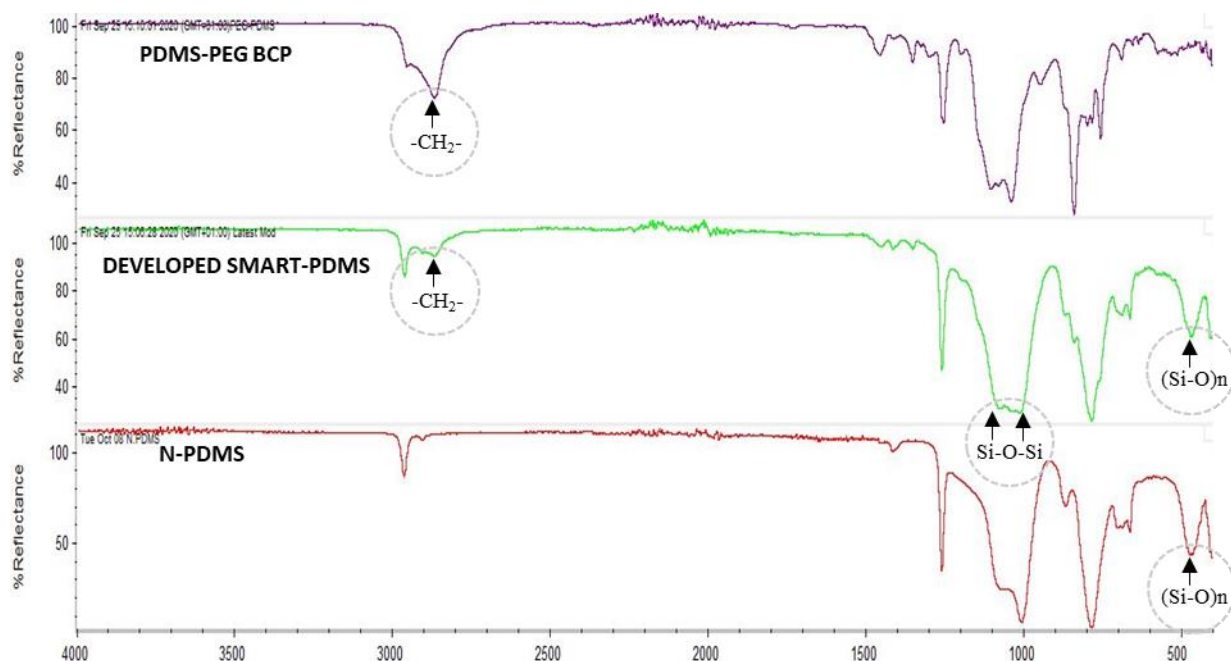


Figure 5. 4 Independent ATR-FTIR spectra for PDMS-PEG BCP, smart-PDMS and PDMS membrane

Upon modifying PDMS membrane with the newly introduced PDMS-PEG BCP reagent, and dimethylphenylsilanol, a chemical change in their respective spectra was observed with the help of ATR-FTIR spectroscopy. In Figure 5.4 notable changes between the three different forms of the membranes included changes in Si-O-Si stretching vibrations, seen in the spectrum of the developed smart PDMS (S-PDMS). This change in bond stretching was attributed to the proposed newly formed alkoxysilane bond, similar to the findings of others (Pissetti, Araújo, Silva, & Poirier, 2015). Additionally, an absorption band at 478 cm^{-1} was attributed to the symmetric stretching of Si-O-Si resulting from the (Si-O) siloxane unit. This was observed in the PDMS spectrum but absent for PDMS-PEG BCP. The bond was seen to appear at 478 cm^{-1} in S-PDMS. This was probably as a result of a local gradient that may draw and integrate the bulk PDMS base to the introduced PDMS-PEG BCP additive, thereby creating some sort of interaction. This phenomenon solidifies a chemical reaction process had occurred amongst the entities present in the modification process.

Another change observed was in the peak at 2874.9 cm^{-1} attributed to the ethylene group (ν_s CH_2) from PDMS-PEG BCP, similar to peak identification presented in (Galhenage et al., 2017). This peak was not present in PDMS, obviously due to the absence of PEG co-polymer. However, following the modification process, a peak at 2883.6 cm^{-1} was observed, also indicating the occurrence of a chemical change. Another interesting aspect noteworthy is how the developed S-PDMS membrane spectrum indicated all expected bonds, in line with the proposed reaction scheme depicted in Figure 5.3.

Other observed bonds included methyl groups which were confirmed by symmetrical stretching vibrations at 2982.4 , 2990.1 and 2991 cm^{-1} for PDMS, PDMS-PEG BCP and S-PDMS membranes respectively. Asymmetric deformations of methyl groups from the membranes were also observed at approximately 1412 cm^{-1} and symmetric deformation of methyl groups for PDMS, PDMS-PEG BCP and S-PDMS membranes were at 1272.7 , 1277.5 and 1278.1 cm^{-1} respectively. The presence of O-SiCH_3 was confirmed by peaks at 771.2 , 778.2 and 783.1 cm^{-1} , the presence of C-SiCH_3 groups were confirmed with peaks at 680.3 , 677.7 and 680.6 cm^{-1} . Peaks from PDMS membrane were in close agreement with those from literature, (Bodas & Khan-Malek, 2006), (Kim & Jeong, 2011).

5.2.4. Permeation analysis and measurement.

A similar permeation analysis methodology as reported in Section 2.3.1.7 was adopted. However, high performance liquid chromatography (HPLC) was introduced to serve as a confirmatory technique, in addition to the previously reported UV-visible technique.

Details of HPLC parameters are presented in Section 2.3.1.8.

5.2.4.1. HPLC Method Development

A series of caffeine (selected model drug) concentrations i.e. 2, 4, 8, 16 and 20 ppm, using de-ionised water, were measured from a prepared stock solution of 1000 ppm, and a calibration

graph with an R^2 value of 0.9998 was obtained. Serial dilutions for the calibration plot were slightly adjusted to 8, 16, 20, 24 and 32 ppm in the subsequent experiments, which was for convenience, but with the same stock solution of 1000 ppm. All subsequent R^2 values were in concordance with the first measurement.

All reported analysis using caffeine were carried out at an established wavelength of 271 nm, which was also in line with reported literature (Seyedabadi, Rostami, Jafari, & Fathi, 2020; Xhaferaj, Peculi, Kopali, Shkurti, & Hoxha) at a total running time of 30 minutes. A single peak was seen at approximately 3.02 minutes, with an injection volume of 10 μL , which was attributed to caffeine (Figures 5.5 and 5.6).

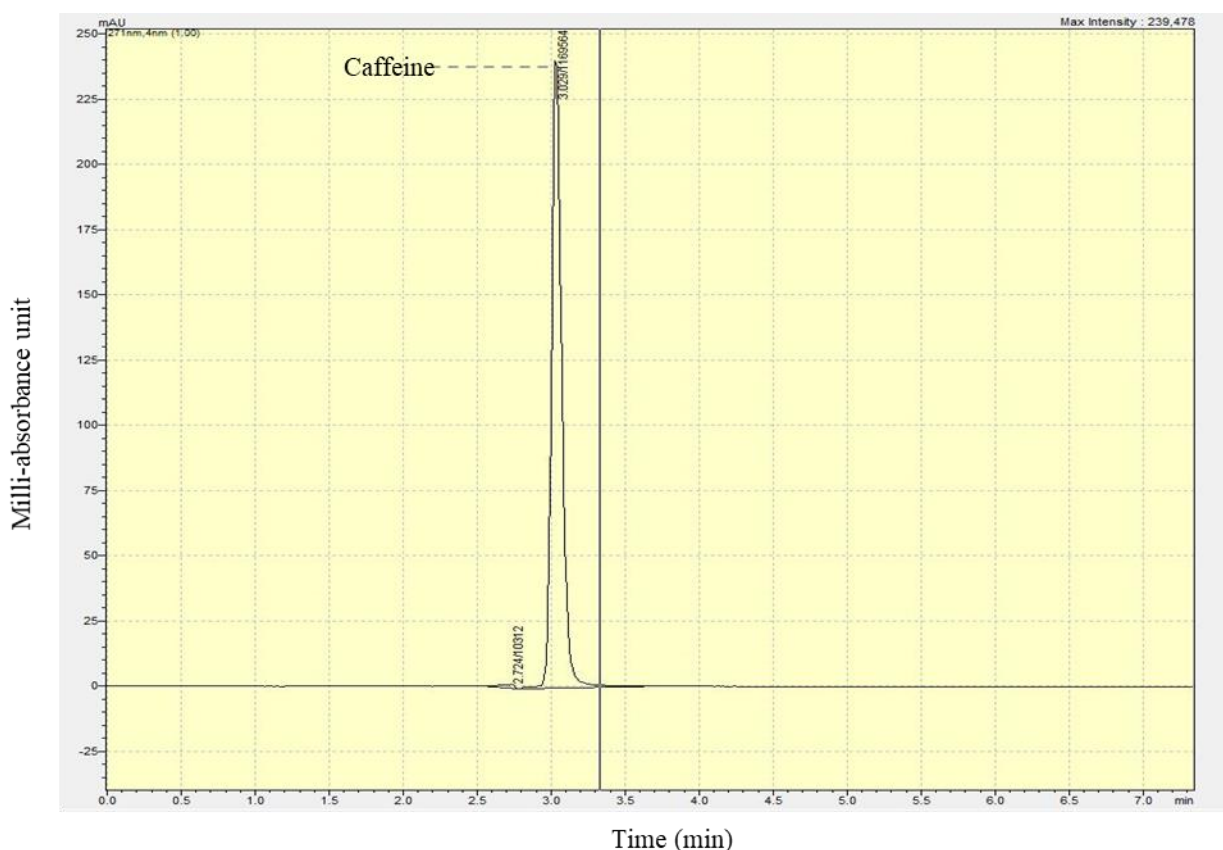


Figure 5. 5 Chromatogram of caffeine at a concentration of 8 ppm, and a peak at approximately 3. 02 minutes.

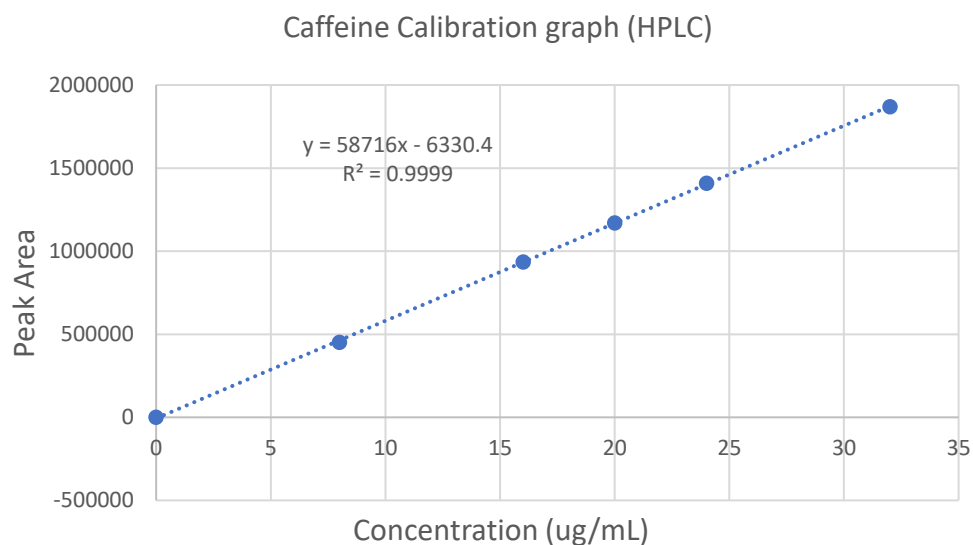


Figure 5. 6 Caffeine calibration at 271 nm using HPLC

Subsequently, after identifying the caffeine peak at a retention time of 3.02 minutes, sample solutions obtained from previously performed permeation analysis using modified smart PDMS membrane were analysed. Peaks with similar retention times (~ 3.0 minutes) were obtained from samples which was easily attributed to caffeine due to the consistency of the retention times (Figure 5.7). The resultant peak area obtained was integrated and drug concentration calculated.

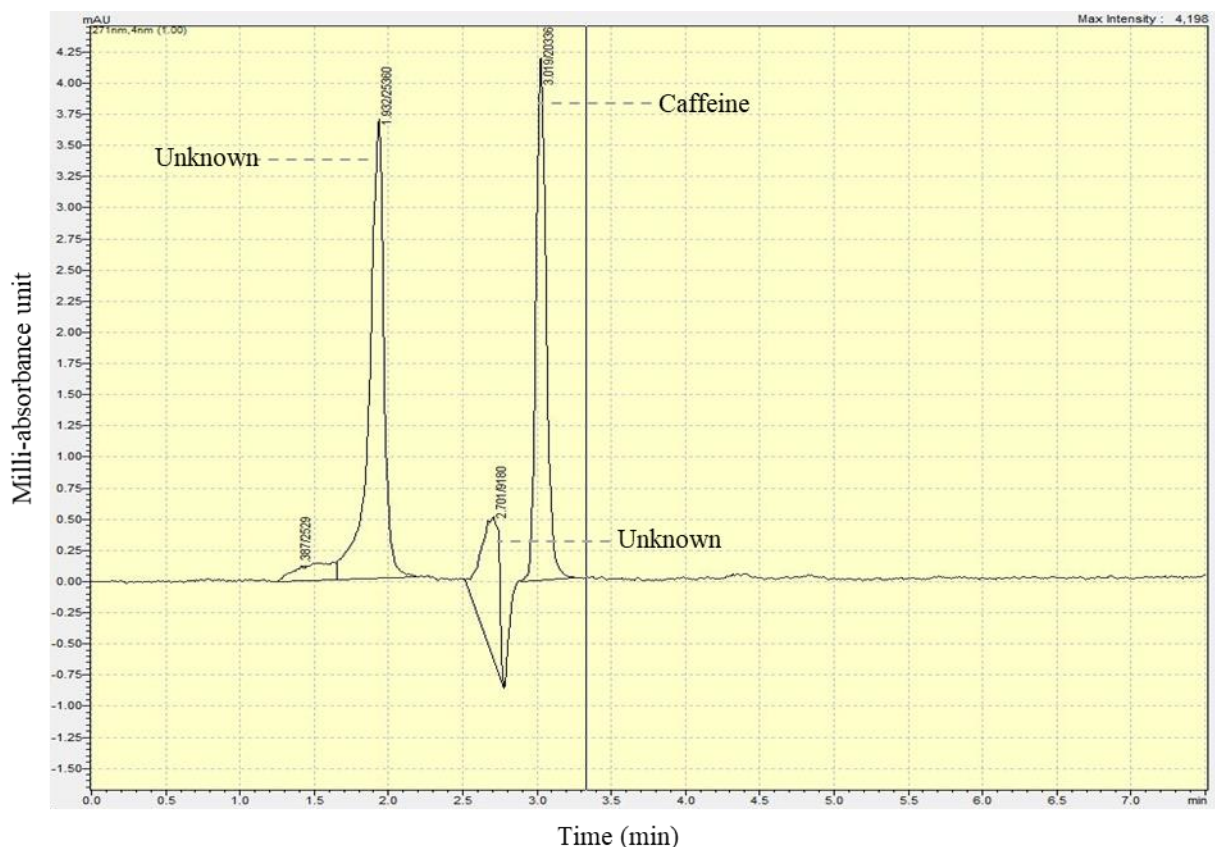


Figure 5. 7 Chromatogram of caffeine solution at a concentration of 8 ppm, indicating a peak at approximately 3.0 minutes

However, a few unknown additional peaks (1.91 and 2.70 minutes) appeared following analysis of the sample, as displayed in Figure 5.7. These peaks were most likely from a leaching effect often attributed to PDMS membrane. As such, a control analysis was employed which comprised of the modified and un-modified membranes under the same experimental conditions without the model drug compound (caffeine), to effectively analyse the disparity (Figure 5.8).

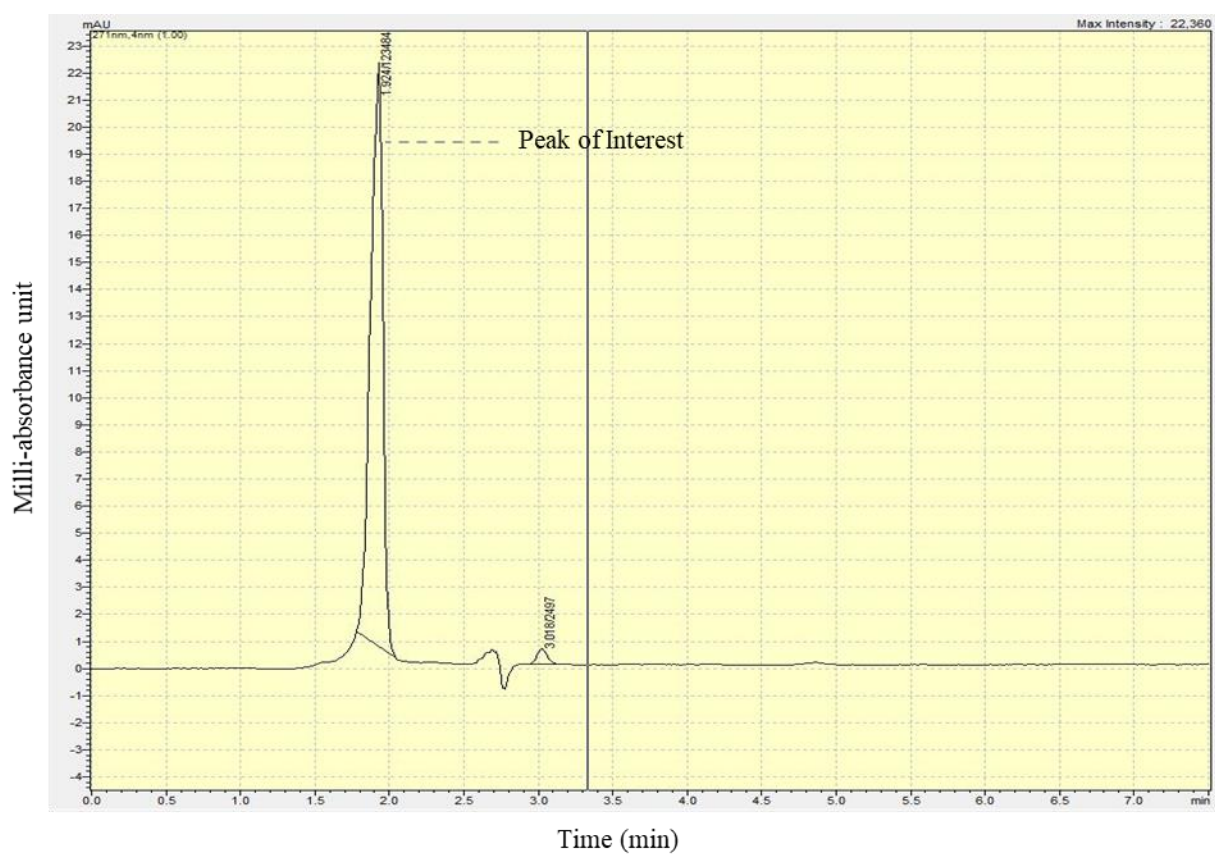
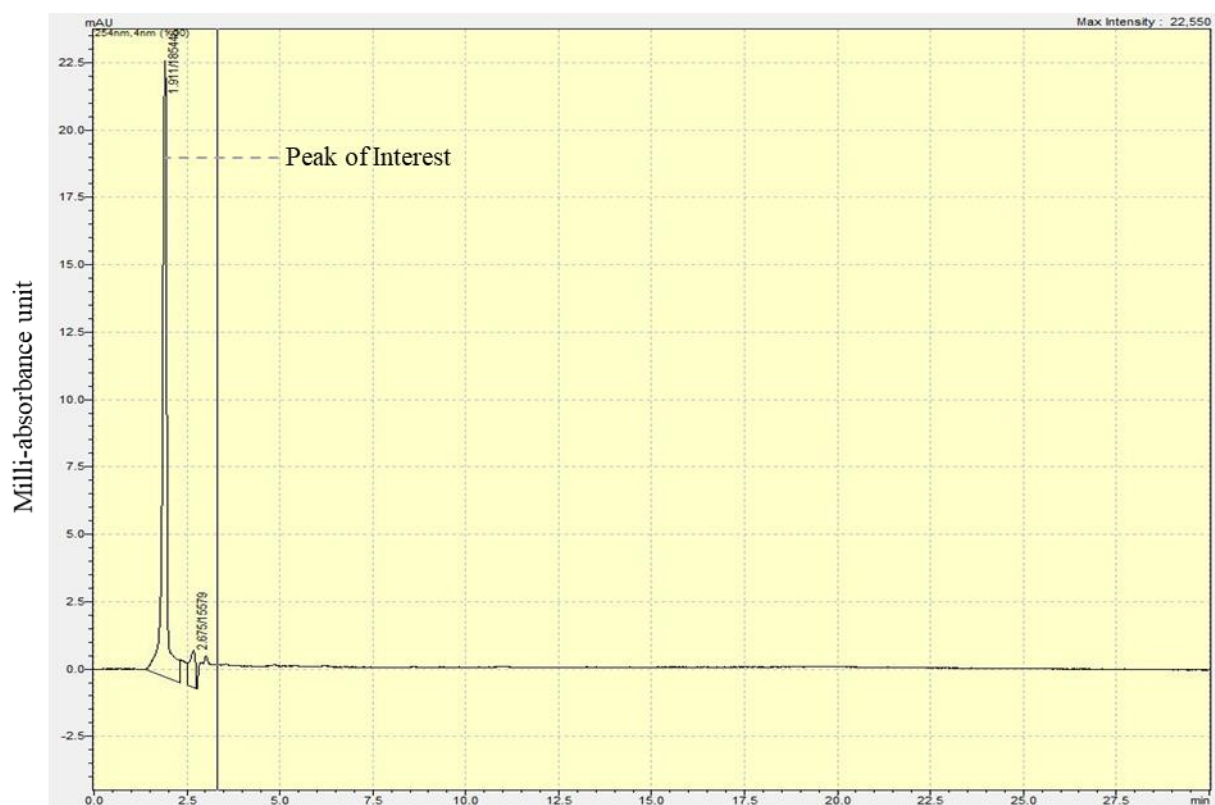


Figure 5. 8 (a and b) Chromatogram of PDMS-PEG and PDMS respectively.

In Figure 5.8 a caffeine peak at ~ 3 minutes was largely absent in the chromatograms. Figure 5.8a (PDMS-PEG) indicated the same unidentified peak at a similar retention time of 1.91 minutes. Figure 5.8b also showed the same peak of interest ascertained by a similar retention time of 1.92 minutes. These results imply a logical conclusion that the peak of interest appearing at a retention time of approximately 1.91 minutes was as a result of a leaching effect from the bulk PDMS membrane. It was also ascertained that this peak has no effect in the overall permeation analysis of the model drug compound.

5.2.4.1 Permeation data

For effective comparison of data presented in this study with data obtainable from literature, flux can be calculated from cumulative amount of drug permeated through any form of silicon membranes using the following equations, which is in line with Flynn's work (G.L. Flynn, 1974).

$$\text{Flux} = \frac{C_v K D}{L} = P \cdot C_v \quad \text{Equation 5.1}$$

$$DL^{-2} = \frac{1}{6 \cdot T_{lag}} \quad \text{Equation 5.2}$$

$$KL = 6 \cdot T_{lag} \cdot P \quad \text{Equation 5.3}$$

Where C_v is concentration of the compound, and T_{lag} is calculated from intercept of the slope on the x-axis of the graph (time axis), obtainable after steady state is achieved (according to Fick's first law) from the permeation profile of each model compound.

A summary of the physicochemical properties and cumulative mass permeated for a group of model compounds is summarised in Table 5.2.

Table 5. 2 Physicochemical properties of ketoprofen (KTF), ethylparaben (EPB), ibuprofen (IBU), lidocaine (LID), tetracaine (TTC), and caffeine (CAF) model compounds used in present study, alongside their cumulative mass permeated ($\mu\text{g}/\text{cm}^2$) through PDMS and modified smart-PDMS

	Cmpds	Log P	Mol.wght (g/mol)	CMP ($\mu\text{g}/\text{cm}^2$) N-PDMS	CMP ($\mu\text{g}/\text{cm}^2$) S-PDMS	HBD	HBA	PSA (\AA^2)	log D (pH 7.4)
1	KTF	3.29	254.28	85.7	45.9	1	3	54	0.06
2	EPB	2.76	166.17	323.7	58.2	1	3	47	2.48
3	IBU	3.5	206.28	1176.2	221.3	1	2	37	0.45
4	LID	1.81	234.34	3351.3	921.3	1	2	36	1.26
5	TTC	3.54	264.36	1551.0	114.7	1	4	42	2.26
6	CAF	-0.24	194.19	72.0	76.2	0	3	58	-

* Mol.wght – Molecular weight

* log D – Distribution coefficient

* PSA – Polar surface area

* CMP ($\mu\text{g}/\text{cm}^2$) N-PDMS – Cumulative mass permeated ($\mu\text{g}/\text{cm}^2$) of normal PDMS membrane

* CMP ($\mu\text{g}/\text{cm}^2$) D-PDMS - Cumulative mass permeated ($\mu\text{g}/\text{cm}^2$) of DMPS modified PDMS membrane

* HBD – Hydrogen bond donor

* HBA – Hydrogen bond acceptor

- log P *source* DrugBank (Uniformly considered for linearity of data)
NB. The value of log P can be different depending on the source and often can be different according to methods used in obtaining the results

Following ATR-FTIR characterisation of the newly developed smart-PDMS (S-PDMS), permeation analysis was employed using the newly modified membrane and results obtained were compared with that of PDMS, as presented in Table 5.2. Evidently, a remarkable difference was observed in the permeation profile of these model drugs. One of the major shortcomings of standard PDMS in permeation analysis is over estimation of percutaneous absorption (Khan, Frum, Sarheed, Eccleston, & Meidan, 2005; Simon, Amaro, Healy, Cabral,

& de Sousa, 2016; Uchida et al., 2016), yet based on this analysis, it can be said that this shortcoming has been potentially resolved, as displayed in Table 5.3.

Table 5. 3 Percentage decrease (% decrse.) of compounds i.e. ketoprofen (KTF), ethyl paraben (EP), ibuprofen (IBU), lidocaine (LID), tetracaine (TTC) and percentage increase (% incr.) of caffeine (CAF), that permeated through smart PDMS membranes

	Compounds	% Decrse
1	KTF	49.4 %
2	EPB	82.0 %
3	IBU	81.1 %
4	LID	72.5 %
5	TTC	92.6 %

	Compounds	% Incrse
6	CAF	4.2%

* % Decrse – Percentage decrease

* % Incrse – Percentage increase

From Chapter 4, model compounds showed very high percentage increases regarding permeation obtained using D-PDMS compared to PDMS. However, upon the modification in this chapter, the same model compounds, and under the same experimental conditions were seen to exhibit a drastic reduction in permeation, except for caffeine. This is to say, the effect of the modification employed in this section of the study has shown an impressive effect in the overall permeation profile behaviour of the membrane. However, due to the complexity of drug compounds, alongside various intrinsic properties often associated with polymer membranes, it is difficult to align this reduction in permeation analysis with a single physicochemical parameter.

Aside from ionisation of drug compounds, lipophilic chemical groups, and bulky oxygenated side chains, solubility is also known to influence permeation of drug compounds, regardless of the process being passive or active. Part of the limitation in analysing the dataset presented herein, in terms of selectivity of the membrane, is the closely related physicochemical properties of the compounds. For instance, with the exception of caffeine, all the model compounds used belong to the Class II division according to the biopharmaceutics classification system. This could be part of the reason why they all show a decrease in their permeation when permeating through the smart membrane. Caffeine on the other hand, is a hydrophilic drug, with a log P value of -0.24, and the fact that an additional layer of PEG introduced in the membrane surface is hydrophilic, could result in an increased affinity of the drug compound to the membrane, thereby increasing permeation, unlike the rest of the compounds that are all lipophilic.

5.3. Conclusion

Overall, the modification process employed has been confirmed using ATR-FTIR, alongside permeation analysis where model compounds used (both hydrophilic and lipophilic) were quantified using UV-visible spectrophotometry and HPLC.

The membrane developed has shown an impressive reduction in permeation compared with PDMS; this was previously a lingering issue when considering PDMS as a substitute for human skin in percutaneous absorption. Enhanced activity of the membrane can be attributed to a suitable balance amongst all the moieties present in the modification process from the co-polymer used. This is to say, the PEG chain length can result in staggered delivery of compounds (Akimoto, Aoyagi, Minoshima, & Nagase, 1997) and, as a result, selectively reduce permeation.

References

- Aguilar, M. R., Elvira, C., Gallardo, A., Vázquez, B., & Román, J. (2007). Smart polymers and their applications as biomaterials. *Topics in tissue engineering*, 3(6).
- Aguilar, M. R., & San Román, J. (2019). *Smart polymers and their applications*: Woodhead publishing.
- Akimoto, T., Aoyagi, T., Minoshima, J.-i., & Nagase, Y. (1997). Polymeric percutaneous drug penetration enhancer: synthesis and enhancing property of PEG/PDMS block copolymer with a cationic end group. *Journal of controlled release*, 49(2-3), 229-241.
- Asatekin, A., Kang, S., Elimelech, M., & Mayes, A. M. (2007). Anti-fouling ultrafiltration membranes containing polyacrylonitrile-graft-poly (ethylene oxide) comb copolymer additives. *Journal of Membrane Science*, 298(1-2), 136-146.
- Asatekin, A., & Mayes, A. M. (2009). Oil industry wastewater treatment with fouling resistant membranes containing amphiphilic comb copolymers. *Environmental science & technology*, 43(12), 4487-4492.
- Bodas, D., & Khan-Malek, C. J. M. e. (2006). Formation of more stable hydrophilic surfaces of PDMS by plasma and chemical treatments. *Microelectronic engineering*, 83(4-9), 1277-1279.
- G.L. Flynn, S. H. Y., T.J. Roseman. (1974). *Journal of pharmaceutical sciences*, 63(4), 479-510. doi:<https://doi.org/10.1002/jps.2600630403>
- Galhenage, T. P., Webster, D. C., Moreira, A. M., Burgett, R. J., Stafslie, S. J., Vanderwal, L., . . . Clare, A. S. (2017). Poly (ethylene) glycol-modified, amphiphilic, siloxane–polyurethane coatings and their performance as fouling-release surfaces. *Journal of Coatings Technology and Research*, 14(2), 307-322.
- Gökaltun, A., Kang, Y. B. A., Yarmush, M. L., Usta, O. B., & Asatekin, A. (2019). Simple Surface Modification of Poly (dimethylsiloxane) via Surface Segregating Smart Polymers for Biomicrofluidics. *Scientific reports*, 9(1), 1-14.
- Hu, S., Ren, X., Bachman, M., Sims, C. E., Li, G., & Allbritton, N. (2002). Surface modification of poly (dimethylsiloxane) microfluidic devices by ultraviolet polymer grafting. *Analytical Chemistry*, 74(16), 4117-4123.
- Kaner, P., Rubakh, E., & Asatekin, A. (2017). Zwitterion-containing polymer additives for fouling resistant ultrafiltration membranes. *Journal of Membrane Science*, 533, 141-159.
- Kang, S., Asatekin, A., Mayes, A. M., & Elimelech, M. (2007). Protein antifouling mechanisms of PAN UF membranes incorporating PAN-g-PEO additive. *Journal of Membrane Science*, 296(1-2), 42-50.
- Khan, G. M., Frum, Y., Sarheed, O., Eccleston, G. M., & Meidan, V. M. (2005). Assessment of drug permeability distributions in two different model skins. *International journal of pharmaceuticals*, 303(1-2), 81-87.
- Kim, H. T., & Jeong, O. C. J. M. E. (2011). PDMS surface modification using atmospheric pressure plasma. *Microelectronic engineering*, 88(8), 2281-2285.
- Majcen, N., Mohsen, R., Snowden, M. J., Mitchell, J. C., & Vancina, B. (2018). The development of a novel smart material based on colloidal microgels and cotton. *Advances in colloid and interface science*, 256, 193-202.
- Pissetti, F. L., Araújo, P. L. d., Silva, F. A., & Poirier, G. Y. (2015). Synthesis of poly (dimethylsiloxane) networks functionalized with imidazole or benzimidazole for copper (II) removal from water. *Journal of the Brazilian Chemical Society*, 26(2), 266-272.

- Seyedabadi, M. M., Rostami, H., Jafari, S. M., & Fathi, M. (2020). Development and characterization of chitosan-coated nanoliposomes for encapsulation of caffeine. *Food Bioscience*, 100857.
- Simon, A., Amaro, M. I., Healy, A. M., Cabral, L. M., & de Sousa, V. P. (2016). Comparative evaluation of rivastigmine permeation from a transdermal system in the Franz cell using synthetic membranes and pig ear skin with in vivo-in vitro correlation. *International journal of pharmaceutics*, 512(1), 234-241.
- Uchida, T., Yakumaru, M., Nishioka, K., Higashi, Y., Sano, T., Todo, H., & Sugibayashi, K. (2016). Evaluation of a silicone membrane as an alternative to human skin for determining skin permeation parameters of chemical compounds. *Chemical and Pharmaceutical Bulletin*, 64(9), 1338-1346.
- Xhaferaj, N., Peculi, A., Kopali, A., Shkurti, A., & Hoxha, F. Evaluation of Caffeine in Soft and Energy Drinks by Means of UV/Visible Spectrophotometer.
- Yao, M., & Fang, J. (2012). Hydrophilic PEO-PDMS for microfluidic applications. *Journal of Micromechanics and Microengineering*, 22(2), 025012.

Chapter 6:

Conclusion and Future work

6.1. Conclusion

The primary aim of this research work was to produce an alternate inorganic synthetic polymer membrane capable of mimicking the surface activity of skin in terms of permeation analysis (primarily the measurement of drug percutaneous absorption), which is necessary before any transdermal drug is released on to the market.

Poly(dimethylsiloxane) PDMS membrane was considered and initially the membrane was plasma treated using a non-thermal plasma technique, which resulted in activating the polymer surface, thereby making it susceptible for further modifications. Reported stability, selectivity and integrity of the membrane were vital in the intended purpose of this work, hence, a cautious approach mainly informed by literature to use a mild and non-invasive chemical method to modify the membrane was adopted. Skin structural activity was also carefully studied and critically analysed to guide direction of the modification. Keeping in mind some imperative constraints often posed by scientists regarding the use of synthetic membranes for *in vitro* analysis, such as the absence of viable cells to mimic activity of the living system with certainty, the approach was instead based on comparisons with permeation data obtainable from literature using skin. It was understood that permeation activity of the skin can be achieved without necessarily replicating its cellular structures or viable cells, as selective permeability of the skin is largely attributed to the topmost stratum corneum layer, which in itself is predominantly not made up of viable cells (Godin & Touitou, 2007; Guy, 2013; Herkenne, Naik, Kalia, Hadgraft, & Guy, 2007; K. W. Ng & Lau, 2015).

Moreover, it was understood that poly(dimethylsiloxane) generally results in overestimation of percutaneous absorption (Simon et al., 2016; Uchida et al., 2016), a phenomenon that seems to persist even after reported attempts to modify the membrane for percutaneous absorption (Feldstein et al., 1998; Miki et al., 2015; Xia et al., 2007). Therefore, the primary focus in this

research work was to try and achieve a noticeable decrease in drug permeation through the membrane. After plasma treating the membrane, a slight reduction was achieved when results of the plasma treated membrane were compared with that of PDMS membrane using a set of model compounds that covered a wide range of therapeutic classes. This finding indicates a change in surface behaviour of the membrane. The change wasn't sufficient enough to form a strong basis for adaptation hence, glycerol was further grafted on the plasma treated membrane via a simple condensation process. Although following this process a surface change of the membrane was confirmed using spectroscopic techniques such as scanning electron microscopy (SEM), water contact angle analysis (WCA), attenuated total reflectance spectroscopy- Fourier transform infrared spectroscopy (ATR-FTIR) and permeation analysis, changes in permeation profiles were not adequately similar to that of skin.

Following on from that result, some chemical entities were also considered, this time focusing mainly on compounds that can incorporate lipophilic properties on the membrane. Compounds such as dimethylphenylsilanol, tertbutyldimethylsiloxane and perfluorophenylsilanol were selected for such purposes, mainly due to their reported lipophilic properties and chemical compatibility with plasma treated PDMS membrane. All the compounds utilised showed some changes in permeation profiles of the modified membrane accordingly, however, membrane that was treated with dimethylphenylsilanol, showed the most desirable change in terms of this research aim. This version of the membrane depicted a heightened affinity to lipophilic compounds ($R^2 = 0.9$, for 13 compounds) when utilised for permeation studies, indicating a rather successful addition of the lipophilic layer on its surface. Moreover, stability and selectivity of the membrane was maintained throughout the duration of permeation analysis (6 hours). This section of the work provided a remarkable avenue for further modifications of the membrane.

Based on these studies, it was apparent that poly(dimethylsiloxane) can be chemically modified to achieve an overwhelming change in permeation profile, more importantly, exhibiting these changes in a controlled and logical manner (Waters & Sabo, 2020), and can be used to achieve data of highly hydrophilic drugs such caffeine, which in the past has also been an issue. Despite these recorded achievements, reduction of permeation through the membrane remained a challenge.

As a result, the concept of a smart PDMS modified membrane was introduced. This concept was not to only selectively allow xenobiotics to permeate the membrane, it was also intended to reduce the permeation ability of compounds through the membrane. Permeation results for six model drugs using this newly developed smart-membrane indicated that five out of the six drugs displayed a remarkable reduction in their permeation profile, compared to PDMS alone. Analytical techniques, namely attenuated total reflectance spectroscopy- Fourier transform infrared spectroscopy (ATR-FTIR) and high-performance liquid chromatography (HPLC), were used to characterise the newly developed membrane. These findings provide the possibility for scientists to utilise this modified membrane to accurately and precisely predict permeation without the need to use animal or human skin, thus achieving the overall aim of this work.

6.2. Future work

Although this study can be deemed successful in regard to creating a polymer-based skin mimic, there are several potential avenues of interest for future work, including:

- ✚ An increase in the number of model drugs used in analysing the newly developed smart PDMS membrane should be pursued, as this will not only allow a better understanding of how the membrane works but will also provide sufficient data to predict a deeper understanding of the membrane. Compounds

of interest to expand the study should span a wide range of log P values and also cut across different therapeutic classes to enable a more robust dataset.

- ✚ The inclusion of alternative analytical techniques that could be used for surface analysis, such as X-ray photoelectron spectroscopy (XPS), and atomic force microscopy (AFM). These should be employed to further understand the surface chemistry of the modified membrane, as this will help in proposing a theory of how it functions.
- ✚ In the long term, mathematical model equations should be generated using data acquired from the newly developed smart membrane as this will serve as a useful tool for primary screening of drugs intended for transdermal delivery.
- ✚ Creation of alternative modified membranes. Promising membranes such as hydro- and microgels capable of exhibiting smart re-orientation have been widely explored. However, there have been limited considerations in modifying them for purposes of permeation analysis. Hence, these promising class of membranes should also be investigated, particularly to modify and tailor-fit them in mimicking skin barrier properties.

References

- Feldstein, M. M., Raigorodskii, I. M., Iordanskii, A. L., & Hadgraft, J. (1998). Modeling of percutaneous drug transport in vitro using skin-imitating Carbosil membrane. *Journal of controlled release*, 52(1-2), 25-40.
- Godin, B., & Touitou, E. (2007). Transdermal skin delivery: predictions for humans from in vivo, ex vivo and animal models. *Advanced drug delivery reviews*, 59(11), 1152-1161.
- Guy, R. (2013). Skin-‘that unfakeable young surface’. *Skin pharmacology and physiology*, 26(4-6), 181-189.
- Herkenne, C., Naik, A., Kalia, Y. N., Hadgraft, J., & Guy, R. H. (2007). Ibuprofen transport into and through skin from topical formulations: in vitro–in vivo comparison. *Journal of Investigative Dermatology*, 127(1), 135-142.
- Miki, R., Ichitsuka, Y., Yamada, T., Kimura, S., Egawa, Y., Seki, T., . . . Morimoto, Y. (2015). Development of a membrane impregnated with a poly (dimethylsiloxane)/poly (ethylene glycol) copolymer for a high-throughput screening of the permeability of drugs, cosmetics, and other chemicals across the human skin. *European Journal of Pharmaceutical Sciences*, 66, 41-49.
- Ng, K. W., & Lau, W. M. (2015). Skin deep: the basics of human skin structure and drug penetration. In *Percutaneous Penetration Enhancers Chemical Methods in Penetration Enhancement* (pp. 3-11): Springer.
- Simon, A., Amaro, M. I., Healy, A. M., Cabral, L. M., & de Sousa, V. P. (2016). Comparative evaluation of rivastigmine permeation from a transdermal system in the Franz cell using synthetic membranes and pig ear skin with in vivo-in vitro correlation. *International journal of pharmaceuticals*, 512(1), 234-241.
- Uchida, T., Yakumaru, M., Nishioka, K., Higashi, Y., Sano, T., Todo, H., & Sugibayashi, K. (2016). Evaluation of a silicone membrane as an alternative to human skin for determining skin permeation parameters of chemical compounds. *Chemical and Pharmaceutical Bulletin*, 64(9), 1338-1346.
- Waters, L. J., & Sabo, S. (2020). Permeation of pharmaceutical compounds through silanised poly (dimethylsiloxane). *Journal of pharmaceutical sciences*. 109 (6), 2033-2037
- Xia, X.-R., Baynes, R. E., Monteiro-Riviere, N. A., & Riviere, J. E. (2007). An experimentally based approach for predicting skin permeability of chemicals and drugs using a membrane-coated fiber array. *Toxicology and applied pharmacology*, 221(3), 320-328.

Appendices

Appendix I

Award

- Best poster presentation award
Africans in STEM Symposium, organised at the University of Cambridge, UK. (April 2021)

Conferences Attended

- *Postgraduate Research Conference, University of Huddersfield, April 2018*
- *10th Association of Pharmaceutical Scientist (APS) International PharmSci Conference, University of Greenwich (Maritime Campus), September 2019.*
- *The JPAG pharmaceutical analysis research awards and careers symposium conference, Royal Society of Chemistry, London UK., November 2019*
- *Postgraduate Research Conference, University of Huddersfield, November 2020*
- *Africans in STEM symposium, University of Cambridge, April 2021*

Poster Presentations

- Modifying polymer membranes to create skin mimic systems for permeation analysis – *APS Conference, University of Greenwich, 2019*
- Chemical modification of poly(dimethylsiloxane) PDMS for permeation analysis - *JPAG Conference, Royal Society of Chemistry/ London UK., 2019*
- Smart Poly(dimethylsiloxane) polymer; A smart alternative to the use of an actual skin for permeation analysis - *Africans in STEM symposium, University of Cambridge, April 2021 (In-view)*

Oral Presentation

- Replacing the use of animal skin with a synthetic polymer membrane in permeation analysis (Drug Delivery).
PGR Conference, University of Huddersfield. 2020

Peer Reviewed Publications

- Permeation of Pharmaceutical Compounds Through Silanized Poly(dimethylsiloxane)
Journal of pharmaceutical sciences 109 (6), 2033-2037
- Poly(dimethylsiloxane): A Sustainable Human Skin Alternative for Transdermal Drug Delivery Prediction (A review)
Journal of pharmaceutical sciences 110 (3), 1018-1024

Appendix II

- BET results for untreated PDMS membrane obtained.

			
ASAP 2020 V3.00 H	Unit 1	Serial #: 517	Page 1
Sample: 000-030 PDMS untreated Operator: GPA Submitter: Sani File: C:\2020\DATA\000-030.SMP			
Started: 23/05/2019 14:28:33PM Completed: 23/05/2019 16:19:20PM Report Time: 28/05/2019 16:20:45PM Sample Mass: 0.1322 g Cold Free Space: 87.7092 cm ³ Low Pressure Dose: None		Analysis Adsorptive: N2 Analysis Bath Temp.: 77.356 K Thermal Correction: No Warm Free Space: 28.5140 cm ³ Measured Equilibration Interval: 5 s Automatic Degas: No	
<hr/>			
Summary Report			
No summary reports could be produced.			

- BET results for chemically treated PDMS membrane obtained.

			
ASAP 2020 V3.00 H	Unit 1	Serial #: 517	Page 1
Sample: 000-029 Treated PDMS Operator: GPA Submitter: Sani File: C:\2020\DATA\000-029.SMP			
Started: 20/05/2019 15:20:37PM Completed: 20/05/2019 17:25:05PM Report Time: 28/05/2019 16:24:38PM Sample Mass: 0.1097 g Cold Free Space: 86.8568 cm ³ Low Pressure Dose: None		Analysis Adsorptive: N2 Analysis Bath Temp.: 77.316 K Thermal Correction: No Warm Free Space: 28.3396 cm ³ Measured Equilibration Interval: 5 s Automatic Degas: No	
Comments: Using piece as recieved degassed at 50 C for 30 min.			
<hr/>			
Summary Report			
No summary reports could be produced.			

